

Cover design: Box press

Print: Box press, proefschriftmaken.nl, Oisterwijk, the Netherlands

ISBN: 978-90-393-5336-3

© Marijke W.A. de Backer, Moordrecht, the Netherlands, 2010

The research presented in this thesis was performed at the Rudolf Magnus Institute of Neuroscience, Department Neuroscience and Pharmacology of the University Medical Centre Utrecht, the Netherlands.

Optimization of viral vector technology to study gene function in the hypothalamus

Optimalisatie van virale vector technologie om de
functie van genen in de hypothalamus te
bestuderen
(met een samenvatting in het Nederlands)

Proefschrift

ter verkrijging van de graad van doctor aan de Universiteit
Utrecht op gezag van de rector magnificus, prof.dr. J.C.
Stoof, ingevolge het besluit van het college voor promoties
in het openbaar te verdedigen op

donderdag 3 juni 2010 des middags te 4.15 uur

door

Maria Wilhelmina Anna de Backer
geboren op 25 november 1980, te 's-Hertogenbosch

Promotor: Prof.dr. R.A.H. Adan

Publication of this thesis was financially supported by the Rudolf Magnus Institute (Utrecht, the Netherlands) and by the Plasmid Factory (Bielefeld, Germany).

The research described in this thesis was supported by the Netherlands Organization for Scientific Research (NWO).

CONTENTS

Abbreviations	7
Chapter 1	11
General introduction	
Chapter 2	31
An adeno-associated viral vector transduced the rat hypothalamus and amygdala more efficient than a lentiviral vector	
Chapter 3	43
Optimization of adeno-associated viral vector mediated gene delivery to the hypothalamus	
Chapter 4	59
Melanocortin receptor mediated effects on obesity are distributed over specific hypothalamic regions	
Chapter 5	81
A new method to deliver neuropeptides to the brain: a von Willebrand factor signal peptide to direct local neuropeptide secretion	
Chapter 6	97
Suppressor of cytokine signaling 3 (Socs3) knockdown in the mediobasal hypothalamus: counterintuitive effects on feeding behavior	
Chapter 7	117
General discussion and summary	
References	127
Nederlandse samenvatting	167
Curriculum Vitae	173
List of publications	175
Dankwoord	177

LIST OF ABBREVIATIONS

AAV	adeno-associated virus/ adeno-associated viral
Acc	nucleus accumbens
ACTH	adrenocorticotrophic hormone
Ad	adenovirus
AgRP	agouti-related peptide
AM	amygdala
ARC	arcuate nucleus
BAT	brown adipose tissue
BDNF	brain-derived neurotrophic factor
CART	cocaine and amphetamine-regulated transcript
CBA	chicken β -actin
CCK	cholecystokinin
CMV	cytomegalovirus
CNS	central nervous system
dsRed	discosoma red fluorescent protein
GABA	gamma-aminobutyric acid
GFP	green fluorescent protein
HSPG	heparin sulfate proteoglycan
HSV	herpes simplex virus
ICV	intracerebroventricular
ITR	inverted terminal repeat
LEPRb	leptin receptor long isoform (b)
LH	lateral nucleus of the hypothalamus
LTR	long terminal repeat
LV	lentivirus/ lentiviral
MBH	mediobasal hypothalamus
MC	melanocortin
MCH	melanin concentrating hormone
MCR	melanocortin receptor
MSH	melanocyte-stimulating hormone
NPY	neuropeptide Y
NSE	neuron specific enolase
NTS	nucleus of the solitary tract
POMC	proopiomelanocortin
PVN	paraventricular nucleus of the hypothalamus
RV	retrovirus
RNAi	RNA interference
shRNA	short hairpin RNA

siRNA	short interfering RNA
Socs3	suppressor of cytokine signaling 3
VMH	ventromedial nucleus of the hypothalamus
VSV-G	vesicular stomatitis virus-g protein
VWF	von Willebrand factor
WAT	white adipose tissue
WPRE	woodchuck hepatitis post-transcriptional regulatory element

Chapter 1

General introduction

GENERAL INTRODUCTION

Outline

1. Viral vector mediated gene delivery to the central nervous system	13
Viral vector mediated gene transfer	14
<i>Lentiviral vectors</i>	17
<i>Adeno-associated viral vectors</i>	18
2. Neurobiology of energy balance	19
Hypothalamic circuits	19
Hindbrain circuits	21
Higher brain areas	22
3. Leptin-Melanocortin signaling	22
Leptin system	22
Melanocortin system	24
4. Aims and outline of the thesis	28

1. Viral vector mediated gene delivery to the central nervous system

Human diseases of the central nervous system (CNS), like Huntington's disease, familiar Alzheimer's disease and familiar amyotrophic lateral sclerosis, have been associated with mutations in genes. In addition, genetic variations can contribute to the susceptibility for a disease or a disorder, such as autism and schizophrenia. To understand how a certain gene is involved in the development of a disease, the function of a gene needs to be determined. In mice a specific gene can be deleted or overexpressed in (all) cells by homologous recombination or transgenesis. Currently, many genetic mouse models are available to investigate gene function; however, rats are often better models for human diseases, such as diabetes, cardiovascular diseases and psychiatric disorders. Unfortunately, genetic modification in rats is hampered, because homologous recombination has a very low success rate in species other than mice. However, viral vectors are able to (locally) modify gene expression and their application is not limited to the mouse, they can be used in any species.

Genetic and pharmacological studies have contributed widely to unravel pathways underlying diseases. *In vivo* drug administration studies and knockout models in rodents have greatly contributed to the knowledge concerning the role of leptin and melanocortin (MC) signaling in modulating energy homeostasis. However, these studies showed some contradictory results, e.g. intracerebroventricular (ICV) infusion of agouti-related peptide (AgRP, a inverse agonist for MC receptors in the brain) increases food intake and body weight significantly, while AgRP knockout mice show relatively normal ingestive behavior and body weight (1, 2). Most pharmacological and knockout studies have focused on the effects of neuropeptides or their receptors in the whole brain by infusing the peptides ICV or investigating whole body knockout mice. When a drug is administrated ICV, the drug can bind to all its receptors in different brain regions, which is not a normal physiological response when a gene product is released locally; therefore the normal function of the gene product may not be seen under these manipulated conditions. A comparable situation occurs in case of transgenic overexpression or knockout of a gene, the gene is expressed in many places at once, even in areas where it normally is not expressed, or the gene is deleted in all places. A gene plays a specific role in a particular neural circuit to control a certain behavior. Therefore, brain nucleus specific studies may help to elucidate the role of a gene more specifically. Local infusion studies with permanent cannulae in the brain have been performed, but the drugs can only be infused for up to a week. In addition, neuron type specific knockout is possible, because there is a wide range of cre-expressing mice available, however, not all brain areas or neuron types can be

targeted and developmental compensation can not be ruled out. In this thesis we used viral vector mediated gene transfer as a complementary approach to study the role of leptin and MC systems in specific brain areas in regulation of energy homeostasis, this as an example of how viral vectors can be applied to determine gene function in the CNS.

Viral vector mediated gene transfer

A viral vector is derived from a wild type virus, by removing most of the viral genome and replacing it with a promoter and a gene sequence of interest (Fig. 1). The recombinant viral genome can be co-transfected with plasmids, which contain the original viral genes for replication and packaging, into cells.

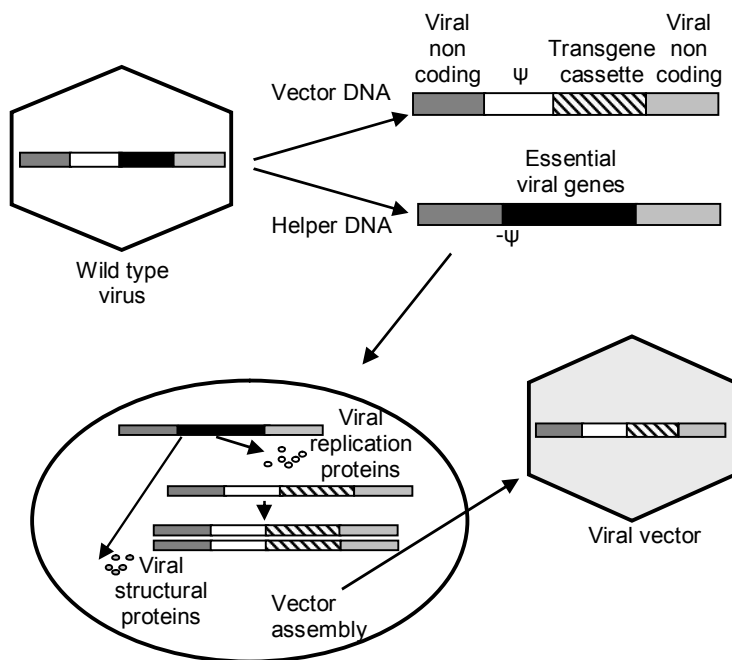


Figure 1 - Schematic overview: how to engineer a viral vector from a virus

The vector DNA contains the transgene expression cassette and non-coding *cis*-acting sequences including the packaging signal (ψ). The helper DNA contains genes which are essential for replication and packaging but lacks ψ . The helper genes can sometimes be split over multiple plasmids to enhance biosafety (more recombination events are needed to end up with a wild type virus). After transfection of the plasmids into cells, the cells will produce replication proteins, that are involved in the synthesis of many copies of vector genome (DNA or RNA, depending on the viral vector). In addition, viral structural proteins are produced and these recognize the ψ sequence in the vector genome and package the vector genome into a viral particle. The helper plasmid does not contain ψ and therefore is not packaged into a particle. Modified from (3).

These cells subsequently produce replication deficient viral particles, because the viral particles only contain the modified viral genome and do not contain genes which are necessary for replication and packaging. This increases the biological safety (reviewed in (3)).

Viral vectors can establish stable gene expression for long periods of time and they can be used at any moment during life to overexpress a specific gene or to suppress a desired gene by RNA interference (RNAi). RNAi can be mediated by small interfering RNAs (siRNAs) or short hairpin RNAs (shRNAs) which target a specific gene and degrade the mRNA and/or block the translation of the mRNA into a protein (reviewed in (4)). Synthetic siRNAs are rapidly degraded in cells, thus they can only decrease gene expression for a short period of time (5, 6). This transient effect may be circumvented by the use of shRNAs. A shRNA is a siRNA with a hairpin structure (loop) and can continuously be transcribed from a RNA polymerase III promoter (6, 7). In addition, shRNAs are more efficiently loaded into the RNA-induced silencing complex (RISC) than siRNAs (8). One aspect to keep in mind when using RNAi is the possibility of unintended regulation of other genes (off-target effects), due to partial complementary sequences or due to a wide range of immune and toxicity effects, e.g. activation of interferon (reviewed in (8)).

There are different classes of viral vectors; all with their own advantages and disadvantages. The classes can be divided in two groups, namely those which integrate into the chromosome (retroviruses and lentiviruses (LV)) and those which persist in the nucleus as extrachromosomal episomes (adeno-associated viruses (AAV), adeno-viruses and herpes simplex viruses). Table 1 shows the properties of these different viral vectors (reviewed in (9)).

LV and retroviral vectors differ in their tropism even when they are both packaged with the G protein of vesicular stomatitis virus (VSV-G) envelop. A retroviral vector, e.g. Moloney murine leukemia virus (MoMLV) only transduces dividing cells, because the pre-integration complex (PIC) enters the cell nucleus when the nuclear membrane breaks down, however LV vectors transduce dividing and non-dividing cells, because their PIC can cross the nuclear cell membrane (10, 11). However, integration in the chromosome by LV and retroviral vectors is not a guarantee for stable expression, since integrated vector genomes can be silenced over time (12, 13). In addition, these integrating vectors have a risk of inducing insertional mutagenesis.

Herpes simplex viral -1 (HSV-1) vectors can be made in two ways. One method is to remove 1 or more essential replication gene(s). These replication deficient recombinant HSV-1 vectors have the capacity to express transgenes after a latent infection in central and peripheral neurons. These vectors can package up to 40 kb of transgenic sequences.

Table 1 - Main classes of viral vectors

Vector	Genetic material	Packaging capacity	Tropism	Inflammatory potential	Vector genome form	Main limitations	Main advantages
<i>Enveloped</i>							
Retrovirus	RNA	8 kb	Dividing cells	Low	Integrated	Only transduces dividing cells; integration might induce oncogenesis	Persistent gene transfer in dividing cells
Lentivirus	RNA	8 kb	Broad	Low	Integrated	Integration might induce oncogenesis	Persistent gene transfer in most cell types
HSV-1	dsDNA	40 kb* 150 kb§	Strong for neurons	High	Episomal	Inflammatory; transient gene expression in cells other than neurons	Large packaging capacity; strong tropism for neurons
<i>Non-enveloped</i>							
AAV	ssDNA	<5 kb	Broad	Low	Episomal	Small packaging capacity	Non-inflammatory; non-pathogenic
Adenovirus	dsDNA	8 kb* 30 kb±	Broad	High	Episomal	Capsid mediates a potent inflammatory response	Extremely efficient transduction of most tissues

* Replication deficient; § Amplicon; ± Helper dependent; dsDNA: double stranded DNA; ssDNA: single stranded DNA; HSV-1: Herpes simplex virus-1; AAV: Adeno-associated virus.

The other method is to remove all viral genes, except for the packaging signal and the origin of replication; these vectors are helper dependent and are called amplicon vectors. Amplicon vectors may contain large inserts up to 150kb, when the inserts are smaller the amplicon vectors carry concatamers of DNA which are derived from the amplicon plasmid (14, 15). In addition HSV-1 vectors are able to spread trans-synaptically from neuron to neuron, in anterograde and retrograde direction (15).

In adenoviruses similar deletions as in HSV-1 vectors can be made to obtain replication deficient or helper dependent adenoviral vectors, the later can have larger transgene inserts (16). In addition, helper dependent adenoviral vectors show a decrease in immunogenicity and a prolonged transgene expression compared to replication deficient adenoviral vectors (3, 17).

AAV (AAV) and LV vectors are attractive tools to modify gene expression, because they can transduce dividing and non-dividing cells, establish stable expression for long periods of times and have low immunogenicity. Therefore in this thesis these two viral vectors were tested in their ability to transduce the adult rat hypothalamus and amygdala. Below there is a short description of the properties of these viruses/vectors.

Lentiviral vectors

LV infects vertebrates, particularly primates and domestic animals. and cause a slowly progressive disease (lenti in Latin means slow). LV is a RNA virus derived from retroviruses with three open reading frames: *gag*, *pol* and *env* which encode for capsid proteins, viral enzymes and envelope glycoproteins. In addition, they carry regulatory and accessory genes to control their own gene expression. A number of LV members have been used as viral vectors, such as human immunodeficiency virus (HIV)-1, simian immunodeficiency virus (SIV), equine infectious anaemia virus (EIAV) and feline immunodeficiency virus (FIV).

A LV vector contains two long terminal repeats (LTRs), a packaging signal (part of *gag*), a rev-responsive element (RRE, to promote nuclear export of viral RNA), a flap region (includes central polypurine tract (cppt), contributes to nuclear import of proviral DNA) and a transgene insert, with a promoter and a gene of interest and often a woodchuck hepatitis post-transcriptional response element (WPRE) (18, 19, 20, 21). Most LV vectors used today are self-inactivating (SIN); the regulatory elements in the 3'LTR are deleted and this prevents vector mobilization by wild type viruses (22).

The normal envelop of LV only has a narrow tropism, it only infects cells that express the CD4 receptor. Therefore LV vectors are often pseudotyped with other viral envelopes, in particular with vesicular stomatitis virus glycoprotein (VSV-G) (23, 24), which appears to interact with a ubiquitous cellular "receptor", rendering a broad tropism (25, 26). In addition, VSV-G pseudotyping increases particle stability

(27). Other envelopes which are used to pseudotype LV vectors are for example rabies glycoproteins, lymphocytic choriomeningitis virus glycoproteins and alphavirus glycoproteins (28).

LV vectors can be used for local gene delivery to the (adult) rodent brain (11, 29, 30, 31). In addition, LV vectors can be used to make transgenic animals, because they can integrate into the chromosome (32, 33).

Adeno-associated viral vectors

AAV is a non-pathogenic virus, which belongs to the family of *Parvoviridae*. AAVs are unique since they require co-infection with an unrelated helper virus, such as adenovirus or herpes virus, for efficient replication (34, 35). The viral genome is a single stranded DNA strand and it contains two open reading frames; *rep* (encoding 4 Rep proteins essential for replication, transcriptional control, site specific integration and accumulation for viral packaging) and *cap* (encoding 3 viral capsids proteins (VP)). The AAV genome is flanked by inverted terminal repeats (ITRs). The 3' ITR is a primer for synthesis of new DNA strands. In addition, the ITRs have a Rep binding site (Rep 78 and 68 can bind and exert site specific endonuclease activities) and a terminal resolution site (that is identical to a sequence in human chromosome 19, AAVS1) to facilitate integration of the viral genome (reviewed in (36)). AAV vectors remain predominantly episomal because, the *rep* and *cap* sequences are removed (reviewed in (37)).

The capsid, surrounding the AAV vector genome, mediates cell surface receptor binding, endocytosis, intracellular trafficking and unpackaging (38, 39, 40).

Capsid diversity is found in natural AAV variants (serotypes) and these serotype capsids account for different tropism, because different serotypes use different receptors and trafficking pathways to enter cells. Until now at least 12 serotypes are discovered (AAV1-AAV12) (41, 42, 43, 44, 45, 46, 47, 48, 49, 50) of these serotypes AAV2 is the most widely used. AAV2 uses heparan sulfate proteoglycans (HSPG) as attachment receptors and at least 3 receptors are reported to act as co-receptor, namely fibroblast growth factor receptor type 1, $\alpha V\beta 5$ integrin and hepatocyte growth factor receptor c-Met (51, 52, 53, 54). For the other serotypes the entry receptors are hardly identified. AAV3 binds to heparin while AAV1 and 5 do not (55), suggesting that AAV3 also uses HSPG as an attachment receptor. In addition, AAV1, 5 and 6 appear to use α -2,3- or α -2,6-N-linked sialic acid as receptors, while AAV4 uses α -2,3-O-linked sialic acid (56, 57). In addition, AAV5 has been shown to use platelet derived growth factor receptor (PDGFR) as a co-receptor (58). However, the attachment receptors and co-receptors for most serotypes are still unknown.

Tropism of rAAV vectors can be altered by pseudotyping the rAAV genome with one or a combination of serotype capsid proteins (mosaic capsids) (55, 59). However, more specific tropism can be obtained by ligand mediated receptor

targeting. There are two ways for receptor targeting; the indirect way, a bispecific adaptor molecule binds to the vector and to the receptor (60) and the direct way, a target-receptor binding ligand is integrated directly into the capsid (reviewed in (61)).

AAV vectors can be used for local gene transfer in (adult) rat brain and can establish long term expression (62, 63, 64, 65, 66).

2. Neurobiology of energy balance

The brain integrates a wide range of informative stimuli for nutritional state and for energy levels of the body, to produce appropriate responses in terms of food intake and energy expenditure to maintain a stable body weight (homeostatic control). However, in the western society, obesity is prevailing because there is plenty of palatable food available and there is less need to exercise. In the case of overconsumption, homeostatic control is overruled by non-homeostatic systems, which influence the hedonic aspects of feeding behavior, i.e. wanting and liking of food. The homeostatic and non-homeostatic systems are regulated by different brain areas. The hypothalamus and the hindbrain are involved in homeostatic control, while higher brain areas such as nucleus accumbens and amygdala are involved in non-homeostatic control (reviewed in (67))(Fig. 2).

Hypothalamic circuits

Already in the 1950's, brain lesions and stimulation studies identified the hypothalamus as a major brain area controlling energy homeostasis (68, 69). However, it has become evident that the hypothalamic regulation of energy balance involves a complex network of integrated pathways.

The arcuate nucleus (ARC) in the hypothalamus is highly sensitive to peripheral signals, such as adiposity signals leptin and insulin, because it is in close proximity to the blood stream (70). In addition, when the ARC is destroyed leptin can no longer reduce food intake (71, 72). The ARC contains two important groups of neurons which are involved in energy balance; one population synthesizes the anorexigenic neuropeptides pro-opiomelanocortin (POMC) and cocaine- and amphetamine-regulated transcript (CART) (73), while the other population produces the orexigenic neuropeptides Agouti-related peptide (AgRP) and neuropeptide Y (NPY) (74). POMC/CART neurons and AgRP/NPY neurons react in opposite manners to different signals, such as leptin or insulin. In addition, activation of AgRP/NPY neurons inhibits the activity of POMC neurons via GABA-ergic projections and/or melanocortin 3 receptor (MC3R, which may function as an autoreceptor)(75) (Fig. 3). Taken together these data suggest that the ARC is an important nucleus for integration of signals related to energy status, such as leptin and insulin, and it is involved in the initiation of a neuronal feeding response via

projections to other hypothalamic areas, but also extra-hypothalamic areas such as the hindbrain (reviewed in (76, 77)).

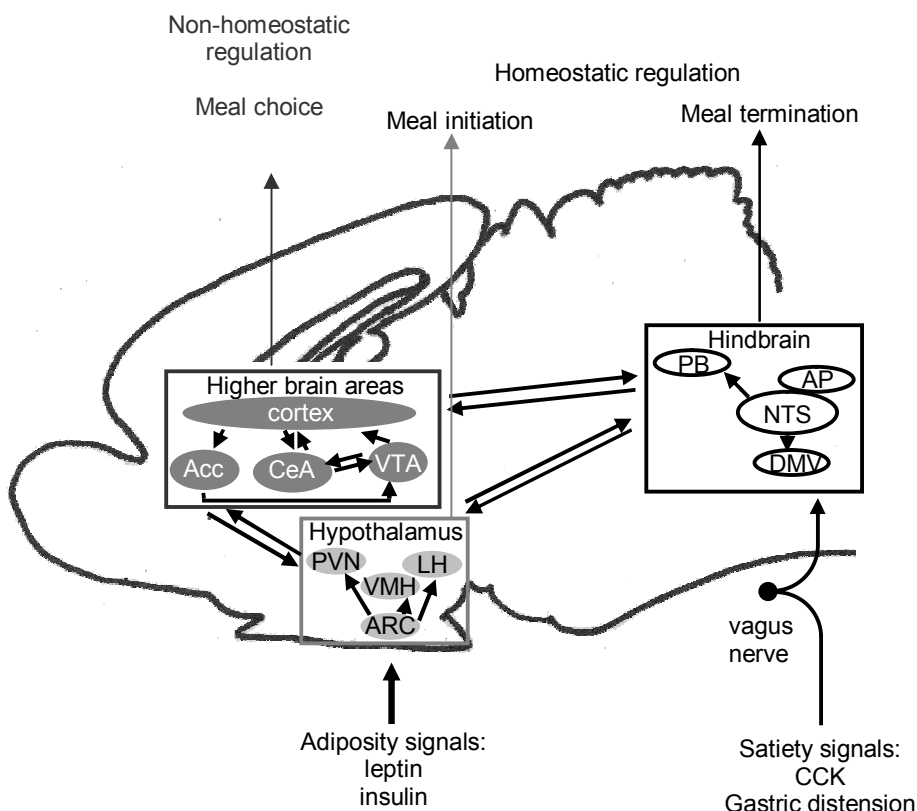


Figure 2 - Simplified overview of neural circuits involved in the energy homeostasis

Acc: nucleus accumbens; AP: area postrema; ARC: Arcuate nucleus; CeA: central amygdala; DMV: dorsomotor nucleus of the vagus; LH: lateral hypothalamus; NTS: nucleus of the solitary tract; PB: parabrachial nucleus; PVN: paraventricular nucleus; VMH: ventromedial hypothalamus. Modified from (78).

Neurons of the ARC project to several hypothalamic nuclei including the paraventricular nucleus (PVN), the lateral hypothalamus (LH) and the ventromedial hypothalamus (VMH) (79). The PVN, VMH and LH play different roles in feeding behavior. Lesioning of the PVN or the VMH increased food intake and resulted in obesity, while electrical stimulation of the PVN or the VMH inhibited food intake (80, 81). The PVN and VMH contain neuronal subsets of neurons which produce anorectic peptides (the subsets in the PVN contain peptides such as corticotropin-releasing factor (CRF), thyrotropin-releasing hormone (TRH) and oxytocin (OT), whereas glucoreponsive neurons of the VMH produce brain-derived neurotrophic factor (BDNF) (82, 83)). The PVN and VMH have projections to

many brain area's, such as the hindbrain, autonomic preganglionic nuclei, and higher brain areas (67, 84, 85, 86).

In contrast to PVN and VMH, lesioning of the LH decreased food intake, while electrical stimulation increased food intake (87, 88). There are two subsets of orexigenic neurons in the LH, namely melanin concentrating hormone (MCH) expressing and orexin expressing neurons (89, 90, 91, 92). The LH also directly innervates autonomic centers in the hindbrain (93).

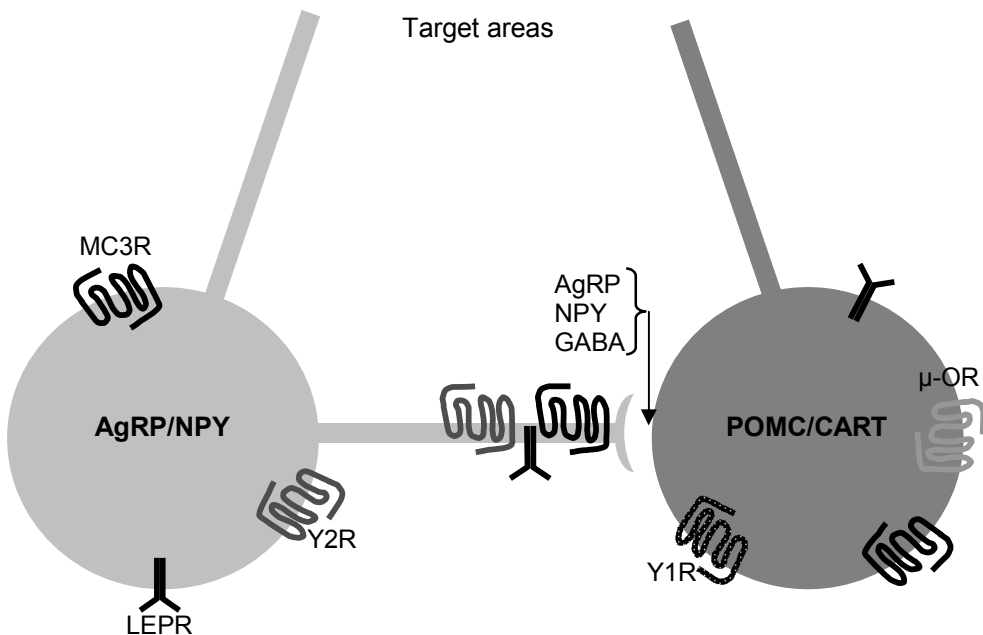


Figure 3 - Schematic overview of melanocortin system within the arcuate nucleus

Some receptors of the large number of neuropeptides and hormones which regulate the network are indicated. However, the localization of the receptors, presynaptic or postsynaptic, is often not known. LepR: leptin receptor; MC3R: melanocortin 3 receptor; μ -OR: μ opioid receptor; Y1R and Y2R: NPY receptor 1 and 2 respectively. Modified from (75).

Hindbrain circuits

Neurons in the hindbrain are involved in ingestive consummatory behaviors such as licking, swallowing and chewing, which generate and terminate food intake; thereby determining meal size. These neurons can be influenced by satiation signals, like sensory signals from gastric distension and release of intestinal hormones (e.g. cholecystokinin (CCK), glucagon like peptide-1 (GLP-1)), because these signals can activate receptors on vagal afferent neurons, which project to the hindbrain (Fig. 2). Rats with transected hypothalamic-caudal brainstem projections

(decerebrated) can decrease meal size when they receive a gastric preload; however, they can not alter the meal size when they are food deprived (94, 95). This suggests that meal size alterations due to gastric components are located in the caudal brainstem; whereas forebrain structures are involved in meal size regulation due systemic/metabolic changes in response to food deprivation. The integration of gastrointestinal (GI) satiation signals and metabolic signals such as leptin may be located in the medial NTS (mNTS). The mNTS contains a subset of neurons which respond to GI signals and to leptin (77). In addition, rats with knockdown of the long form leptin receptor (LEPRb) in the mNTS are less sensitive for intake suppressive effects of CCK and show an increase in food intake (96). Besides leptin, MCs are also able to modulate sensitivity of NTS neurons for GI signals (reviewed (77)).

Higher brain areas

The higher brain areas regulate non-homeostatic control of food intake and can overrule homeostatic control, i.e. you can eat a dessert because you like and want it, while you are already satiated by the main course. In addition, non-homeostatic control of food intake also plays a role in food preference, e.g. to eat food which is rich in carbohydrates and fat. Brain areas involved in this control include several regions of the cortex, nucleus accumbens (Acc), amygdala and ventral tegmental area (VTA). These areas are involved in the motivation to eat by interpreting sensory factors (e.g. smell, taste), emotional processes (e.g. stress can make you eat) and decision making processes (e.g. you want to diet) (97). The processes depend on multiple neurotransmitter systems, such as GABA, glutamate, opioids and dopamine. It is suggested that liking (the pleasure derived of a palatable food) involves opioid and GABA systems, while wanting (motivation component) is associated with the dopamine system (67). The higher brain areas are also connected to the hypothalamus and hindbrain (67, 97).

The hypothalamic circuit, hindbrain and higher cortical areas are all interconnected and may regulate distinct components of energy balance.

3. Leptin-melanocortin signaling

In the brain the MC signaling pathway is downstream of the leptin system, since leptin can activate transcription of POMC derived melanocortins and inhibits AgRP transcription in the ARC, thereby leptin increases MC signaling (75, 98, 99). In addition, leptin can also decrease transcription of NPY (100).

Leptin system

Leptin is a adipocyte-derived hormone which circulates in the blood at levels which are roughly proportional to body fat (101) and it has anorexigenic properties; leptin

decreases food intake and increases energy expenditure (reviewed by (102)). Spontaneous leptin deficiency (obese (*ob/ob*) mice), leptin receptor deficiency (diabetes (*db/db*) mice, Koletsky rat) or leptin receptor missense mutation (Zucker fatty rats) results in hyperphagia and obesity mice and rats (103, 104, 105, 106). Most obese humans and rodents appear to be resistant to leptin, since they have high leptin levels, but still over-consume calories (101, 107, 108, 109). Several mechanisms to mediate leptin resistance have been proposed like impaired leptin transport from the blood to the brain cerebrospinal fluid, impaired leptin receptor b (LEPRb) expression and impaired LEPRb signaling pathways (see review (102)). Under normal circumstances binding of leptin to the LEPRb induces tyrosine phosphorylation of this receptor and this activates multiple signaling pathways, such as JAK2-STAT3/STAT5 signaling, PI3K-Akt-FOXO1 pathway, SHP2-MAPK-ERK1/2 (Fig. 4).

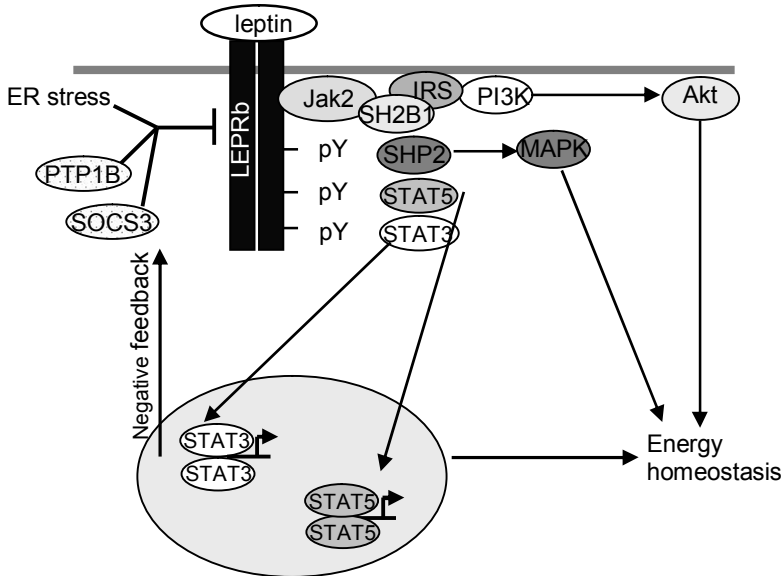


Figure 4 - Schematic, simplified overview of leptin signaling

Leptin binds to the long form of the leptin receptor (LEPRb) and activates JAK2. JAK2 phosphorylates LEPRb on tyrosine residues 985, 1077 and 1138. SH2 containing protein tyrosine phosphatase 2 (SHP2) binds to phosphorylated tyrosine 985 and activates MAPK pathway. STAT5 and STAT3 bind to phosphorylated tyrosine 1077 and 1138, respectively, and are phosphorylated by JAK2. STAT3 and STAT5 translocate to the nucleus and activate their target genes, which mediate leptin's anorexigenic effect. STAT3 also induces transcription of suppressor of cytokine signaling-3 (Socs3) which can bind phosphorylated tyrosine 985 and inhibits leptin signaling (negative feedback).

JAK2 autophosphorylates on tyrosine 813, which binds SH2B1. SH2B1 recruits insulin receptor substrate-1 and 2 (IRS-1 and IRS-2) to the LEPRb/JAK2 complex. Phosphorylation of the IRS proteins by JAK2 activates the phosphoinositide 3-kinase (PI3K) pathway. Therefore, SH2B1 is a positive regulator of the LEPRb signaling pathway. In contrast, Socs3, protein tyrosine phosphatase B (PTP1B) and endoplasmic reticulum stress are negative regulators of the LEPRb signaling pathway. Modified from (102)

Leptin signaling can be influenced by positive and negative regulators, such as SH2B1, a positive regulator, and PTP1B and Socs3, which are negative regulators. It is suggested that an increase in Socs3 contributes to the development of leptin resistance. Leptin binding to the receptor leads to STAT3 phosphorylation. Phosphorylated STAT3 induces the expression of Socs3, Socs3 in turn reduces the phosphorylation of JAK2 and the LEPRb, thereby reducing receptor sensitivity for leptin (110, 111, 112). Administration of leptin increases Socs3 mRNA and SOCS3 mRNA is elevated in hypothalami of obese animals (110, 113, 114, 115, 116, 117). In addition, Socs3 haplo-insufficient mice or mice with deletion of neuronal Socs3 are resistant to diet induced obesity (115, 118, 119, 120). These data suggest that Socs3 is a possible target to prevent leptin resistance and diet induced obesity.

Under normal circumstances, leptin decreases food intake. This decrease can be achieved by a decrease in the number of meals taken (frequency), which is a measure for hunger, or by a decrease in meal size, which is a measure for satiation. When humans and rodents are quickly satiated they will take smaller meals. However, when people and rodents feel hunger frequently, they will take more meals (121, 122). Intracerebroventricular (ICV) administration of leptin reduces meal size and has no effect on meal frequency (123, 124, 125). Leptin can exert its effects in many brain regions, because leptin receptors are found in several brain areas including ARC, PVN, VMH and LH (126, 127). The ARC is implicated as one of the important regions mediating the effects of leptin. Re-expression of LEPRb in the ARC of Koletsky rats decreases food intake and restores meal size back to normal (128). It is suggested that meal size is regulated via descending pathways from the hypothalamus to hindbrain and may involve melanocortin signaling, since leptin increases MC signaling. MC agonists and the inverse agonist AgRP can influence the sensitivity for satiety signals, such as CCK, in hindbrain neurons, directly by binding to MC4R in the hindbrain, or indirectly by binding to oxytocin neurons in the PVN, which send projections to the hindbrain (129, 130, 131, 132, 133, 134). This indicates that the leptin induced alterations in MC signaling may affect satiation and thereby meal size. However, leptin may also mediate the effects on satiation directly in the NTS via LEPRb (77).

Melanocortin signaling

Melanocortins (MCs) are peptides derived from POMC via splicing by prohormone convertases. POMC is processed into adrenocorticotrophic hormone (ACTH), α -, β - and γ -melanocyte stimulating hormone (MSH) and the opiod peptide β -endorphin. The POMC neurons project to many areas in the brain, including the PVN, LH, brainstem and amygdala (135, 136, 137, 138). POMC neurons also project directly to preganglionic neurons in the spinal cord, suggesting a direct influence on the

regulation of energy expenditure via modulation of the sympathetic system (139, 140). Melanocortins exert their effects via one of the five melanocortin receptors (MC1R-MC5R). The MC receptors are G-protein coupled receptors and differ in function, expression pattern and binding affinities for their ligands (141) (Table 2 (modified from(142), data from (143, 144, 145, 146, 147, 148, 149, 150, 151, 152, 153, 154, 155)).

Table 2 - Some characteristics of MC

Receptor	Main distribution	Main functions	Agonists (order of affinity)	Inverse agonists
MC1R	Melanocytes, keratinocytes, macrophages, monocytes, neutrophils, fibroblasts, astrocytes, pituitary, Leydig cells, corpus luteum, neurons of periaqueductal gray	Pigmentation, anti-inflammatory	α -MSH= β -MSH = ACTH > γ -MSH	Agouti
MC2R	Adrenal cortex, murine adipocytes	Glucocorticoid production, stress induced lipolysis	ACTH	Agouti
MC3R	Hypothalamus, brainstem, limbic system, heart, gut, thymus, placenta	Energy homeostasis, sexual arousal, inflammation	γ -MSH= α -MSH = β -MSH = ACTH	AgRP
MC4R	Brain (almost all areas), adipose tissue, sensory peripheral neurons	Body weight regulation, grooming, anti-inflammatory	α -MSH= β -MSH = ACTH $\geq \gamma$ -MSH	AgRP
MC5R	Peripheral tissue (including adrenal glands, adipose tissue), brain (cortex, cerebellum, striatum)	Production sebum, lipogenesis	α -MSH= β -MSH = ACTH > γ -MSH	Agouti

The MC3R and MC4R are implicated in energy balance and are predominantly expressed in the brain (156, 157, 158), but the MC4R is expressed more widely in the CNS than the MC3R (139, 146, 147, 159).

The melanocortin system is regulated by two endogenous antagonists, namely agouti and AgRP. Agouti is normally not expressed in the CNS, but it regulates skin pigmentation by antagonizing MC1 receptor (160, 161). AgRP is expressed in the brain, only in a subpopulation of ARC neurons, and functions as an inverse agonist on constitutively active MC3R and MC4R (145, 162, 163).

Knockout of POMC or overexpression of AgRP results in obesity due to hyperphagia and a decrease in energy expenditure (145, 163, 164, 165). In contrast, overexpression of POMC or knockout of AgRP has no effects on energy balance in normal situations (1, 166, 167, 168). However, in obese rodents POMC overexpression (transiently) decreases food intake and body weight (167, 169). In addition, aged AgRP^{-/-} mice show a decrease in body weight and adiposity, due to increased metabolism (170). Thus, under normal circumstances inhibition of the MC3R and MC4R signaling results in more obvious effects than stimulation of these signaling pathways.

AgRP and POMC derived MCs mediate their effects by binding to the MC3R and MC4R. Deletion of MC3R only modestly affects feeding behavior, but these animals are more efficient in storing energy, i.e. they need fewer calories to gain a gram of body weight, therefore these animals are only fatter, but not heavier than controls (157, 158). However, MC4R^{-/-} mice show hyperphagia and a decrease in energy expenditure (156, 171, 172). In addition, MC4R^{-/-} mice are not sensitive for intake suppressive effects of MTII and this underscores the role of MC4R in food intake (172, 173). Nevertheless, other receptors also are implicated in regulation of food intake since administration of AgRP to MC4R^{-/-} still induces a small increase in food intake (174, 175). In addition, the MC4R^{-/-} mice are obese before the onset of hyperphagia, suggesting that a decrease in energy expenditure contributes to the MC4R^{-/-} phenotype (171). The food intake and energy expenditure effects of the MC4R may be located in different brain areas; since re-expression of MC4R in the PVN and amygdala corrected the hyperphagia, but only partially reduced obesity (176).

The effects of MC3R and MC4R on energy balance are additive since mice which lack both the MC3R and the MC4R are more obese than mice lacking the MC4R only (157).

ICV administration of non-selective MC agonists, α -MSH, β -MSH and ACTH(1-24), or inverse agonist AgRP and antagonist, SHU9119 all have a significant effect on food intake, while the MC3R specific agonist, γ -MSH, only has a modest effect on food intake (2, 146, 177, 178, 179, 180, 181, 182). This supports the idea that

predominantly the MC4R is involved in feeding response and not the MC3R. In addition, MC agonist and inverse agonist have effects on energy expenditure (145, 172, 183, 184, 185, 186). However, MC agonist and inverse agonist differ in their effects over time. Chronic application of MC agonists only decreases food intake for the first days, while chronic application of AgRP increases food intake during the entire experiment (183, 187, 188, 189).

Knockout studies and ICV administration studies have shown that the MC system contributes to food intake and energy expenditure. Local interference of MC receptor signaling is required to unravel which neural substrates are underlying the different behaviors, such as food intake and energy balance. Until now only a few studies have infused MC receptor ligands in local brain areas to investigate the role of these areas in energy balance. Multiple studies have focused on the PVN and investigated the acute effects. Local injections with MC ligands stimulating or inhibiting MC receptors in the PVN, indicate that MC receptors in the PVN are involved in meal duration rather than initiation ((182, 190, 191, 192) and reviewed in (78)). In addition, injections of MTII in the PVN increase body temperature and spontaneous locomotor activity (193). This suggests that MC signaling in the PVN contributes to food intake and energy expenditure. In addition, the DMH and MPO are also indicated as primary sites in the hypothalamus to mediate effects on energy balance (194). However, it is poorly understood via which neuronal substrates, that express MC receptors, the different effects of MC are mediated.

4. Aims and outline of the thesis

The neural circuits involved in energy homeostasis are complex and involves multiple brain regions and neuropeptides. The many functions of the different neuropeptide systems in the hypothalamus have been described; however, the specific roles of the different neuropeptides in specific hypothalamic areas are not fully understood. The overall aim of this thesis was to modify the leptin and MC system with viral vectors in order to further determine the role of leptin and MC signaling in food intake and energy expenditure.

In order to achieve this goal, the first experiments assessed the ability of AAV and LV vectors to transduce the hypothalamus and subsequently optimize the transduction of the hypothalamus by AAV vectors. These experiments are described in **chapter 2 and 3**.

The most optimal method to transduce a nucleus in the hypothalamus was used to investigate the role of long term suppression of MC receptor activity in different brain areas, namely PVN, VMH, LH and Acc. Long term suppression of the MC receptors was achieved by AAV-mediated overexpression of AgRP in the different brain areas. This approach was taken, because continuous long term infusion in a specific brain nucleus is not feasible. The results of this study are described in **chapter 4**.

One disadvantage of neuropeptide overexpression with AAV vectors is that AAV vectors may transduce projection neurons and this causes the product of the expressed transgene to be released at distant projection sites and not in the targeted area. The interpretation of the data may be complicated when a transgene product is released at distant sites and not at the site of injection; therefore a novel method was developed and tested, to establish local release of a neuropeptide at the cell body instead of release at axon terminals. These results are described in **chapter 5**.

Leptin influences MC and NPY signaling. In addition, leptin upregulates Socs3 mRNA and this increase may contribute to leptin resistance which is observed in diet-induced obesity. In **chapter 6** an AAV vector with a shRNA against Socs3 was injected in the mediobasal hypothalamus to determine if Socs3 knockdown in the mediobasal hypothalamus prevented the development of diet-induced obesity in these rats.

Finally, in **chapter 7** the main findings of these studies are summarized and discussed.

Chapter 2

An adeno-associated viral vector transduces the rat hypothalamus and amygdala more efficient than a lentiviral vector

Marijke W.A. de Backer¹, Carlos P. Fitzisimons², Maïke A.D. Brans¹, Mienieke C.M. Luijendijk¹, Keith Garner¹, Erno Vreugdenhil², Roger A.H. Adan¹

¹ Rudolf Magnus Institute of Neuroscience, Department of Neuroscience and Pharmacology, University Medical Centre Utrecht, Utrecht, the Netherlands.

² Medical Pharmacology Department, Leiden/Amsterdam Center for Drug Research, Leiden University Medical Center, Leiden University, the Netherlands.

AN ADENO-ASSOCIATED VIRAL VECTOR TRANSDUCES THE RAT HYPOTHALAMUS AND AMYGDALA MORE EFFICIENT THAN A LENTIVIRAL VECTOR

Abstract

We compared the transduction efficiencies of an adeno-associated viral (AAV) vector, encoding the green fluorescent protein (GFP), with a lentiviral (LV) vector, encoding the discosoma red fluorescent protein (dsRed). The LV and AAV vector were mixed and injected into the lateral hypothalamus or into the amygdala of adult rats. Immunostaining for GFP and dsRed showed that AAV-GFP transduced significantly more cells than LV-dsRed in both areas. LV-dsRed transduced few cells in the lateral hypothalamus and amygdala. AAV-GFP was more efficient in transduction of the lateral hypothalamus and amygdala. In addition, the number of LV particles that were injected can not easily be increased, while the number of AAV particles can be increased easily with a factor 100 to 1000.

In this study we showed that AAV vectors are better tools to overexpress or knockdown genes in the lateral hypothalamus and amygdala of adult rats, since more cells can be transduced with AAV than with LV vectors and the titer of AAV can easily be increased.

Introduction

Viral vectors are used as tools to introduce genes or shRNAs into the brain in order to unravel the role of genes. The advantages of viral vectors are that they can be injected locally and establish long term expression of the gene or the shRNA.

Several viral vectors have been tested *in vivo* in the central nervous system: adeno-associated viral (AAV), lentiviral (LV), adenoviral (AdV) and herpes simplex viral (HSV) vectors (195, 196, 197, 198). To date, studies in the rodent hypothalamus and amygdala have mainly used AAV or AdV and to a lesser extent LV vectors (199, 200, 201, 202, 203, 204). It is important to know which viral vector, AAV or LV, is most efficient in transducing brain areas involved in energy homeostasis, because then it is possible to efficiently alter gene expression in specific brain nuclei to further investigate the function of genes involved in feeding behavior. The lateral hypothalamus (LH) and amygdala (AM) are important brain areas involved in energy homeostasis (205).

In this study we compared the transduction efficiencies of a LV and an AAV vector in the LH and AM of the rat brain. The LV and AAV vector both used the CMV promoter to drive the expression of a fluorescent marker, dsRed or GFP respectively.

Materials and methods

Cell lines and constructs

Human embryonic kidney (HEK) 293T cells were maintained at 37°C with 5% CO₂ in Dulbecco's modified Eagles medium (DMEM) supplemented with 10% fetal calf serum (FCS), 2mM glutamine, 100 units/ml penicillin, 100 units/ml streptomycin and non-essential amino acids.

pAAV-CMV-GFP was constructed by removing the CMV promoter with a part of the GFP gene from pTRCGW (206) through digestion with KpnI and BsrGI. Subsequently this fragment was ligated into a KpnI-BsrGI digested backbone of pAAV-CBA-GFP (kind gift from M. Sena-esteves (207)). This digestion removed the CBA promoter and a part of the GFP gene.

The construction of LV-CMV-dsRED was previously described (208).

To check the specificity and intensity of staining of the GFP and dsRed antibodies, 2.5 µg of pPRIME-CMV-GFP and pPRIME-CMV-dsRed (209) was transfected, alone or together, on 10cm dishes with polyethylenimine (PEI). The morning after transfection the cells were trypsinized and seeded in 24 wells plates containing poly-L-lysine coated glass cover slips. Seventy-two hours after transfection cells were washed with phosphate buffered saline (PBS), fixated for 20 minutes with 4% paraformaldehyde (PFA) and stored in PBS at 4°C until immunohistochemistry was performed.

Virus production and purification

AAV production was performed with 15x15 cm dishes containing 293T cells at 80-90% confluency on the day of transfection. Two hours before transfection, the 10% FCS-DMEM was replaced with 2% FCS-DMEM. The transfections were performed with polyethylenimine (PEI) as described by Reed S.E. et al. (210). pAAV-CMV-GFP was co-transfected with the helper plasmid pDP1 (211) (Plasmid factory, Bielefeld, Germany) in a molar ratio of 1:1. The transfection mix remained on the cells until the next day, then the 2% FCS-DMEM was refreshed. The AAV production and purification was essentially performed as described by Zolotukhin et al. (212). Briefly, sixty hours after transfection, the cells were harvested in their medium, centrifuged and washed with PBS containing 5mM ethylenediaminetetraacetic acid (EDTA). Finally, the cells were collected in 12 ml ice cold buffer (150 mM sodium chloride (NaCl), 50 mM 2-amino-(hydroxymethyl)-1,3-propanediol (Tris), pH 8.4) and stored at -20°C until further use. Usually after three days the cells were freeze-thawed twice, incubated for 30 minutes with Benzonase (end concentration 50 units/ml, Sigma, The Netherlands) at 37°C and centrifuged. After centrifugation, the supernatant was loaded onto an iodixanol gradient (60%, 40%, 25%, 15%, supernatant (Optiprep, Lucron bioproducts, Belgium)) in Quickseal tubes (Beckman Coulter, The Netherlands). After 1 hour of ultracentrifugation (70.000 rpm at 20°C) in Ti70 rotor (Beckman Coulter, The Netherlands), the 40% layer was extracted. This 40% layer was used for ion-exchange chromatography with 5ml Hitrap Q HP columns (GE Healthcare, The Netherlands). Subsequently PCR was used to determine AAV positive fractions, these were pooled and desalted/concentrated on Centricon Plus-20 Biomax-100 concentrator columns (Millipore, The Netherlands). The titer, in genomic copies per ml (g.c./ ml), was determined by qPCR with sybergreen mix in a LightCycler (Roche) (213). The qPCR primers were designed to detect BGHpolyA and were BGHpolyA_F: 5' CCTCGACTGTGCCTTCTAG; BGHpolyA_R: 5' CCCAGAAATAGAATGACACCTA. The titer obtained for AAV-CMV-GFP was 6.6×10^{13} genomic copies (g.c.)/ml. In addition we also performed a serial dilution with AAV-CMV-GFP virus on HT1080 cells, to obtain an indication of the transducing units in this AAV preparation. Seventy-two hours after infection GFP positive cells were counted and a titer was calculated. This serial dilution showed that a titer of 5×10^8 transducing units (t.u.)/ml of AAV-CMV-GFP was achieved. Lentivirus with a CMV promoter driving dsRED expression (LV-CMV-dsRED) was produced as described previously (208). In short, 293T cells were transfected using the ViraPower Lentiviral Expression System (Invitrogen, Breda, The Netherlands) according to manufacturer's instructions. Forty-eight hours after transfection virus containing supernatant was harvested, centrifuged at 2.000 rpm for 3 minutes to remove cell debris and concentrated by two rounds of ultracentrifugation (19.400 rpm, 4 °C, 2hours each), resuspended in PBS,

aliquoted and stored at -80 °C until use. Virion titers were measured by real-time PCR and biological titers calculated from those and verified by dsRED expression (214). The titer of LV-CMV-dsRED was 3.9×10^8 t.u./ml.

Animals

Male Wistar rats of 220–250 g, were purchased from Charles River (CrI-Wu, Germany). All rats were individually housed in filtertop cages with *ad libitum* access to food (CRM pellets; Special Diet Services, Whitham, Essex, UK) and water. Animals were kept in a temperature- and humidity-controlled room ($21 \pm 2^\circ\text{C}$) with a 12 h light/dark cycle (lights on at 7:00 A.M.). All experimental procedures were approved by the Committee for Animal Experimentation of the University of Utrecht (Utrecht, The Netherlands).

Just before stereotactic injections AAV-CMV-GFP was diluted in PBS to 2×10^8 g.c./ μl or 2×10^9 g.c./ μl and LV-CMV-dsRed was diluted to 2×10^8 tu/ μl . The diluted AAV and LV vectors were mixed 1:1 and 1 μl of this mixture was injected in the LH or in the AM of rats. The injections were performed with a micro-infusion pump. The injection speed was 0.2 μl /minute. After the injection the needle remained in the injection site for 10 minutes.

Twelve rats were anesthetized with 0.1 ml/100 g Hypnorm intramuscular (Janssen Pharmaceutica, Beerse, Belgium) and 0.05 ml/100 g Dormicum intraperitoneal (Hoffman-LaRoche, Woerden, the Netherlands). Rimadyl (Pfizer animal health, Capelle a/d IJssel, the Netherlands) was administrated as pain medication before surgery and on day 1 and 2 after surgery. Four rats were injected bilaterally in the LH (coordinates AP-2.56, ML+2.00, DV-8.60) with 1 μl of AAV-LV mixture containing 1×10^8 gc of AAV-CMV-GFP and 1×10^8 tu of LV-CMV-dsRed. Another four rats also received 1 μl AAV-LV mixture in the LH. Here LV-CMV-dsRed remained 1×10^8 tu, however, the titer of AAV-CMV-GFP was raised 10 times to 1×10^9 gc. In addition, four rats received injections in the central AM (coordinates AP-2.10, ML+4.00, DV -8.00) with a mixture of 1×10^8 gc of AAV-CMV-GFP and 1×10^8 tu of LV-CMV-dsRed. Four weeks after the injections the rats were anesthetized and perfused with 4% PFA containing 0.05% glutaraldehyde. Subsequently, the brains were isolated and placed in 4%PFA overnight at 4°C . The next morning the brains were placed in PBS and stored at 4°C until further use. The perfused brains were sectioned on a vibratom (Leica) at 40 μm in series of 10. Thus every tenth section was used for immunohistochemistry.

Immunohistochemistry

Every tenth 40 μm section was used for GFP-dsRed co-immunostaining. The free floating sections were washed 3 times with PBS, permeabilized for 30 minutes in PBS supplemented with 0.5% triton X-100 at room temperature (RT), blocked for 1 hour in PBS with 1.5% normal goat serum (NGS) at RT and incubated overnight in

PBS supplemented with mouse monoclonal anti-dsRed (1:400, Clontech), rabbit polyclonal anti-GFP (1:1000, Invitrogen) and 1.5% NGS at 4°C. The next morning sections were washed 3 times for 10 minutes with PBS and incubated for 1 hour with secondary antibodies (ALEXA 555 conjugated goat anti mouse (1:500) and ALEXA 488 conjugated goat anti rabbit (1:1000) both Invitrogen) in 1.5% NGS at RT. After 3 times 10 minutes wash with PBS, the sections were transferred to microscope slides and kept over night in the dark to dry. All sections were embedded in 90% glycerol and stored flat at 4°C.

Imaging and data analysis

The number of positive cells for GFP and dsRed were counted in every section, except the positive cells in the injection tract which are probably macrophages. The MCID system was used to digitize pictures from sections containing endogenous or immunohistochemistry signals.

GraphPad Prism was used for data analysis and treatment effects were evaluated with two-tailed *t*-test.

Results

In vitro testing of antibodies

To confirm that the GFP and dsRed antibodies were able to detect the respective proteins with similar efficiencies, 293T cells were transfected with constructs encoding CMV-GFP and CMV-dsRed individually and together (Fig. 1 A, B). Since the promoter driving the expression of the fluorescent proteins was the same, we expected similar levels of fluorescent protein expression. The endogenous fluorescence of GFP and dsRed was compared with the immunostained fluorescence. The cells transfected with only one construct showed co-localization of endogenous fluorescence and immunostained fluorescence (Fig. 1C). In addition, cells co-transfected with CMV-GFP and CMV-dsRed showed co-localization of both immunohistochemistry signals (Fig. 1D). The pictures showed that red fluorescent signals, endogenous or immunostained, were at least threefold stronger in intensity than green fluorescent signals.

AAV-GFP and LV-dsRed transduction in vitro

AAV-GFP was pseudotyped with an AAV1 coat, which was previously shown to be more effective in transduction of hypothalamic areas, such as the LH, than AAV2 coated vectors (215). It is still unknown which entry receptors AAV1 uses to enter cells and it is therefore unknown which cell line is optimal for determining transducing units. Nevertheless we performed a serial dilution with AAV-GFP on HT1080 cells to obtain an indication of transducing units. These results showed that the titer of AAV-GFP was 5×10^8 t.u./ml, which is substantially lower than the 6.6×10^{13} g.c./ml. The LV-dsRed had a titer of 3.9×10^8 t.u./ml.

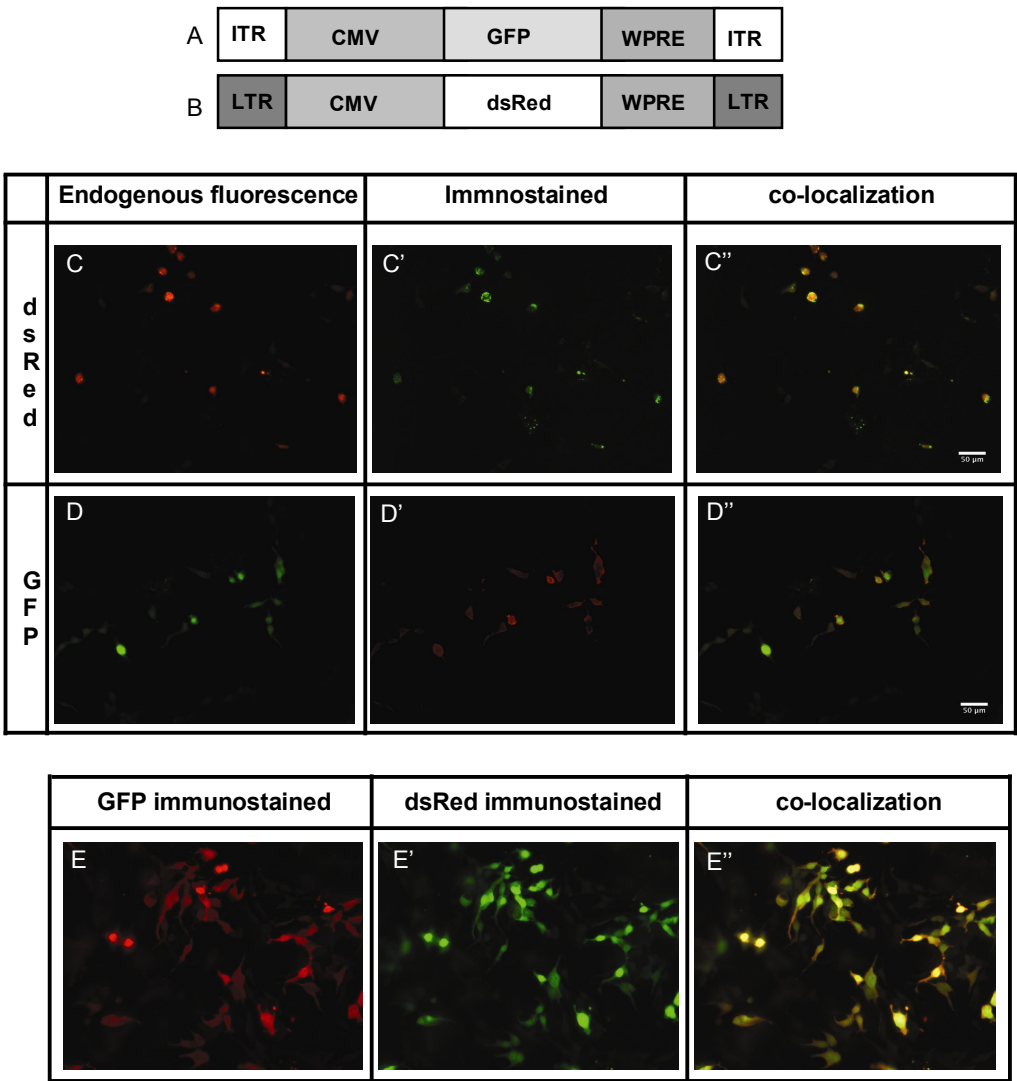


Figure 1 - *In vitro* testing of the antibodies against GFP and dsred
A a schematic overview of AAV vector used. B a schematic overview of LV vector used. C shows endogenous dsRed fluorescence (red) of 293T cells transfected with CMV-dsRed. C' panel shows immunostaining for dsRed (green) of these cells. C'' shows co-localization of the immunostained and endogenous fluorescence (yellow). D shows endogenous GFP fluorescence (green) of 293T cells transfected with CMV-GFP. D' immunostaining for GFP (red) and D'' shows the overlay of D and D' (green nucleus with red cytoplasm). E 293T cells co-transfected with CMV-GFP and CMV-dsred were immunostained for GFP (red (E)) and dsRed (green (E')). These stainings overlap (yellow (E'')). The scalebar is 50µm.

Before mixing the two viruses, the preparations were diluted. AAV was diluted to 2×10^8 and 2×10^9 g.c./µl, thus 1.5×10^3 and 1.5×10^4 t.u./µl on HT1080 respectively. LV-dsRed was diluted to 2×10^5 t.u./µl. Subsequently the diluted viruses were mixed

1:1 and 1 μ l of this mix was injected in each brain area. This resulted in 1×10^8 or 1×10^9 g.c. (7.5×10^2 or 7.5×10^3 t.u.) of AAV-GFP and 1×10^5 t.u. of LV-dsRed per site.

Transduction of the LH by AAV-GFP and LV-dsRed

To determine the transduction efficiencies of AAV and LV in the LH, animals were perfused four weeks after injection with viral vectors. Immunostaining for GFP and dsRed showed positive staining in the injection tract. These were probably apoptotic cells and were not included in our quantification (Fig. 2, upper panel). Counting of GFP and dsRed immunostained positive cells revealed that AAV-GFP, at 1×10^8 g.c., transduced significantly more cells in the LH compared with LV-GFP, at 1×10^5 t.u. (Fig. 3).

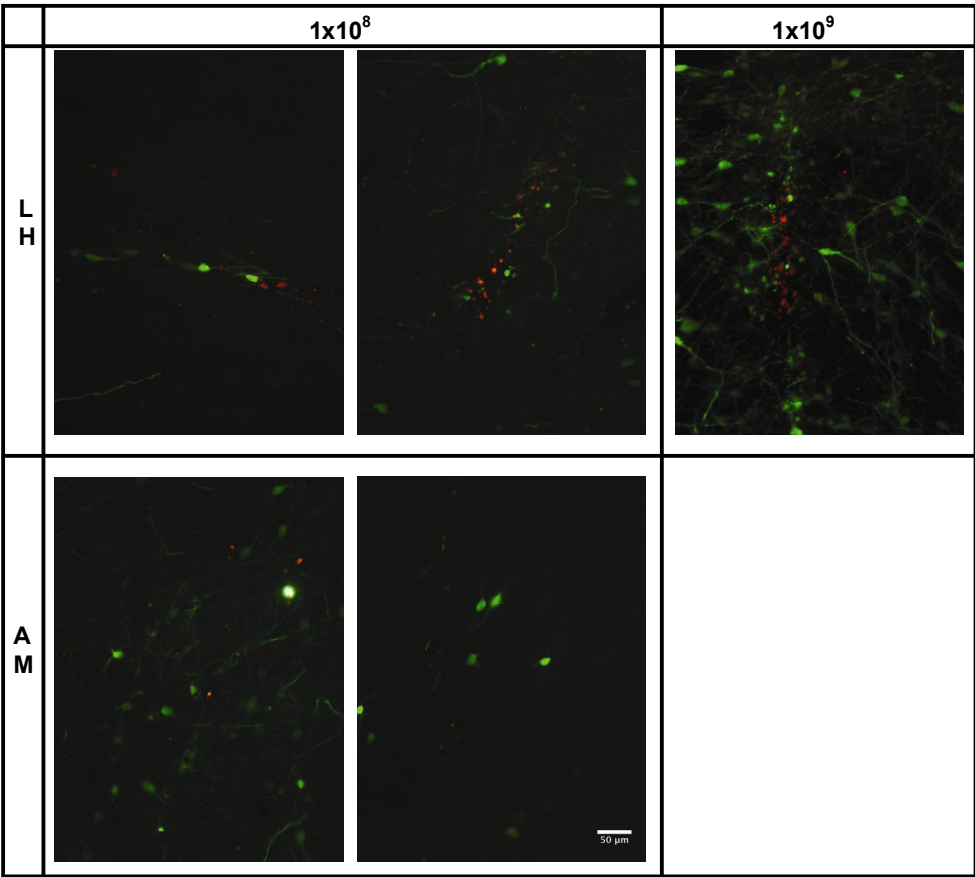


Figure 2 - *In vivo* transduction of the LH and AM by AAV-CMV-GFP and LV-CMV-dsRed

The titer of LV-CMV-dsRed was kept constant at 1×10^5 t.u., while the titer of AAV-CMV-GFP was 1×10^8 or 1×10^9 g.c.. Immunostaining for GFP is shown in green and for dsRed in red. Scalebar is 50 μ m.

As expected, an increase in titer of AAV-GFP, from 1×10^8 to 1×10^9 g.c., resulted in 14.2 fold increase in the area transduced at the injection site. The area increased from $3338 (\pm 599) \mu\text{m}^2$ to $47525 (\pm 10822) \mu\text{m}^2$ ($p=0.0005$).

Transduction of the AM by AAV-GFP and LV-dsRed

In addition, we studied the transduction efficiencies of AAV-GFP and LV-dsRed in the AM. Similar to the LH, AAV-GFP transduced significantly more cells than LV-dsRed in the AM (Fig. 2 lower panel and Fig. 3). The number of cells transduced by AAV or LV in the AM was comparable to the number of cells in the LH.

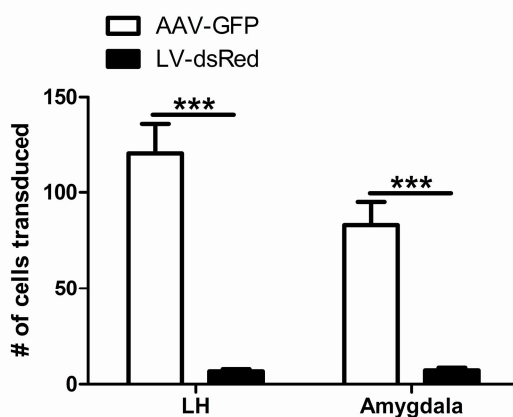


Figure 3 - Quantification of the number of cells transduced

Number of cells transduced by 1×10^8 g.c. of AAV-CMV-GFP and 1×10^5 t.u. of LV-CMV-dsRed. *** $p < 0.0001$

Discussion

This study showed that an AAV vector transduced significantly more cells in the LH and AM of adult rats than a LV vector. This is in agreement with previous studies in the rat that reported low levels of transgene expression after injection of $1 \mu\text{l}$ of LV vectors in other rat brain nuclei, namely the red nucleus (66) and the retina (216). However, several studies reported substantial levels of transduction by LV in the rat striatum and hippocampus. However, these groups injected larger volumes of LV, namely 2 or $3 \mu\text{l}$ (30, 31, 217). In contrast, LV vectors have been reported to efficiently transduce cells in the mouse hippocampus and striatum (29, 218). In addition, AAV and LV vectors were reported to transduce approximately the same numbers of cells after injection in the hippocampus or hippocampal slices (219, 220). This indicates that there may be species differences and/or brain area differences which account for the differences in transduction efficiencies by LV and AAV vectors in rat and mouse brain.

The titer of our AAV-GFP preparation was 6.6×10^{13} g.c./ml, this is a titer in the range that we usually obtain with AAV production. The number of transducing units/ml will be lower than genomic copies/ml since not all vector DNA is properly packaged into infectious particles. The optimal cell line for determining the t.u./ml of AAV1 preparations is unknown. In order to have some indication of the t.u. we assessed the t.u./ml of AAV-GFP on HT1080 cell line. The titer of AAV-GFP was 5×10^8 t.u./ml, and this preparation was diluted 330 times, to 1.3×10^3 t.u./ μ l before mixing with LV-dsRed. The LV-dsRed was only diluted 2 times until 2×10^5 t.u./ μ l. Since the number of t.u. of AAV-GFP injected was much lower than the t.u. of LV-dsRED, we concluded that AAV is more efficient in transduction of the LH and AM than LV.

We only observed 6-7 cells positive for dsRed after injection of 1×10^5 t.u. of LV. Thus, ideally the titer of LV-dsRed should be increased to transduce more cells in the LH and AM. The methods we used for LV preparation and titer determination are standard procedures in the field. Normally, titers of concentrated LV vectors are reported to be in the range of 5×10^7 to 1×10^9 t.u./ml (30, 218, 221). Thus compared with results from others, 3.9×10^8 t.u./ml is in the normal titer range. Therefore, it is technically difficult to increase the LV titer to transduce more neurons in the AM and LH of rats.

The differences in transduction by AAV-GFP and LV-dsRed in the LH and AM may be explained by the fact that the vectors probably used different receptors to enter cells. The LV-dsRed used in this study was pseudotyped with the G protein of the vesicular stomatitis virus (VSV-G). VSV-G transduces many cell types from different species, but it is still unknown how VSV-G enters these cells. For a long time it was thought that phosphatidylserine (PS) was the receptor to mediate membrane fusion (25). However, more recent data indicated that PS is not the entry receptor (26). AAV-GFP was pseudotyped with AAV1 capsid proteins. The entry receptor for AAV1 also is unknown, but there are indications that α -2,3 and α -2,6 N-linked sialic acids facilitate transduction by AAV1 vectors (222).

We have chosen the 4 week time point to compare transduction by AAV and LV vectors, since on this time point LV and AAV transduce predominantly neurons. AAV1 was previously reported to transduce predominantly neurons in different rat brain regions at all investigated time points after injection (62, 64). However, the transduction pattern of LV with a CMV promoter seems to shift from glial and neuronal cells at 1 week post injection to predominantly neuronal cells at 3 weeks post injection. This shift in transduction pattern with CMV promoter was reported to be accompanied by a small decrease in transgene expression, probably because the glia cells returned to resting state in which CMV driven expression is low (30).

In conclusion, when a substantial part or the entire LH or amygdala of rats needs to be transduced AAV vectors are preferred over LV vectors, since more cells can be transduced with AAV than with LV vectors and the titer of AAV can easily be increased.

Acknowledgements

This work was supported by the Netherlands Organization for scientific research (NWO grant No. 90339175).

Chapter 3

Optimization of adeno-associated viral vector mediated gene delivery to the hypothalamus

Marijke W.A. de Backer, Maïke A.D. Brans, Mienieke C.M.
Luijendijk, Keith M. Garner,
Roger A.H. Adan

Human Gene Therapy, (Epub 14 Jan), 2010

OPTIMIZATION OF ADENO-ASSOCIATED VIRAL VECTOR MEDIATED GENE DELIVERY TO THE HYPOTHALAMUS

Abstract

In order to efficiently deliver genes and shRNA's to the hypothalamus we aimed to optimize the transduction efficiency of adeno-associated virus (AAV) in the rat hypothalamus. We compared the transduction efficiencies of AAV2 vectors pseudotyped with AAV1, 8 and mosaic 1/2 and 2/8 coats with an AAV2 coated vector after injection in the lateral hypothalamus of adult rats. In addition, we determined the transduction areas and the percentage of neurons infected after injection of different titers and volumes of two AAV1 pseudotyped vectors in the paraventricular hypothalamus (PVN). Successful gene delivery to the hypothalamus was achieved by using AAV1 pseudotyped AAV vectors. The optimal approach to transduce an area, with the size of the PVN, was to inject 1×10^9 genomic copies of an AAV1 pseudotyped vector in a volume of $1 \mu\text{l}$. At a radius of 0.05 mm from the injection site almost all neurons were transduced. In addition, overexpression of AgRP with the optimal approach resulted in an increase in food intake and bodyweight when compared to AAV-GFP.

Introduction

Dysregulation of energy balance involves genetic, environmental and cognitive factors and may result in obesity or eating disorders (122). These disorders are associated with substantial morbidity, mortality and socioeconomic burden.

Although genes expressed in the hypothalamus have repeatedly been shown to contribute to obesity (223, 224, 225, 226), gene therapy thus far has hardly been considered as therapeutic strategy (227). Animal studies with spontaneous gene mutations, which resulted in obesity and/ or diabetes, have greatly contributed to our knowledge which role certain genes play in energy balance (226). The importance of genes for regulation of energy balance was confirmed by knockout mice, although these mice may display the capacity to compensate for the lack of that gene during development rather than demonstrating the function of a certain gene in adult stage. One of the neuropeptides involved in feeding is Agouti-related protein (AgRP) (163). AgRP is a peptide that is produced in the arcuate nucleus of the hypothalamus and is secreted in many brain regions, including multiple hypothalamic nuclei such as paraventricular nucleus (PVN) and the lateral hypothalamic nucleus (LH) (137, 228). In the projection areas, AgRP can bind the melanocortin receptors and reduce their activity. Reduction of melanocortin signaling is suggested to induce hyperphagia and lower energy expenditure, resulting in obesity in rodents and humans (reviewed in (225, 229)).

In view of the development of gene therapy to modify gene expression in the hypothalamus, it is important to determine the local effect of genes in the hypothalamus. We have chosen to use AAV vectors for local overexpression and knockdown of genes in the brain, because AAV vectors can transduce non-dividing neurons and the gene cassettes are expressed for long periods of time, up to 25 months in rats (230). AAV vectors have been reported to transduce specific cell types *in vitro* and *in vivo* by using cell type-specific promoters and/or by packaging the AAV DNA in different serotype capsids or in capsids that have been genetically or chemically altered (231, 232, 233, 234, 235). AAV2 serotype AAV vectors were the first to be used for gene transfer (236). Since the 1980s many other serotypes have been identified and investigated for their cell tropism (231, 235). Until now, the most widely used AAV serotype to modify gene expression in the hypothalamus has been AAV2 (201, 237, 238). However, recent studies have shown that serotypes other than AAV2 were more efficient in transducing rat primary cortical and hippocampal cultures (232, 239). In addition, AAV1 and AAV8 coated vectors have been shown to transduce more neurons *in vivo*, for example in the rat striatum (62, 64), hippocampus (62, 63, 240) and midbrain (62, 65).

Therefore, in this study, we aimed to characterize how different capsids affect AAV-mediated transduction of selected areas in the hypothalamus. We packaged an AAV-CBA-GFP-WPRE vector, containing AAV2 ITRs, with single AAV1 and AAV8 capsids or with mosaic capsids AAV1/2 and 2/8. This was done to compare

the transduction efficiencies of AAV1 and AAV8, which most often show higher transduction efficiencies than AAV2, with the “golden standard” AAV2 after injection in the lateral hypothalamus. The mosaic vectors were tested, because some studies have shown that combination of two serotype capsids may confer (synergistic) effects of both parental strains (241, 242). In addition, we investigated the area of transduction after administration of different titers (1×10^8 , 1×10^9 and 1×10^{10} genomic copies (g.c.)) and different volumes (1 μ l versus 0.3 μ l) of AAV1 coated vectors aimed at the paraventricular nucleus (PVN) of the hypothalamus. From these results we obtained an indication for the optimal titer and volume to transduce a nucleus of a certain size in the hypothalamus. Our major findings were that AAV1 was more efficient than the AAV2, 8, 1/2 and 2/8 pseudotyped AAV vectors in neuronal transduction of the LH. In addition, a titer of 1×10^9 g.c., in a volume of 1 μ l, transduced an area of 0.5mm² successfully. At a distance of 0.05 mm from the injection site almost all neurons were transduced when AAV1 pseudotyped AAV vectors were used. As a proof of principle of gene delivery to induce a phenotype we injected AAV1-AgRP in the PVN.

Materials and methods

Cell lines and plasmids

Human embryonic kidney (HEK) 293T cells were maintained at 37°C with 5% CO₂ in Dulbecco's modified Eagles medium (DMEM) supplemented with 10% fetal calf serum (FCS) and penicillin-streptomycin.

The helper plasmids used to produce AAV vectors were pDP1, pDP2 and pAR-8 in combination with pXX6. The pDP1 and pDP2 helper plasmids have been described (211) and were obtained from Plasmid factory (Germany). The packaging plasmid pAR-8 and the transgene vector pAAV-CBA-GFP-WPRE, with AAV2 inverted terminal resolutions sites, were both previously described (207) and were a kind gift from M. Sena-Esteves (University of Massachusetts, Worcester, MA, USA). pAR-8 lacks the adeno-helper genes, therefore pXX6 is necessary as an additional helper plasmid. PXX6 has been described (243). We constructed pAAV-CBA-AgRP-ires-gfp by removing the green fluorescent protein (GFP) from pAAV-CBA-GFP-WPRE with the restriction enzymes Agel and BsrGI. Subsequently, agouti-related protein (AgRP)-ires-GFP, was isolated from pIRES2-AgRP with Afel and BsrGI, and was ligated in the pAAV-CBA-GFP-WPRE, from which the GFP was removed. This ligation generated pAAV-CBA-AgRP-ires-GFP.

AAV production

To produce AAV-GFP with single capsids of AAV1, AAV2 and AAV8, we co-transfected pAAV-CBA-GFP-WPRE with the individual helper plasmids pDp1, pDp2 or pAR-8+pXX6, in a molar ratio of 1:1 (AAV vector plasmid: helper plasmid). Mosaic coated AAV-GFP with AAV1/2 and AAV2/8 capsids were produced by

mixing the packaging vectors (pDp1 or pAR-8 with pDp2) in a molar ratio of 1:1. Subsequently, pAAV-CBA-GFP-WPRE was co-transfected, in a 1:1 molar ratio, with either the pDp1+pDp2 or the pAR-8+pDp2 mix. pAAV-CBA-AgRP-ires-GFP was only co-transfected with pDp1. Each AAV production was performed with 15 dishes 293T cells at 80-90% confluency on the day of transfection. Two hours before transfection, the 10% FCS-DMEM was replaced with 2% FCS-DMEM. The transfections were performed with polyethylenimine (PEI) as described by Reed S.E. et al. (210). The transfection mix remained on the cells until the next day, then the 2% FCS-DMEM was refreshed. The purification was performed as described by Zolotukhin et al. (212). Briefly, sixty hours after transfection, the cells were harvested in their medium, centrifuged and washed with phosphate buffered saline (PBS) containing 5mM ethylenediaminetetraacetic acid (EDTA). Finally, the cells were collected in 12 ml ice cold buffer (150 mM sodium chloride (NaCl), 50 mM 2-amino-(hydroxymethyl)-1,3-propanediol (Tris), pH 8.4) and stored at -20°C until further use. Usually after three days the cells were freeze-thawed twice, incubated for 30 minutes with 50units/ml Benzonase (Sigma, The Netherlands) at 37°C and centrifuged. After centrifugation, the supernatant was loaded onto an iodixanol gradient (60%, 40%, 25%, 15%, supernatant (Optiprep, Lucron bioproducts, Belgium)) in quickseal tubes (Beckman Coulter, The Netherlands). After 1 hour of ultracentrifugation (70.000 rpm at 20°C) in Ti70 rotor (Beckman Coulter, The Netherlands), the 40% layer was extracted. This 40% layer was used for ion-exchange chromatography with 5ml Hitrap Q HP columns (GE Healthcare, The Netherlands). The AAV positive fractions, determined by PCR, were pooled and concentrated on Centricon Plus-20 Biomax-100 concentrator columns (Millipore, The Netherlands). The titer, in genomic copies per ml (g.c./ ml), was determined by qPCR with sybergreen mix in a LightCycler (Roche) (213). The qPCR primers were designed to detect BGHpolyA and were BGHpolyA_F: 5' CCTCGACTGTGCCTTCTAG; BGHpolyA_R: 5' CCCAGAATAGAATGACACCTA.

Animals

Male Wistar rats, weight ranging from 220–250 g, were purchased from Charles River (CrI-Wu, Germany). All rats were individually housed in filtertop cages with *ad libitum* access to food (CRM pellets; Special Diet Services, Whitham, Essex, UK) and water. Animals were kept in a temperature- and humidity-controlled room (21 ± 2°C) with a 12 h light/dark cycle (lights on at 7:00 A.M.). All experimental procedures were approved by the Committee for Animal Experimentation of the University of Utrecht (Utrecht, The Netherlands).

Surgical procedures

In study 1 the transduction efficiency of different capsids surrounding AAV-CBA-GFP-WPRE after injection in the lateral hypothalamus was studied. 20 rats were

anesthetized with 0.1 ml/100 g Hypnorm intramuscular (Janssen Pharmaceutica, Beerse, Belgium) and 0.05 ml/100 g Dormicum intraperitoneal (Hoffman-LaRoche, Mijdrecht, The Netherlands). Rimadyl (Pfizer animal health, Capelle a/d IJssel, the Netherlands) was administered as pain medication before surgery and on day 1 and 2 after surgery. After this, the rats were injected bilaterally in the lateral hypothalamus (LH, coordinates AP-1.8, ML+1.7, DV-8.6) with 1.5 μ l of AAV-CBA-GFP-WPRE coated with respectively AAV2, AAV1, AAV8, AAV1/2 and AAV2/8. The injected volume contained 1×10^8 g.c. of AAV vector and was delivered at a rate of 0.2 μ l/ minute. After the injection the needle remained in the injection site for 10 minutes. Four weeks after injection the rats were anesthetized and perfused with 4% paraformaldehyde (PFA) containing 0.05% glutaraldehyde. After perfusion the brains were isolated and were placed in 4%PFA overnight at 4°C. The next morning the brains were placed in PBS and stored at 4°C until further use. The perfused brains were sectioned on a vibratome at 40 μ m in series of 10. The 1st and 6th series of sections were combined and used for double immunohistochemistry against GFP and the neuronal marker NeuN.

In study 2 the effect of different titers of AAV1 coated AAV vectors on transduction efficiency was explored. Twenty-four rats received bilaterally 1 μ l of AAV-CBA-GFP-WPRE or AAV-CBA-AgRP-ires-GFP coated with AAV1 aimed at the paraventricular nucleus (PVN, coordinates AP -1.8, ML +1.7, DV -8.1, angle 10 degrees). The injections contained respectively 1×10^{10} (2 rats), 1×10^9 (2-3 rats) or 1×10^8 g.c. (3-4 rats) of the AAV vectors. Each rat was injected at both sides of the brain and these sides were analyzed separately. After 4 weeks the rats were decapitated and the brains were removed, quickly frozen on dry-ice and stored in -80°C until they were sectioned on a cryostat (Leica, The Netherlands) at 20 μ m. The sections were used for *in situ* hybridization with GFP-dig labeled mRNA probe to show the transduction area of the AAV vectors.

In study 3 the effect of an injection volume smaller than 1 μ l, of AAV1 coated vectors, was investigated. Twenty rats received injections with 0.3 μ l of AAV-CBA-GFP-WPRE or AAV-CBA-AgRP-ires-GFP-WPRE, coated with AAV1, containing 1×10^9 (3 rats), 5×10^8 (4 rats) and 1×10^8 (3 rats) g.c. aimed at the PVN (coordinates AP -1.80, ML +1.70, DV -8.10, angle 10 degrees). After 31 days animals were decapitated and processed as described in study 2.

Immunohistochemistry

40 μ m sections of study 1 were used for GFP-NeuN staining (series 1 and 6 were pooled). The free floating sections were washed 3 times with PBS, permeabilized for 30 minutes in PBS supplemented with 0.5% triton X-100 at room temperature (RT), blocked for 1 hour in PBS with 1.5% normal goat serum (NGS) at RT and

incubated overnight in PBS supplemented with mouse monoclonal anti-NeuN (1:2000, Chemicon), rabbit polyclonal anti-GFP (1:1500, Invitrogen) and 1.5% NGS at 4°C. The next morning sections were washed 3 times for 10 minutes with PBS and incubated for 1 hour with secondary antibodies (ALEXA 555 conjugated goat anti mouse (1:1000) and ALEXA 488 conjugated goat anti rabbit (1:1000) both Invitrogen) in 1.5% NGS at RT. After 3 times 10 minutes wash with PBS, the sections were transferred to microscope slides and kept over night in the dark to dry. All sections were embedded in 90% glycerol and stored flat at 4°C.

In situ hybridization

The brains of study 2 and 3 were sectioned on cryostat at 20 µm thickness and were used for *in situ* hybridization with a 720 basepair long digoxigenin (DIG)-labeled eGFP riboprobe (antisense to NCBI gene DQ768212). The *in situ* hybridization was performed as described by Schaeren-Wiemers and Gerfin-Moser (244) with small modifications in the fixation procedure and hybridization temperature. Briefly, sections were fixed in 4% PFA for 20 minutes and rinsed 3 times for 3 minutes in PBS. After acetylation for 10 minutes (0.25% acetic anhydride in 0.1 M triethanolamine), the sections were washed 3 times in PBS for 5 minutes and prehybridized at RT in hybridization solution, containing 50% deionized formamide, 5xSSC, 5xDenhardt's solution, 250 µg/ml tRNA Baker's yeast and 500 µg/ml sonicated salmon sperm DNA. After 2 hours 150µl of hybridization mixture containing 400 ng/ml DIG-labeled riboprobe was applied per slide, covered with Nescofilm and hybridized overnight at 72°C. The next morning the slides were quickly washed in 2xSSC followed by 0.2xSSC for 2 hours, both wash steps were performed at 72°C. DIG was detected with an alkaline phosphatase labeled antibody (1:5000, Roche, Mannheim) using nitroblue tetrazolium and bromochloroindolylphosphate (NBT/BCIP, Roche) as a substrate. After overnight incubation at RT with NBT/BCIP mixture, sections were quickly dehydrated in ethanol, cleared in xylene and mounted using Entellan.

Imaging, quantitation and statistical analysis

The MCID system was used to digitize pictures from sections containing the injection site and a section 400 µm more posterior. The images were analyzed blind with ImageJ (<http://rsb.info.nih.gov/ij/>). This program was used to transform the digitized, color pictures into binary (black and white) pictures (Figs. 2A, B), the scale was set and total black area was measured. The total black area was used as a value for the total area which was transduced by the different serotypes in one section (Fig. 2B). In addition ImageJ was used to obtain an indication for the percentage of area transduced at a certain distance from the injection site, as a measure for spread from injection site (Fig. 2B). This was done by using the macro: measure and label tool circle. Circles of different radiuses were placed at

the site of injection and total black area and % black area in a certain sized circle were measured. From this the percentage transduced per circle radius was calculated.

SPSS 15.0 was used for statistical analysis. The total area transduced and percentage transduced area per circle were compared using ANOVA analysis. The post-hoc Bonferroni correction was used when 3 or more groups were compared

Results

AAV1 transduces the LH most efficiently

In order to compare the efficiency of different AAV serotypes in transducing the LH, we packaged pAAV-GFP with capsids derived from serotypes 1, 2, 8 or combined packaging plasmids to obtain mosaic capsids 1/2 and 2/8. These pseudotyped AAV vectors were bilaterally injected into the LH of rats ($n=2-4$) with 1×10^8 g.c. in a volume of 1.5 μ l. Free floating brain sections (thickness, 40 μ m) were used for double immunohistochemistry against GFP (green signal) and the neuronal marker NeuN (red signal). Co-localization of GFP and NeuN showed that all AAV serotypes transduced primarily neurons (>95%), since there were only few GFP stained cells that lacked staining for the neuronal marker NeuN (Figs. 1A, 1B).

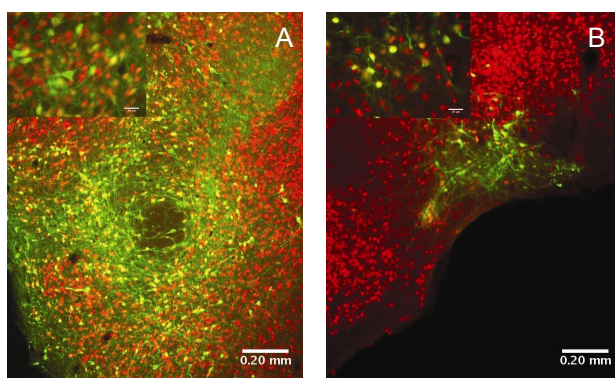


Figure 1 - Transduction by AAV1-GFP or AAV2-GFP *in vivo*

A Co-localization of GFP (green) and NeuN (red) at injection site, 4 weeks after injection with 1×10^8 g.c. of AAV1-GFP. **B** Co-localisation of GFP and NeuN after injection of titer matched AAV2-GFP. Scalebar is 0.20 mm.

The area transduced by AAV vectors was quantified using imaging software (Fig 2A, 2B). Analysis of the brains injected with AAV-GFP coated with different serotypes in the LH revealed that the total area transduced was 0.025 mm^2 with AAV2-GFP.

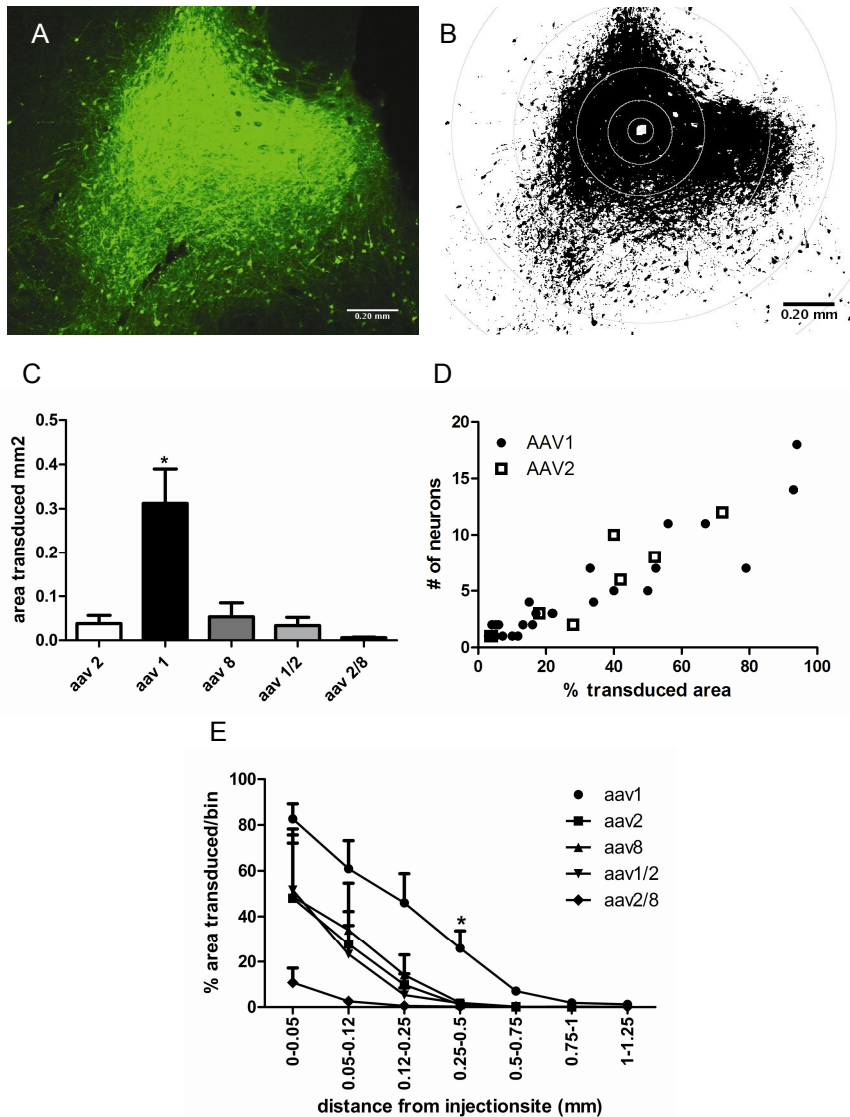


Figure 2 - Effect of AAV serotype capsids on transduction efficiency in the lateral hypothalamus

A: GFP immunostaining of a 40 μ m slice containing the lateral hypothalamus, four weeks after injection with AAV1-GFP at a titer of 1×10^8 genomic copies in 1.5 μ l. **B:** A binary picture made with ImageJ through conversion of the original picture (2A) to a binary picture. Subsequently, ImageJ was used to measure the total area which is GFP positive (black). **C** Total area transduced (in mm²) by AAV-GFP coated with different serotype capsids. **D** A graphical representation of the relationship between percentage transduced area and the number of neurons transduced in an area of 0.115 mm² by AAV1-GFP (closed circles) and AAV2-GFP (open squares). This area contains approximately 19-20 neurons. **E** The percentage of area transduced at certain radii from the injection site (see circles in 2B). * $p < 0.05$ compared to AAV2-GFP.

The total area transduced with serotypes 8, 1/2 and 2/8 was not significantly different from AAV2 (respectively 0.05, 0.03 and 0.005 mm², $p>0.05$; Fig. 2C). However, AAV1-GFP transduced a significantly larger total area than AAV2-GFP (0.312 mm², $p=0.042$).

In addition to the total area of transduction, we also investigated whether the percentage of transduced cells at different radii from the injection site was different for the different AAV serotypes. The percentage of the area transduced was positively correlated to the number of neurons transduced (Fig. 2D). The results in Fig. 2e show that serotypes 2, 8 and 1/2 transduced approximately 50% of the neurons at a distance of 0.05mm from the injection site at a titer of 1×10^8 g.c. The AAV2/8-GFP only transduced an area of approximately 20% at a distance of 0.05mm. Again AAV1-GFP appeared to be superior, transducing almost 90% of the neurons at 0.05mm from the injection site. In addition, AAV1 transduced neurons could be found at distances further from the injection site, namely up to 1mm instead of 0.5mm (Fig 2E). AAV1 also showed a significantly larger spread in rostral to caudal direction. Ten sections (~2mm, $p=0.002$ compared to AAV2) were positive for GFP protein in the AAV1 group compared to 4, 3, 5 and 6 sections for AAV2, 8, 1/2 and 2/8, respectively ($p>0.05$ for AAV8, 1/2 and 2/8 compared to AAV2). These results together suggest that AAV1 coated AAV-vectors are more efficient in transducing neurons after injection in the LH than AAV2, AAV8 or the mosaic 1/2 and 2/8 coated AAV-vectors.

Effect of titer on transduction area and on percentage transduction

To investigate the effect of different titers, we tested two AAV-genomes packaged with AAV1 capsids, namely pAAV-GFP and pAAV-AgRP. These AAV vector preps were diluted in PBS to obtain 1×10^8 , 1×10^9 and 1×10^{10} g.c./ μ l. One μ l of these diluted preps was bilaterally injected in the PVN. As expected, an increase in titer of AAV1-AgRP (Fig. 3A) and AAV1-GFP (data not shown) augmented the total transduction area as determined with a GFP *in situ* hybridization (ISH). Increasing the amount of viral particles from 1×10^8 g.c. to 1×10^9 g.c. of AAV1-AgRP resulted in a total transduction area that was eight times larger; it increased from 0.08 to 0.65 mm² ($p=0.004$). An additional ten times rise in total viral particles, from 1×10^9 g.c. to 1×10^{10} g.c., did not transduce a significant larger area than 1×10^9 g.c.. The total transduced area only increased from 0.65 to 0.77 mm² ($p>0.05$). Figure 3b shows that the percentage of transduced area at a certain distance from the injection site with 1×10^9 g.c. was not significantly different from 1×10^{10} g.c., while both 1×10^9 g.c. and 1×10^{10} g.c. are significantly different from 1×10^8 g.c. (Fig. 3B). The total area transduced and the percentage transduced by AAV1-GFP (Fig. 3C) did not significantly differ from AAV-AgRP at comparable titers (1×10^9 $p>0.05$, 1×10^{10} $p>0.05$).

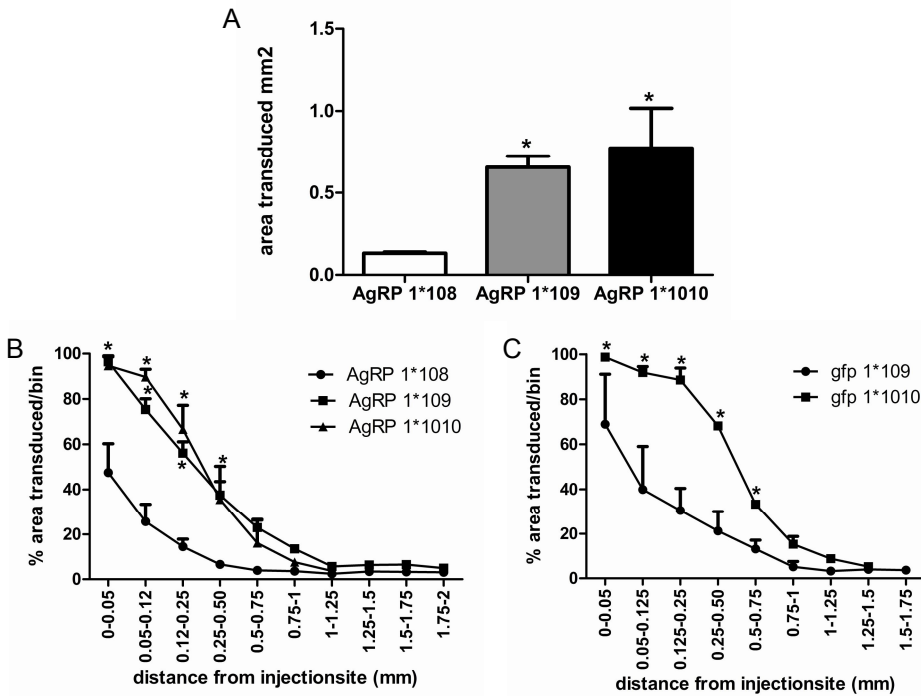


Figure 3 - Effects of different titers of AAV1 coated vectors on transduction efficiency in the paraventricular hypothalamus

A total area transduced, in mm², by AAV1-AgRP at different titers in the rat PVN. **B**: percentage transduced area per circle with AAV1-AgRP. **C** percentage transduced area per circle with AAV-GFP. * $p < 0.05$ compared to AgRP 1×10^8

Effects of injection volume on transduction area and percentage transduction

In addition to variation in titer, we also varied the injection volume to investigate the effect on transduction area. We injected AAV1-GFP and AAV1-AgRP at similar genomic copy numbers (1×10^8 and 1×10^9 g.c.), but in different end volumes (1 and 0.3 μ l), into the PVN. As can be seen in Figures 4A and 4B, the injection volume of 0.3 μ l resulted in significantly smaller transduction areas ($p = 0.029$) (Figs. 4A, 4B). In addition, 0.3 μ l resulted in a lower percentage transduced area per circle than injections with similar amounts of viral particles, but in volumes of 1 μ l. We observed more often a GFP positive injection track in 0.3- μ l groups than in the 1- μ l groups (Figs. 4C, 4D).

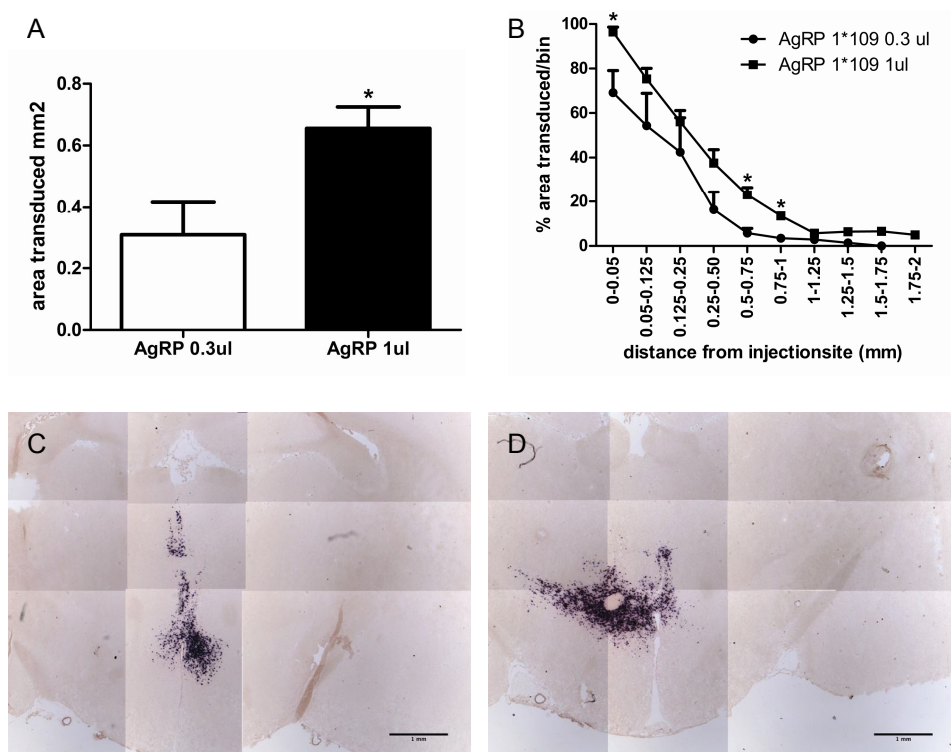


Figure 4 - Effects of different volumes of AAV1 coated vectors on transduction efficiency in the paraventricular hypothalamus

A Total transduced area with injection volumes of 0.3 µl and 1 µl. Both volumes contained 1×10^9 g.c. of AAV1-AgRP. **B** Percentage area transduced per circle with AAV1-AgRP. **C** GFP ISH picture with injection volume of 0.3 µl. **D** GFP ISH picture with injection volume of 1 µl. The 0.3 µl injection volume more often resulted in GFP positive injection tracts than 1 µl injection volumes. Scalebar is 1mm.

* $p < 0.05$ compared to 0.3 µl.

Behavioral effects of AAV-AgRP overexpression in the PVN

Injection of AAV1-AgRP and AAV1-GFP at the optimal dose of 1×10^9 g.c., in 1 µl, into the PVN resulted in an increase in body weight in the AAV1-AgRP rats compared to AAV1-GFP rats. On day 28 AAV1-AgRP rats had accumulated 147 ± 5.4 % ($p = 0.0002$) more weight than did the AAV1-GFP rats (Fig. 5A). The increased body weight in AAV1-AgRP rats was, at least partly, caused by an increase in daily caloric intake in the AAV1-AgRP rats ($p = 0.0001$) (Fig. 5B).

Discussion

Recent studies have shown that AAV vectors coated with serotypes other than AAV2 are more efficient in the transduction of several brain areas, like striatum, hippocampus and substantia nigra (62, 63, 64, 65, 240). However, most studies using AAV vectors for transduction of the hypothalamus have been conducted with

AAV2 coated vectors (201, 237, 238). Therefore, we compared the transduction efficiency of AAV1, 8 or mosaic capsids 1/2 and 2/8 with that of AAV2 in the hypothalamus. We injected AAV-GFP coated with different capsid proteins in the LH at a titer of 1×10^8 g.c.. The results showed that AAV1-GFP transduced a significantly larger total area than AAV2. However, AAV-GFP coated with AAV8, 1/2 and 2/8 did not significantly differ from AAV2-GFP in the total area transduced after injection in the LH. In addition, the AAV1-GFP transduced more neurons at a certain radius from the injection site in comparison with the other serotypes AAV2, 8, 1/2 and 2/8; AAV1 also showed a significantly larger dispersion in rostral to caudal direction. It is possible that the mosaic capsids transduced a different set of neurons, however, we did not investigate this. In addition, we can not exclude that other AAV serotypes, such as AAV5, 6, 9 and 10, are more efficient than AAV1 in transduction of the hypothalamus. To our knowledge this is the first study to determine the efficacy of different AAV serotypes in the adult hypothalamus.

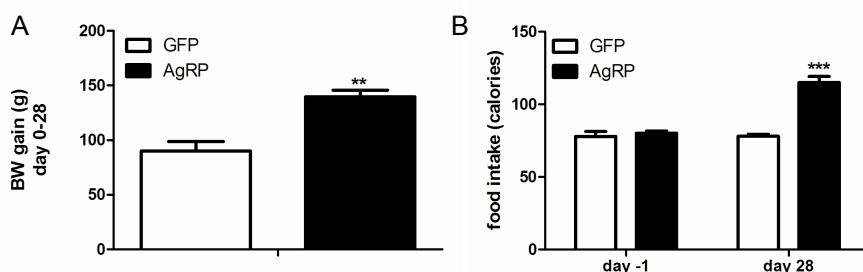


Figure 5 - Effects of AAV1-AgRP on body weight and caloric food intake

A cumulative body weight gain of rats receiving AAV1-AgRP or AAV1-GFP in the PVN. The body weight gain is from day 0 until day 28 after injection. Both vectors were injected at a titer of 1×10^9 g.c. in 1 μ l. **B** total caloric food intake per day one day before injection and 28 days after injection of AAV1-AgRP or AAV1-GFP in the PVN. ** $p < 0.01$, *** $p < 0.001$ compared to AAV1-GFP.

In this study, we determined which titer was required to transduce a brain area of a certain size. We injected two vectors, namely AAV1-GFP and AAV1-AgRP, at different titers (1×10^8 , 1×10^9 and 1×10^{10} g.c. in 1 μ l) into the PVN. These results showed that a titer of 1×10^9 g.c. was able to transduce an area of approximately 0.5 mm^2 . There were some differences in total transduction areas between AAV1-GFP and AAV1-AgRP. 1×10^9 g.c. AAV1-AgRP transduced an total area of 0.65 mm^2 (sem: ± 0.07), while 1×10^9 g.c. AAV1-GFP transduced 0.38 mm^2 (sem: ± 0.18); at 1×10^{10} g.c. the transduction areas were 0.77 mm^2 (sem: 0.24) for AAV1-AgRP and 1.08 mm^2 (sem: 0.09) for AAV1-GFP. However, these differences were not significant. A reason for this variation may be that there is a difference in the ratio of transducing particles and genomic particles between the different AAV preparations. We determined the titers with qPCR and this resulted in a value representing the amount of genomic particles. The determination of transducing

particles is not feasible, because the receptors and pathways by which AAV1, 8 and other serotypes enter cells are still (largely) unknown. The mechanisms for uptake and trafficking, of AAV to the cell nucleus are probably different for each serotype (245, 246). In addition, Rabinowitz J.E. et al. (2004) demonstrated that one dose of AAV vectors coated with AAV1/2 yielded different percentages GFP expression in different cell lines (241). We also confirmed that different serotypes with similar genomic particles resulted in different transducing particles values in HEK293T, HeLa and HT1080 cell lines (data not shown). Thus, comparison of different AAV serotyped AAV vectors on cell lines most probably does not reflect transduction efficiency in the brain and therefore we determined g.c. for comparison between different coats. However, transduction of a cell line with AAV vectors can be used to determine whether different batches of AAV vectors, with identical serotype capsids, have comparable ratios of transducing particles to genomic particle; this to ensure consistent AAV production over time.

When the titer of AAV1-AgRP and AAV1-GFP was increased from 1×10^9 g.c. to 1×10^{10} g.c. we did not observe a significant increase in the total area transduced. This ceiling effect was previously reported by Klein et al. (2002). They showed that AAV-NSE-GFP (AAV2 coat) at a titer of 3×10^{10} particles was not significantly different from a titer of 5×10^9 particles. In addition, they demonstrated that a minimum dose of 5×10^7 AAV particles was necessary to obtain GFP expression in rat hippocampus (230). Together, these data suggests that injection of different amounts of AAV genomic particles, to transduce a brain region, can be described by an S-shaped dose-response curve.

Besides the effect on the total area transduced, we also investigated the effect of the titer on the percentage of neurons that were transduced at a certain radius from the injection site. The results showed that with an increase in titer, the percentage transduced area at a certain radius increased. This is in concordance with the larger total area that was transduced. Thus, more neurons in a certain area were transduced when the titer was increased.

We also studied the effect of different injection volumes, 1 μ l versus 0.3 μ l, on the total area transduced. As expected, an injection volume of 1 μ l transduced a larger total area. In addition, the 1- μ l injection volume showed a trend toward a higher percentage transduced area per circle. This difference was probably due to a difference in diffusion, because the viral preparation, titer and flow rate were comparable.

AAV-mediated overexpression of AgRP in the PVN increased food intake and body weight. This is in accordance with previous studies where acute and chronic

intracerebroventricular (ICV) administration of AgRP increased food intake and body weight (247, 248). In addition, overexpression of agouti with AAV2-pseudotyped vector in the PVN also resulted in an increase in food intake and body weight (249). Similar amounts of AAV-AgRP that missed the PVN did not result in an increase in food intake or body weight (data not shown), showing that local delivery at precise locations is necessary for AAV vectors to result in a phenotype.

Taken together, the results we obtained with regard to titer, volume and type of coat to transduce a certain area in the hypothalamus are similar to those obtained in the striatum, hippocampus and substantia nigra (62, 63, 64, 65, 240) and may therefore be informative for AAV mediated transduction of other brain regions. AAV vectors are effective tools with which the exact role of specific genes and brain areas in the dysregulation of energy balance can be dissected. The further optimization of the AAV technology for transduction of the hypothalamus, which we showed here, will be helpful in designing experiments in this field. Most investigators in this area still use AAV2-coated vectors, whereas we have shown here that an AAV1-pseudotyped vector transduces hypothalamic neurons more efficiently. In the future, AAV-mediated gene therapy may be considered as a new approach to treat obesity (227). In particular, in view of the burden and high mortality associated with bariatric surgery and the limited efficacy that is obtained with lifestyle adaptations, such as diets and exercise (250), local injection of viral vectors to downregulate or to deliver genes to the human hypothalamus may be considered as an alternative therapeutic strategy.

In summary, this study showed that AAV1-GFP was most efficient for transduction of the lateral hypothalamus when compared to AAV2, 8, 1/2 and 2/8 pseudotyped vectors. We were able to transduce an area of approximately 0.5mm^2 with AAV1-pseudotyped vectors at titer of 1×10^9 g.c., in an injection volume of $1\text{ }\mu\text{l}$. An area of 0.5 mm^2 , 4-5% of the total hypothalamic area in the analyzed plane, corresponds to a brain nucleus such as the PVN. These results also imply that for transduction of larger areas, multiple injections are required with distances of 0.5-1 mm between injection sites.

Acknowledgements

M.W.A. de Backer was supported by the Netherlands Organization for Scientific Research (NWO grant No. 90339175) and by the Foundation "De Drie Lichten" in The Netherlands.

Chapter 4

Melanocortin receptor mediated effects on obesity are distributed over specific hypothalamic regions

Marijke W.A. de Backer¹, Susanne E. la Fleur^{1,2}, Maike A.D. Brans¹, Rea J. van Rozen¹, Mienieke C.M. Luijendijk¹, Myrte Merkestein¹, Keith M. Garner¹, Esther M. van der Zwaal¹, Roger A.H. Adan¹

¹ Rudolf Magnus Institute of Neuroscience, Department of Neuroscience and Pharmacology, University Medical Centre Utrecht, Utrecht, the Netherlands.

² Department of Endocrinology and Metabolism, Academic Medical Center, University of Amsterdam, Amsterdam, the Netherlands.

MELANOCORTIN RECEPTOR MEDIATED EFFECTS ON OBESITY ARE DISTRIBUTED OVER SPECIFIC HYPOTHALAMIC REGIONS

Abstract

Reduction of melanocortin signaling in the brain results in obesity. However, where in the brain reduced melanocortin signaling mediates this effect is poorly understood. Therefore, we determined the effects of long term inhibition of melanocortin receptor activity in specific brain regions, namely the paraventricular nucleus (PVN), the ventromedial hypothalamus (VMH), the lateral hypothalamus (LH) and accumbens shell (Acc). Melanocortin signaling was inhibited by recombinant adeno-associated viral (rAAV) vector mediated overexpression of the inverse agonist Agouti-related peptide (AgRP). Overexpression of AgRP in the PVN, VMH or LH increased food intake, bodyweight, percentage white adipose tissue and leptin concentration. In these areas food intake was increased due to an increase in meal size. Overexpression of AgRP in the Acc did not have any effect on the measured parameters. Although the orexigenic peptides AgRP and NPY are co-released from neurons of the arcuate nucleus, the effects of AgRP clearly differ from those of NPY, which suggests complementary roles for these neuropeptides in energy balance.

Introduction

Overconsumption plays an important role in the current obesity epidemic. One of the major neuropeptides which stimulates food intake is Agouti-related peptide (AgRP). AgRP is produced in neurons within the arcuate nucleus of the hypothalamus and functions as an inverse agonist at the melanocortin 3 and 4 receptors (MC3R and MC4R) (162, 251). Constitutive inhibition of the MC-Rs through (ectopic) overexpression of AgRP or agouti, or central infusion of AgRP results in hyperphagia and reduces energy expenditure (145, 163, 247, 248, 249, 252). Furthermore, knockout studies have shown that reduced activity of both the MC3R and MC4R contribute to obesity and have additive effects (156, 157, 158, 171, 172, 253). Although reduced activation of brain MC-Rs results in obesity, it is poorly understood where in the brain this effect is mediated since the MC-Rs are expressed in multiple sites of the brain (139, 146, 159). We previously showed that ectopic overexpression of Agouti in the paraventricular nucleus (PVN) of rats resulted in hyperphagia and obesity (249). In addition, local acute injection studies with AgRP₈₃₋₁₃₂ and MC-R antagonists in different brain nuclei, demonstrated that when MC-R activity is reduced, food intake is stimulated (190, 194, 254). Thus, multiple brain regions are involved in the effects of MC-Rs on food intake. It is, however, unclear whether chronic inhibition of MC-R activity in these different nuclei contributes to the development of obesity, since it is not feasible to locally infuse ligands in the brain over extended periods of time.

To investigate whether the effects of long term inhibition of MC-R activity are brain site specific, we used viral mediated gene transfer to deliver AgRP to the PVN, the lateral hypothalamus (LH), the ventromedial hypothalamus (VMH) and the nucleus accumbens shell (Acc), which are all brain regions with high levels of MC receptor expression (139, 146, 159) and an established role in the regulation of energy balance (67). After injection of rAAV particles containing AgRP or only GFP cDNA in the PVN, LH, VMH or Acc, rats were monitored for 50 days. During this time effects on body weight, caloric intake (including meal patterns), locomotor activity and body core temperature were examined. At the end of the experiments, the effects on white adipose tissue and endocrine parameters were analyzed. In addition, we carefully compared the effects of overexpression of AgRP with those of NPY overexpression, for which a similar approach was used in a previous study (255).

Materials and Methods

Cell lines and plasmids

Human embryonic kidney (HEK) 293T cells were maintained at 37°C with 5% CO₂ in Dulbecco's modified Eagles medium (DMEM) supplemented with 10% fetal calf

serum (FCS), 2mM glutamine, 100 units/ml penicillin, 100 units/ml streptomycin and non-essential amino acids.

pAAV-CBA-GFP with AAV2 inverted terminal resolutions sites, as previously described by (207), was a kind gift from M. Sena-Esteves (University of Massachusetts, Worcester, MA, USA). pAAV-CBA-flAgRP-ires-GFP was constructed by cloning the full length mouse Agouti-related peptide (AgRP) cDNA in pIRES2-EGFP (Clontech). Subsequently, AgRP-ires-EGFP was isolated and ligated in pAAV-CBA-GFP-WPRE, after removing GFP from the AAV plasmid. The pDP1 helper plasmid has been described previously (211) and was obtained from Plasmid factory (Bielefeld, Germany).

Virus production and purification

AAV production was performed with 15x15 cm dishes of 293T cells, 80-90% confluent at day of transfection. Two hours before transfection, the 10% FCS-DMEM was replaced with 2% FCS-DMEM. The transfections were performed with polyethylenimine (PEI) as described by Reed S.E. et al. (210). pAAV-CBA-GFP-WPRE or pAAV-CBA-flAgRP-ires-GFP were co-transfected with the helper plasmid pDP1 (211) (Plasmid factory, Germany) in a molar ratio of 1:1. The transfection mix remained on the cells until the next day, then the 2% FCS-DMEM was refreshed. AAV production and purification were essentially performed as described by Zolotukhin et al. (212). Briefly, sixty hours after transfection, the cells were harvested in their medium, centrifuged and washed with PBS containing 5mM ethylenediaminetetraacetic acid (EDTA). Finally, the cells were collected in 12 ml ice cold buffer (150 mM sodium chloride (NaCl), 50 mM 2-amino-(hydroxymethyl)-1,3-propanediol (Tris), pH 8.4) and stored at -20°C until further use. Usually after three days the cells were freeze-thawed twice, incubated for 30 minutes with 50 units/ml Benzonase (Sigma, The Netherlands) at 37°C and centrifuged. After centrifugation, the supernatant was loaded onto an iodixanol gradient (60%, 40%, 25%, 15%, supernatant (Optiprep, Lucron bioproducts, Belgium)) in quickseal tubes (Beckman Coulter, The Netherlands). After 1 hour of ultracentrifugation (70.000 rpm at 20°C) in Ti70 rotor (Beckman Coulter, The Netherlands), the 40% layer was extracted. This 40% layer was used for ion-exchange chromatography with 5ml Hitrap Q HP columns (GE Healthcare, The Netherlands). The AAV positive fractions, determined by PCR, were pooled and concentrated on Centricon Plus-20 Biomax-100 concentrator columns (Millipore, The Netherlands). The titer, in genomic copies per ml (g.c./ ml), was determined by qPCR with SYBR Green mix in a LightCycler (Roche) (213). The qPCR primers were designed to detect BGHpolyA and were BGHpolyA_F: 5' CCTCGACTGTGCCCTTCTAG; BGHpolyA_R: 5' CCCGAGAATAGAATGACACCTA. The titer obtained for AAV-CBA-GFP-WPRE was 9.9×10^{12} g.c./ml and for AAV-CBA-flAgRP-ires-GFP was 1.7×10^{14} g.c./ml.

Animals

Male Wistar rats, weight ranging from 220–250 g, were purchased from Charles River (Crl-Wu, Germany). All rats were individually housed in filtertop cages with *ad libitum* access to food (CRM pellets; Special Diet Services, Whitham, Essex, UK) and water. Animals were kept in a temperature- and humidity-controlled room (temperature $21 \pm 2^\circ\text{C}$, humidity $55\% \pm 5\%$) with a 12 h light/dark cycle (lights on at 7:00 A.M.). All experimental procedures were approved by the Committee for Animal Experimentation of the University of Utrecht (Utrecht, The Netherlands).

Surgical procedures

After 1½ week of acclimatization the rats were anesthetized with 0.1 ml/100 g hypnorm intramuscular (Janssen Pharmaceutica, Beerse, Belgium), 0.05 ml/100 g dormicum intraperitoneal (Hoffman-LaRoche, Mijdrecht, The Netherlands) and 0.1 ml/100g Carprofen (5mg/ml, Vericore, UK) to relieve pain. After this, the rats received an abdominal transmitter (TA10TA-F40; Data Science International, St. Paul, Minnesota, USA), to measure core temperature and locomotor activity. Immediately after transmitter placement the rats were injected bilaterally in the different brain areas with use of a stereotact. Twenty-five rats were injected in the PVN (coordinates anterior posterior (AP) -1.8 mm from bregma; mediolateral (ML) ± 1.7 mm from bregma; dorsoventral (DV) -8.2 mm below the skull; with 10 degrees angle), 9 rats were injected with AAV-GFP and 16 with AAV-AgRP. Twenty-two rats were injected in the LH (coordinates AP -2.6, ML ± 2.0 , DV -8.6), n=9 AAV-GFP and n= 13 AAV-AgRP. Twenty-one rats were injected in the VMH (coordinates AP -2.6, ML ± 1.2 , DV -9.4 with 5 degrees angle), 9 rats were injected with AAV-GFP and 12 with AAV-AgRP. Finally, twenty-one rats were injected in the shell of the Acc (coordinates AP +1.2, ML ± 2.8 , DV -8.0 with 10 degrees angle), n=9 AAV-GFP and n=12 AAV-AgRP. Per site 1 μl of virus containing 1×10^9 g.c. of rAAV was injected, at a rate of 0.2 μl / minute. After the injection the needle was kept in place for 10 minutes before removal. After surgery the rats received carprofen (5 mg/kg, Vericore, UK) for post-operative pain control during 2 days.

Data recordings

After viral injections the rats were monitored for approximately 50 days for effects on bodyweight, food intake, body core temperature and locomotor activity. Bodyweight gain and food intake were measured three times a week at 10.00 A.M.. Core temperature and locomotor activity were automatically recorded via the transmitters that sent digitized data to a nearby receiver. These data were recorded every 10 minutes using DSI software (DSI, St. Paul, MN). On days 20-21 and 40-41, meal patterns were recorded as described previously (Tiesjema et al. 2007). Food hoppers were automatically weighed using scales (Dept. Biomedical Engineering, UMCU, Utrecht, the Netherlands) and data was sent to a computer

every 12s for 48 hrs. The data of 48 hours were averaged to obtain 24 hr values. A meal was defined as an episode of food intake with a minimal consumption of 0.5 g of chow and an intermeal interval of 5 min.

Collection of blood and tissues

On day 48-50, rats were decapitated in the morning and trunk blood was collected in heparinized tubes containing 83µmol EDTA and 1 mg aprotinin. The blood was immediately placed on ice. After centrifugation blood plasma was stored at -20°C until additional analysis.

After decapitation the brains were immediately removed, quickly frozen on dry ice and stored at -80°C. Retroperitoneal, epididymal, mesenteric and subcutaneous white adipose tissue were isolated and weighed, as well as adrenals and thymus.

DIG in situ hybridization

To verify injection sites, brains were sectioned on a cryostat into 20 µm thick slices and were used for *in situ* hybridization with a 720 basepair long digoxigenin (DIG)-labeled eGFP riboprobe (antisense to NCBI gene DQ768212). The *in situ* hybridization was performed as described by Schaeren-Wiemers and Gerfin-Moser (244) with small modifications in the fixation procedure and hybridization temperature. Briefly, sections were fixed in 4% PFA for 20 minutes and rinsed 3 times for 3 minutes in PBS. After acetylation for 10 minutes (0.25% acetic anhydride in 0.1 M triethanolamine), the sections were washed 3 times in PBS for 5 minutes and prehybridized at RT in hybridization solution, containing 50% deionized formamide, 5xSSC, 5xDenhardt's solution, 250 µg/ml tRNA Baker's yeast and 500 µg/ml sonicated salmon sperm DNA. After 2 hours 150µl of hybridization mixture containing 400 ng/ml DIG-labeled riboprobe was applied per slide, covered with Nescofilm and hybridized overnight at 72°C. The next morning the slides were quickly washed in 2xSSC followed by 0.2xSSC for 2 hours, both wash steps were performed at 72°C. DIG was detected with an alkaline phosphatase labeled antibody (1:5000, Roche, Mannheim) using nitroblue tetrazolium and bromochloroindolylphosphate (NBT/BCIP, Sigma) as a substrate. After overnight incubation at RT with NBT/BCIP mixture, sections were quickly dehydrated in ethanol, cleared in xylene and mounted using Entellan.

Radioactive in situ hybridization

Adjacent cryostat brain sections were used for radioactive ISH with ³³P-labeled antisense RNA probes for agouti-related peptide (AgRP, 396 bp mouse AgRP cDNA (256)), neuropeptide Y (NPY, 287 rat NPY cDNA), pro-opiomelanocortin (POMC, 350bp rat POMC cDNA fragment (256)), suppressor of cytokine signaling 3 (SOCS3, 1200bp SOCS3 cDNA). The procedure for radioactive ISH and analysis has been described previously (257).

Plasma analysis

Plasma concentrations leptin and insulin were measured in duplicate using radioimmunoassay kits (Millipore, Billerica, MA, USA). Plasma glucose was analyzed in triplicate using a glucose/GOD- perid method (Boehringer Mannheim, Mannheim, Germany).

Statistical analysis

Data are presented as group means \pm SEM. Differences in bodyweight and food intake were assessed using repeated measure analysis. When significant overall interactions were found, post hoc analyses were performed with two sided *t* tests. Additional statistical analysis was performed with two sided *t*-test. Differences were considered significant at $p < 0.05$.

Results

Localization of rAAV injections

In situ hybridization with a DIG-labeled GFP probe was performed for each rat to verify injection sites. Rats injected with AAV-AgRP were only included in the study when GFP signals were observed bilaterally in the Acc (AP between +2.2 and +0.7 mm; ML between 1 and 2 mm from bregma), PVN (AP between -1.3 and -2.3 mm; ML between 0 and 1 mm from bregma), VMH (AP between -2.1 and -3.6 mm; ML between 0.2 and 1 mm) or LH (AP between -2.3 and -3.8 mm; ML between 1 and 2.5 mm from bregma). Bilateral injection of AAV-AgRP was confirmed for 8 rats in the PVN, 7 rats in the VMH, 9 rats in the LH and 10 rats for the Acc. Unilateral injections were observed in 5 rats in the PVN, 5 rats in the VMH, 4 rats in the LH and 2 rats in the Acc. Unilateral and missed injections of AAV-AgRP were analyzed separately and are indicated as such. Since expression of GFP would not be expected to have any effects on energy balance, we tested whether there were differences between the bilateral and unilateral transduced AAV-GFP rats. When the different control groups were compared to each other, rats with GFP-expression in different brain areas displayed similar bodyweight gain, food intake and meal patterns, supporting the assumption that GFP-expression had no effects on energy balance.

Effects of rAAV-AgRP on body weight and food intake

All injection groups showed a similar transient decrease in body weight gain, caloric intake and water intake in the days after surgery. In PVN-AgRP and LH-AgRP rats body weight gain was significantly increased compared to controls, starting from day 8 and 11, respectively, until the end of the experiment (Fig. 1A and 1C). In addition, rats which received rAAV-AgRP in the VMH showed a significant increase in body weight from day 14 onwards when compared to VMH-GFP (Fig. 1B).

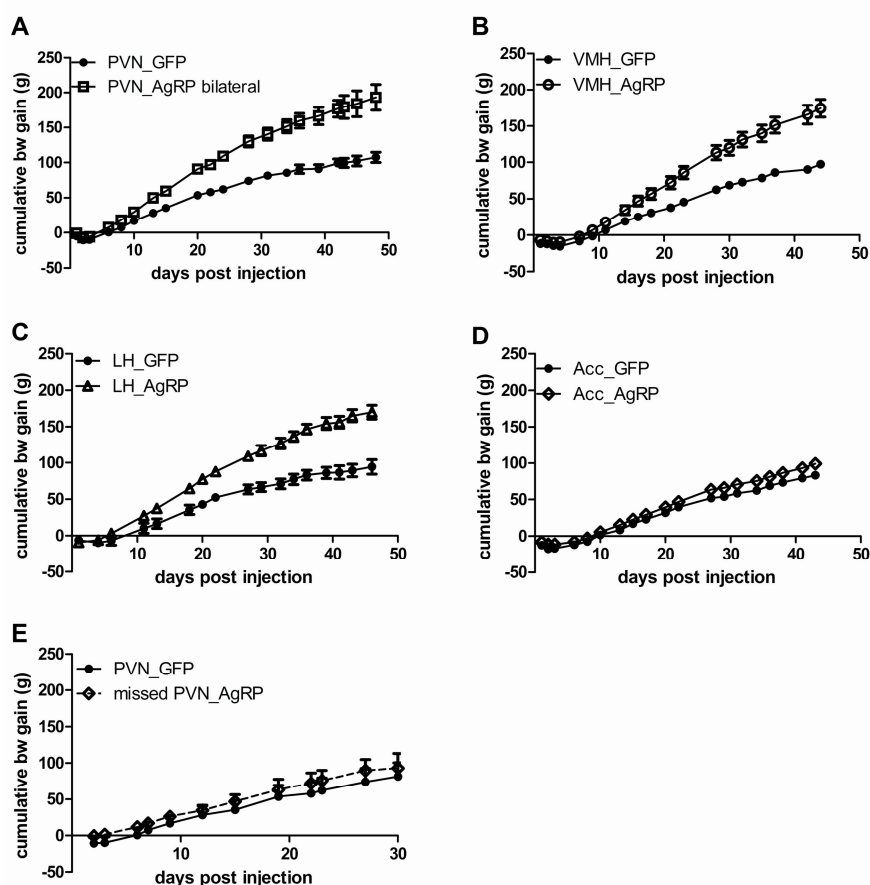


Figure 1 - Cumulative body weight gain

Cumulative body weight gain of rats injected with rAAV-AgRP or rAAV-GFP in PVN (A), VMH (B), LH (C) or Acc (D). Injections of rAAV-AgRP which missed the PVN did not show increase in body weight (E).

The increase in body weight gain in rats injected in these three hypothalamic areas was highest when AgRP was expressed in both sides, since unilateral rAAV-AgRP expression in the PVN, LH or VMH resulted in body weight gain values in between those of controls and the bilateral transduced rats (average at day 50: unilateral PVN $173.7 \text{ g} \pm 11.8$; unilateral LH $122.7 \text{ g} \pm 15.0$; unilateral VMH $139.0 \text{ g} \pm 10.5$). In contrast, AgRP overexpression in the Acc shell did not increase body weight gain when compared with controls (Fig. 1D). In addition, when AgRP expression was mis-targeted, for instance too rostral or caudal of the PVN (missed PVN injection), there was no increase in body weight gain (Fig. 1E). At the end of the experiment PVN-AgRP, LH-AgRP and VMH-AgRP rats had an approximately 80% increase in body weight gain compared with controls (PVN: $79.8\% (\pm 17.2)$ $p=0.0002$; LH: $80.1\% (\pm 10.1)$ $p<0.0001$; VMH $78.8\% (\pm 12.6)$ $p<0.0001$).

During the second week the PVN-AgRP, LH-AgRP and VMH-AgRP rats all increased their daily food intake compared to controls (increased food intake was significant from day 10 for PVN-AgRP, day 8 for LH-AgRP and day 14 for VMH-AgRP). Food intake remained significantly elevated during the course of the experiment (Fig. 2A-C). Daily food intake in the Acc-AgRP and missed PVN-AgRP groups were similar to control groups (Fig. 2D, E).

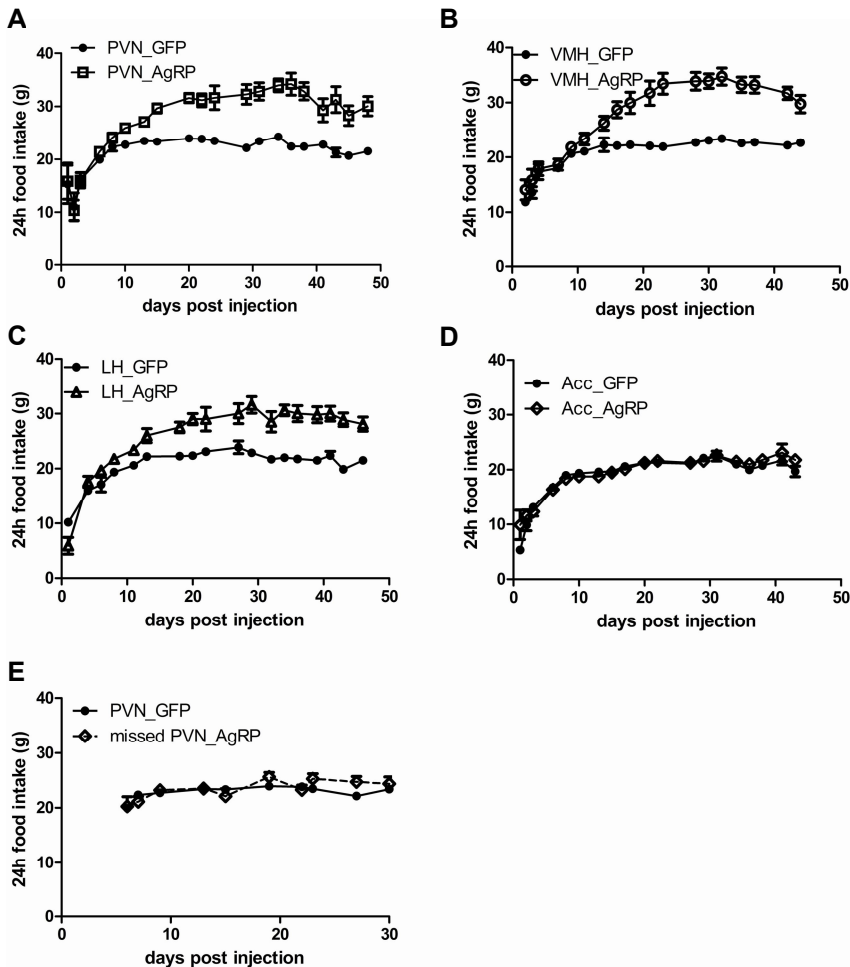


Figure 2 - Daily food intake

Daily food intake of rats injected with rAAV-AgRP or rAAV-GFP in PVN (**A**), VMH (**B**), LH (**C**) or Acc (**D**). Injections of rAAV-AgRP which missed the PVN did not show increase in food intake (**E**).

Daily water intake of PVN-AgRP and VMH-AgRP rats followed the food intake pattern and was significantly increased compared to controls from day 13 and 23, respectively (PVN-AgRP average of 28.2 ± 1.02 ml/day vs. 24.3 ± 0.50 ml/day for PVN-GFP; VMH-AgRP average of 26.5 ± 0.93 ml/day vs. 21.9 ± 0.49 ml/day for

VMH-GFP). LH-AgRP and Acc-AgRP did not differ in water intake compared to their controls (data not shown).

Effects of rAAV-AgRP on meal patterns

The PVN-AgRP, VMH-AgRP and LH-AgRP rats showed significant increase in 24h food intake at day 20 and day 40 (Fig. 3A; 4A; 5A). This was due to an increase in food intake in both the light and dark period (Fig. 3B, C; 4B, C; 5B, C). Acc-AgRP rats were not different in their 24h food intake compared to Acc-GFP rats (Fig. 6A-C).

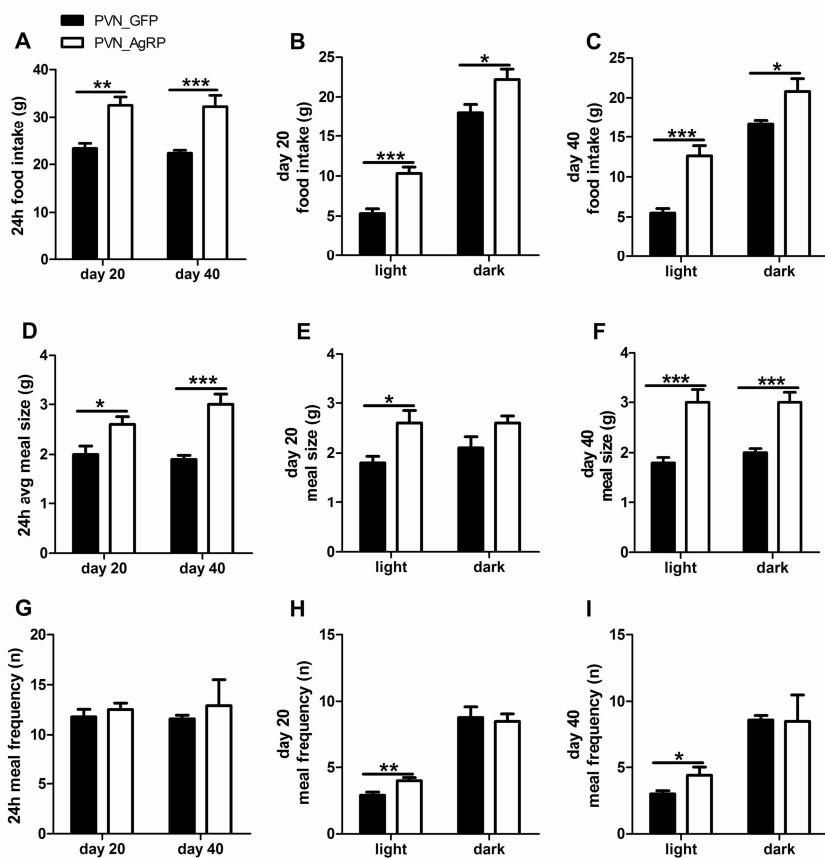


Figure 3 - Effects of AgRP overexpression, in the PVN, on meal patterns

Graphs showing 24 hr food intake (A), 24h average meal size (D) and 24h average meal frequency (G) at day 20 and 40 post injection. The effects on food intake (B,C), average meal size (E,F) and meal frequency (H,I) in the light and dark period of day 20 and 40, respectively. Significance * $p < 0.05$, ** $p < 0.01$, *** $p < 0.001$ versus control group.

To investigate if the increase in daily food intake was due to a difference in the number of meals (meal frequency, a measure of meal initiation) or in meal size (a measure of satiation) meal patterns were analyzed on day 20 and day 40. Gene

expression from a rAAV vector increases during the first weeks to reach a plateau after 2-3 weeks (depending on AAV serotype and tissue), which is probably due to the fact that single stranded genome has to be converted into double stranded DNA (64, 258, 259). Therefore day 20 was analyzed in detail. Day 40 was chosen to compare the results to an earlier study, in which AAV mediated overexpression of NPY in the PVN resulted in compensatory changes after day 20. On day 40, food intake and body weight gain returned to levels similar to controls (255).

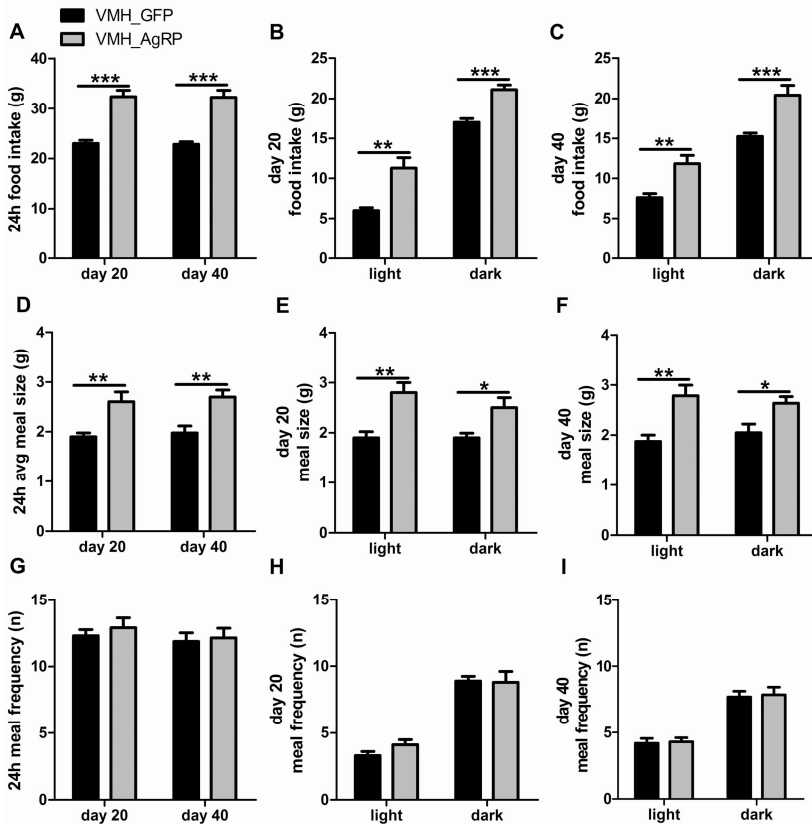


Figure 4 - Effects of AgRP overexpression, in the VMH, on meal patterns

Graphs showing 24 hr food intake (A), 24h average meal size (D) and 24h average meal frequency (G) at day 20 and 40 post injection. The effects on food intake (B,C), average meal size (E,F) and meal frequency (H,I) in the light and dark period of day 20 and 40, respectively.

Significance * $p < 0.05$, ** $p < 0.01$, *** $p < 0.001$ versus control group.

On day 20 and day 40 the 24h meal size of PVN-AgRP, VMH-AgRP and LH-AgRP was significantly increased compared to controls (Fig. 3D, 4D, 5D), while the 24h meal frequency was similar to the respective control groups (Fig. 3G, 4G, 5G). Both 24h meal size and frequency were not different between Acc-AgRP and Acc-GFP rats (Fig. 6D,G)

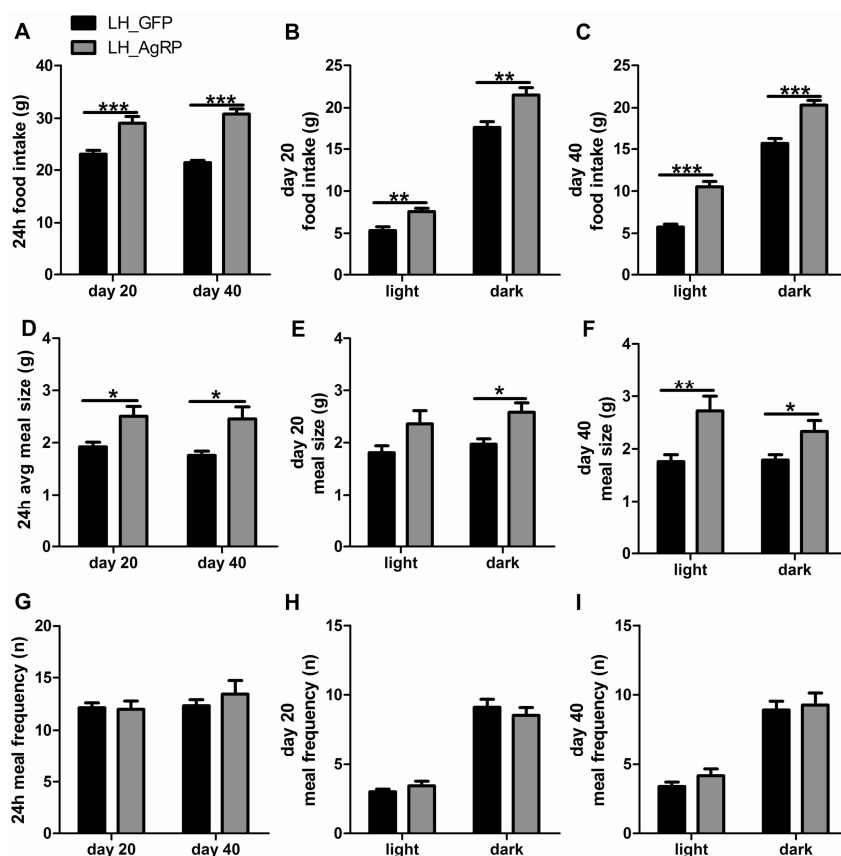


Figure 5 - Effects of AgRP overexpression, in the LH, on meal patterns

Graphs showing 24 hr food intake (A), 24h average meal size (D) and 24h average meal frequency (G) at day 20 and 40 post injection. The effects on food intake (B,C), average meal size (E,F) and meal frequency (H,I) in the light and dark period of day 20 and 40, respectively.

Significance * $p < 0.05$ ** $p < 0.01$, *** $p < 0.001$ versus control group.

On day 20 the increase in 24h food intake in PVN-AgRP rats was due to a significant increase in size and frequency in the light phase only (Fig. 3E, H). On day 40 the increase in 24h food intake of PVN-AgRP rats was due to a significant increase in meal size in both the light and dark phase (Fig. 3F). In addition, the frequency in the light phase was still increased in PVN-AgRP rats compared to PVN-GFP rats (Fig. 3I).

The VMH-AgRP rats showed an increase in food intake on day 20 and day 40. This increase was due to an increase in meal size in both the light and dark phase (Fig 4E,F). There was no difference between VMH-AgRP and VMH-GFP rats in meal frequency on day 20 and day 40 (Fig 4H,I).

The increase in food intake of LH-AgRP rats on day 20 was due to an increase in meal size, which was statistically significant in the dark phase (Fig. 5E). There was

no effect on meal frequency in the light or dark phase (Fig. 5H). On day 40 the increase in food intake of LH-AgRP rats was caused by increased meal size in both the light and dark phase (Fig. 5F). There was no difference in frequency between LH-AgRP and LH-GFP rats (Fig. 5I).

The Acc-AgRP rats were similar to Acc-GFP rats in meal size and frequency on both days in both light and dark phase (Fig 6E, F, H, I).

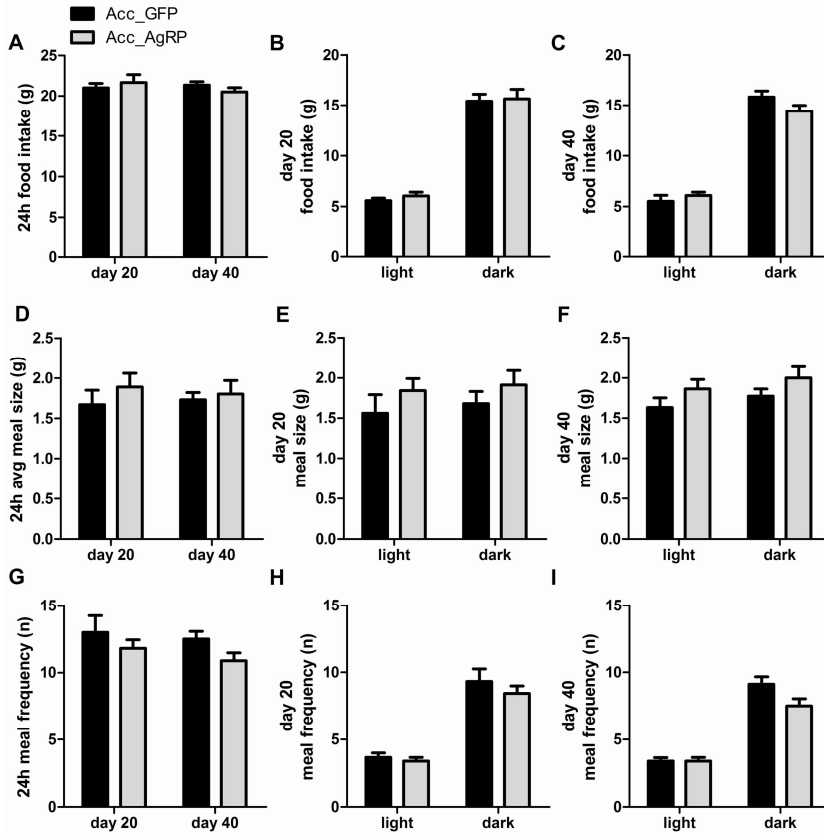


Figure 6 - Effects of AgRP overexpression, in the Acc, on meal patterns

Graphs showing 24 hr food intake (A), 24h average meal size (D) and 24h average meal frequency (G) at day 20 and 40 post injection. The effects on food intake (B, C), average meal size (E, F) and meal frequency (H, I) in the light and dark period of day 20 and 40, respectively.

Effects of rAAV-AgRP on body core temperature and locomotor activity

rAAV-AgRP had only modest effects on body core temperature and activity (Table 1).

Table 1- Effect of AAV-AgRP injections on average core body temperature and locomotor activity in light and dark period

	PVN-GFP	PVN-AgRP	LH-GFP	LH-AgRP	VMH-GFP	VMH-AgRP	acc-GFP	acc-AgRP
<i>Body temperature (°C)</i>								
Day 20								
Light	36.88 ± 0.06	37.05 ± 0.03	36.97 ± 0.02	36.98 ± 0.07	37.04 ± 0.05	37.00 ± 0.05	36.93 ± 0.02	36.92 ± 0.03
Dark	37.72 ± 0.04	37.60 ± 0.06	37.69 ± 0.04	37.62 ± 0.04	37.72 ± 0.07	37.58 ± 0.03	37.62 ± 0.03	37.68 ± 0.04
Day 40								
Light	36.92 ± 0.03	36.94 ± 0.03	36.99 ± 0.03	36.97 ± 0.03	37.04 ± 0.02	36.96 ± 0.07	36.87 ± 0.04	36.87 ± 0.03
Dark	37.62 ± 0.03	37.46 ± 0.07*	37.63 ± 0.04	37.54 ± 0.06	37.69 ± 0.06	37.44 ± 0.07*	37.57 ± 0.03	37.63 ± 0.04
<i>Activity (a.u.)</i>								
Day 20								
Light	86 ± 21	80 ± 9	67 ± 5	62 ± 9	66 ± 6	78 ± 10	88 ± 6	80 ± 11
Dark	310 ± 41	183 ± 25*	215 ± 14	196 ± 24	275 ± 45	184 ± 28	281 ± 13	246 ± 21
Day 40								
Light	77 ± 10	77 ± 7	60 ± 7	57 ± 11	50 ± 4	62 ± 9	82 ± 9	67 ± 6
Dark	257 ± 26	181 ± 21*	181 ± 18	154 ± 19	181 ± 17	147 ± 30	243 ± 21	224 ± 15

* p<0.05 versus control group

In the dark phase of day 40, the temperature of PVN-AgRP rats was significantly decreased. In addition, the temperature of VMH-AgRP rats was decreased in the dark phase of day 40. LH-AgRP and Acc-AgRP rats were similar in body temperature to their controls in both light and dark phase of day 20 and 40. Locomotor activity was decreased in the dark phase of day 20 and 40 in PVN-AgRP rats (Table 1). The LH-AgRP and Acc-AgRP rats showed no significant differences in their locomotor activity compared with their controls, whereas VMH-AgRP rats tended ($p=0.1542$) to decrease locomotor activity at day 20 in the dark phase.

Effects of rAAV-AgRP on endocrine parameters and body composition

The effects of AgRP overexpression in the PVN, VMH and LH on endocrine parameters and body composition are summarized in Table 2. PVN-AgRP, LH-AgRP and VMH-AgRP rats all had significantly increased amounts of subcutaneous and abdominal white adipose tissue compared to controls. Similarly, plasma concentration of leptin and insulin were significantly increased for each of these groups.

However, plasma leptin concentrations of PVN-AgRP and VMH-AgRP rats were significantly higher than leptin concentrations of LH-AgRP rats ($p=0.0253$ LH-AgRP vs. PVN-AgRP; $p=0.0431$ LH-AgRP vs. VMH-AgRP). Rats injected with AgRP in the Acc shell did not show any significant differences from controls. Furthermore, no differences were observed in plasma glucose concentrations or adrenal weights for any of the AgRP-group. However, the weight of the thymus was decreased in PVN-AgRP rats compared to controls.

Effects of rAAV-AgRP on neuropeptide expression

There were no differences in NPY, AgRP, POMC and SOCS3 mRNA levels in the arcuate nucleus between rAAV-AgRP rats and their controls in the PVN, VMH and LH (*NPY mRNA levels*: PVN-GFP 100 ± 6.2 ; PVN-AgRP 84.8 ± 17.9 ; VMH-GFP 100 ± 11.4 ; VMH-AgRP 100.4 ± 12.2 ; LH-GFP 100 ± 6.6 ; LH-AgRP 70.1 ± 14.3 . *AgRP mRNA levels*: PVN-GFP 100 ± 37.4 ; PVN-AgRP 115.8 ± 29.7 ; LH-GFP 100 ± 18.5 ; LH-AgRP 76.4 ± 12.9 . *POMC mRNA levels*: PVN-GFP: 100 ± 6.7 ; PVN-AgRP 106.5 ± 16.7 ; VMH-GFP 100 ± 8.4 ; VMH-AgRP 114.2 ± 16.7 ; LH-GFP 100 ± 18.7 , LH-AgRP 101.7 ± 8.8 . *SOCS3 mRNA levels*: PVN-GFP 100 ± 3.9 ; PVN-AgRP 88.2 ± 7.6 ; VMH-GFP 100 ± 4.3 ; VMH-AgRP 100.7 ± 6.5 ; LH-GFP 100 ± 4.2 ; LH-AgRP 96.5 ± 6.2). VMH-AgRP rats showed ectopic AgRP expression in VMH, which in many rats extended towards the arcuate nucleus; therefore we did not quantify AgRP expression in the arcuate nucleus of these animals.

Table 2- Effect of AAV-AgRP injections on endocrine parameters and body composition

	PVN-GFP	PVN-AgRP	LH-GFP	LH-AgRP	VMH-GFP	VMH-AgRP	acc-GFP	acc-AgRP
Leptin (ng/ml)	7.28 ± 0.87	37.84 ± 6.72***	8.24 ± 0.51	18.96 ± 3.95*	7.87 ± 0.41	35.98 ± 7.14***	7.59 ± 0.30	9.06 ± 0.83
Insulin (ng/ml)	2.53 ± 0.37	8.04 ± 1.42***	2.51 ± 0.31	7.09 ± 2.14	3.26 ± 0.32	7.60 ± 1.29**	2.97 ± 0.28	3.06 ± 0.18
Glucose (mmol/L)	9.45 ± 0.28	9.38 ± 0.47	8.68 ± 0.48	9.25 ± 0.37	9.22 ± 0.35	9.59 ± 0.49	9.70 ± 0.22	9.04 ± 0.45
SWAT (%bw)	0.93 ± 0.06	1.95 ± 0.17***	0.99 ± 0.03	1.65 ± 0.10***	0.91 ± 0.06	2.21 ± 0.12***	0.92 ± 0.06	0.99 ± 0.07
AWAT (%bw)	2.46 ± 0.18	4.44 ± 0.08***	2.48 ± 0.05	4.83 ± 0.05***	2.18 ± 0.09	4.39 ± 0.05**	2.21 ± 0.18	2.24 ± 0.13
Adrenals (% bw)	0.09 ± 0.007	0.08 ± 0.007	0.09 ± 0.006	0.09 ± 0.009	0.09 ± 0.013	0.07 ± 0.013	0.08 ± 0.010	0.06 ± 0.008
Thymus (% bw)	1.19 ± 0.08	0.85 ± 0.11*	1.16 ± 0.10	1.10 ± 0.05	1.02 ± 0.07	1.03 ± 0.07	1.19 ± 0.05	1.19 ± 0.06

SWAT: subcutaneous white adipose tissue; AWAT: abdominal white adipose tissue; % bw: dissected WAT/body weight*100; % bw: dissected tissue/body weight*1000. * $p < 0.05$, ** $p < 0.01$, *** $p < 0.001$ versus control group

Discussion

Reduced brain MC-R activity results in increased food intake and obesity, but it was poorly understood where in the brain this was mediated. In this study we showed that long term inhibition of the MC-R, by overexpression of AgRP, in either PVN, VMH or LH increased body weight gain, fat mass and food intake mainly by increasing meal size. The increase in caloric intake was clearly not an effect of global overexpression of AgRP in the hypothalamus, because rats with mistargeted AgRP overexpression in the hypothalamus were not different from controls.

Together these results suggest that chronic inhibition of MC-R activity at multiple sites in the hypothalamus contributes to the hyperphagia and obesity that are associated with reduced MC-R activity in knockout models and humans with mutations in MC4R. This is in agreement with data from local injections in the LH, VMH and PVN, which showed an increase in food intake after injection of AgRP₈₃₋₁₃₂ in these areas (190, 194, 254). Re-expression of the MC4R in the PVN and amygdala which normalized the hyperphagia seen in MC4R^{-/-} mice suggested that the PVN and amygdala are sufficient for the anorectic effect of melanocortins (176). However, regaining MC sensitivity in a MC4R knockout background clearly differs from reducing MC sensitivity in a wild-type background as was performed in this study. Our current study indicates that the PVN is probably not the only hypothalamic nucleus that contributes to hyperphagia when MC-R activity is reduced.

AgRP overexpression in the Acc shell did not have any effect on caloric intake, body weight gain or any other parameter measured in this study. This is in agreement with a previous study that showed that injections of the MC4R antagonist HS014 in the Acc did not alter food intake (191).

Effects on meal patterns

Hyperphagia can result from an increase in meal size, an increase in meal number or both. It has been hypothesized that meal size is a measure for satiation and that the number of meals is a measure for hunger (260, 261). For all hypothalamic nuclei injected, AgRP increased caloric intake by increasing meal size in both light and dark phase. This was similar for day 20 and day 40 and thus not compensated for over time. Overexpression of AgRP in the PVN, but not in the other targeted nuclei, resulted in different distribution of meals over the light-dark cycle, with more meals consumed in the light period, whereas total 24h frequency was not affected. The increase in meal size observed in this study is in accordance with previous studies which showed that MC-R antagonist increased meal size and not meal frequency (134, 262, 263). In addition, an agonist for the MC3R and MC4R specifically reduced meal size and not meal frequency (134, 264, 265). Taken together, our data suggest that inhibition of MC-R activity in the PVN, LH and VMH, decreases satiation irrespective of the time of day. This effect on satiation has also

been reported in humans with MC4R deficiency. During an *ad libitum* test meal, these patients eat larger meals, indicating a decrease in satiation, similar to our observations (266).

Effects on energy expenditure

Body temperature was differentially affected by AgRP depending on the area in which it was overexpressed. AgRP overexpression in the PVN or VMH reduced body temperature in the dark phase of day 40, whereas AgRP overexpression in the LH or Acc did not change body temperature. The decrease in body temperature shown in PVN and VMH rats may be due to the reduced levels of locomotor activity observed in these rats. A decrease in locomotor activity and core body temperature was previously reported after ICV administration of AgRP₈₃₋₁₃₂ (262, 267). In addition, 6 month old mice deficient of AgRP were reported to be hyperactive (170). However, re-expression of MC4R in the PVN and amygdala of MC4R^{-/-} mice had no effects on locomotor activity (176). MC3R^{-/-} mice did show a decrease in locomotor activity and MC3Rs are also expressed in the PVN (146, 157, 158). Therefore, reductions in locomotor activity by AgRP may be due to inhibition of MC3R.

Effects on body composition and endocrine parameters

The increase in body weight by AgRP overexpression in PVN, LH and VMH was reflected in the amount of white fat mass, which was also increased. As expected with larger fat mass, the plasma leptin concentrations were also increased in these groups. However, leptin concentrations in PVN-AgRP and VMH-AgRP rats were significantly higher than concentrations in the LH-AgRP rats, while all rats had comparable AWAT and SWAT percentages. A decrease in sympathetic nervous system (SNS) activity may have contributed to the increase in leptin secretion in VMH and PVN rats. Retrograde tracing experiments have shown that PVN, LH and VMH are connected to adipose tissue (268, 269, 270) and sixty percent of these projections from the brain to WAT and BAT co-express MC4R mRNA (269, 270). In addition, obese MC4R^{-/-} mice and humans were reported to have decreased SNS activity (271, 272) and ICV administration of MC-R ligands affected SNS activity (273).

Lesions in the VMH and PVN increase food intake and decrease sympathetic activity, while lesions in the LH decrease food intake and increase sympathetic activity (274, 275, 276, 277, 278). Thus the SNS activity is controlled in a similar manner in VMH and PVN, which clearly differs from LH. The SNS activity is relayed to the periphery via noradrenalin which binds β -adrenoreceptors and *in vitro* studies showed that β receptor agonists decreased leptin secretion by adipocytes (279, 280). Therefore, overexpression of AgRP in the LH may increase the levels of SNS activity, thereby decreasing leptin secretion by adipocytes, while

AgRP in the PVN and VMH decreases SNS activity and increases leptin secretion relative to the amount of WAT.

Table 3 - Comparison of parameters affected by AAV-NPY or AAV-AgRP overexpression in different brain areas at 20/21 days p.i.

DAY 20/21	PVN-AgRP	PVN-NPY	LH-AgRP	LH-NPY	VMH-AgRP	Acc-AgRP
Body weight gain	↑	↑	↑	↑	↑	-
Food intake	↑	L↑	↑	L↑	↑	-
Meal size	↑	-	↑	↑	↑	-
Meal frequency	L↑	L↑	-	-	-	-
Water intake	↑	↑	-	-	-	-
Body temperature	-	L↑, D↓	-	L↑, D↓	-	-
Locomotor activity	D↓*	D↓	-	↓	-	-

↑ increased by AgRP or NPY overexpression; ↓ decreased by AgRP or NPY overexpression; L: light phase; D: dark phase; * data to be interpreted with care

Table 4 - Comparison of parameters affected by AAV-NPY or AAV-AgRP overexpression in different brain areas at 40/48 days p.i.

DAY 40/48	PVN-AgRP	PVN-NPY	H-AgRP	LH-NPY	VMH-AgRP	Acc-AgRP
Body weight gain	↑	-	↑	↑	↑	-
Fat %	↑	↑	↑	↑	↑	-
Food intake	↑	L↑	↑	L↑	↑	-
Meal size	↑	-	↑	↑	↑	-
Meal frequency	L↑	-	-	-	-	-
Water intake	↑	-	-	-	↑	-
Body temperature	D↓	D↓	-	D↓	D↓	-
Locomotor activity	D↓*	D↓	-	D↓	-	-
Plasma leptin	↑	↑	↑	↑	↑	-
Plasma insulin	↑	↑	↑	↑	↑	-
Plasma glucose	-	↑	-	-	-	-

↑ increased by AgRP or NPY overexpression; ↓ decreased by AgRP or NPY overexpression; L: light phase; D: dark phase; * data to be interpreted with care

Comparison to AAV mediated overexpression of NPY

The orexigenic peptides, NPY and AgRP, are produced by the same neurons in the arcuate nucleus and NPY1R and MC4R co-localize in several brain areas, e.g. PVN and central amygdala (281). After binding to their receptors AgRP and NPY

both reduce cAMP levels (282, 283). Thus, one might expect that NPY and AgRP overexpression act similarly at projection sites of the arcuate nucleus to increase food intake and body weight. To test the validity of this assumption we compared our current data on AgRP overexpression in the LH and PVN with previous data on NPY overexpression in the same areas (255) (Table 3 and 4).

In the PVN clear differences were found between overexpression of the two peptides. Overexpression of NPY in the PVN temporarily increased food intake, but due to compensatory mechanisms food intake returned to control levels (199). The temporary increase in food intake was caused by a transient increase in meal frequency in the light period only. In contrast, AgRP overexpression in the PVN increased food intake during the entire experiment and was due to increase in meal size in both the light and dark period as well as an increase in meal frequency during the light period. In the LH both overexpression of NPY and AgRP increased food intake due to an increase in meal size without affecting meal frequency, during the entire experiment. Thus in the LH, AgRP and NPY show similar effects on meal patterns. However, energy expenditure appears to be differently regulated; overexpression of NPY in LH decreased locomotor activity and core body temperature, whereas AgRP overexpression in the LH did not affect these parameters.

Overexpression of NPY in both LH and PVN decreased the endogenous expression of AgRP mRNA in the arcuate nucleus, whereas overexpression of AgRP did not affect POMC, NPY, SOCS3 or AgRP mRNA in the ARC. This suggests that the effects of NPY overexpression can be partially compensated by an increase in MC-R signaling, while the effects of AgRP overexpression are not compensated by a decrease in NPY signaling.

The increased meal size which is associated with reduced MC-R activity is distributed over distinct hypothalamic nuclei. Nevertheless, there were brain area specific effects of AgRP on locomotor activity, body temperature, diurnal rhythm of food intake and plasma leptin concentrations. Finally, comparison of AgRP overexpression data with NPY overexpression data showed that although NPY and AgRP are co-released by ARC neurons, they affect food intake and energy expenditure through different mechanisms.

Acknowledgements

This work was supported by the Netherlands Organization for Scientific Research (NWO grant No. 90339175).

Chapter 5

A new method to deliver neuropeptides to the brain: a Von Willebrand factor signal peptide to direct local neuropeptide secretion

Marijke W.A. de Backer, Maïke A.D. Brans, Mienieke C.M. Luijendijk, Keith M. Garner, Dianne M.A. van den Heuvel, R. Jeroen Pasterkamp, Roger A.H. Adan

A NEW METHOD TO DELIVER NEUROPEPTIDES TO THE BRAIN: A VON WILLEBRAND FACTOR SIGNAL PEPTIDE TO DIRECT LOCAL NEUROPEPTIDE SECRETION

Abstract

Multiple neuropeptides, sometimes with opposing functions, can be produced from one precursor gene. To study the roles of the different neuropeptides encoded by one large precursor we developed a method to overexpress minigenes which were released locally. We fused the signal peptide from the Von Willebrand Factor (VWF) to a furin site followed by a processed form of the Agouti related protein (AgRP), AgRP₈₃₋₁₃₂ or α -melanocyte stimulating hormone. *In vitro*, these minigenes were secreted and biologically active. Additionally, the proteins of the minigenes were not transported into projections of primary neurons, thereby ensuring local release. *In vivo* administration of VWF-AgRP₈₃₋₁₃₂, using an adeno-associated viral vector as a delivery vehicle, in the rat paraventricular hypothalamus increased body weight and food intake compared to controls. This study demonstrated that changing the signal peptide of a neuropeptide for a VWF signal peptide is a successful strategy to deliver neuropeptides to the brain and establish local neuropeptide secretion.

Introduction

Numerous neuropeptide precursors have been implicated in the regulation of energy balance, such as pro-opiomelanocortin (POMC), melanin concentrating hormone (MCH) and ghrelin. Neuropeptide precursors have a signal peptide which translocates the neuropeptide precursors from the rough-endoplasmatic reticulum to the trans-golgi network (TGN). From the TGN the peptide precursors traffic into immature secretory vesicles where they are cleaved once or multiple times by prohormone convertases (PC) 1/3 and/or 2 to generate functional neuropeptides (284, 285, 286). Through budding and fusion the immature vesicles become mature, dense, vesicles which release their content upon a specific signal (287). The processing of neuropeptide precursors results in multiple biologically active peptides, sometimes with opposing effects; an example is the POMC gene. Pre-pro POMC is processed into several neuropeptides with anorexigenic function, e.g. α -melanocyte stimulating hormone (MSH) and β -MSH, but also an opioid with "orexigenic" function, namely β -endorphin (178, 288, 289, 290, 291). Loss of the whole POMC gene results in hyperphagia and obesity (164). Although there is strong evidence that the lack of melanocortin signaling in POMC knockout mice explains the phenotype, mice lacking only the β -endorphin part of the POMC gene are also hyperphagic and obese (292). Another example of a precursor gene that encodes for peptides with diverse effects is pre-pro-ghrelin which encodes for ghrelin, an appetite stimulating hormone, and obestatin, an appetite suppressing hormone (293). Therefore, it is important to determine the role of individual neuropeptides encoded by the precursor gene.

To investigate the role of specific neuropeptides, synthesized neuropeptides can be injected through intracerebroventricular (ICV) or local cannulae in the brain. However, there are drawbacks to these techniques. ICV administration of neuropeptides can be done long term, but administration is not local. In contrast, neuropeptides remain local with local cannulae, but these experiments are usually short term, because the cannulae can not be maintained over weeks. To overexpress neuropeptides locally and for long periods of time one can use viral vectors, such as the adeno-associated viral (AAV) vector (169, 230, 255). There are two problems with the long term overexpression of neuropeptide genes. Firstly, the precursor gene encodes for multiple peptides, which may serve different functions (see above). Therefore, overexpression of the precursor gene may show the effects multiple peptides. The second problem, with overexpression of neuropeptides via viral vectors, is that the neuropeptide is potentially released in the area the transduced neuron projects to rather than locally at the site of transduction; with AAV mediated overexpression of neuropeptide Y (NPY) in the paraventricular nucleus (PVN) (199, 255) the release of NPY may not be limited to the PVN. In the hypothalamus there are many interneurons and local connections, therefore NPY will probably be secreted locally. However, even in the absence of

staining in the projection areas one can not exclude that a projection neuron is releasing the neuropeptide elsewhere.

In order to circumvent that overexpression of a neuropeptide gene generates multiple messages and that the peptide may be released at distant sites, we developed an AAV vector based method to overcome these problems. In short, we fused a signal peptide with HA tag and furin site to the cDNA of a specific minigene, namely AgRP₈₃₋₁₃₂ or α -MSH. To prevent trafficking of the minigene into the regulated secretion pathway we used a signal peptide from the Von Willebrand Factor (VWF). This peptide has been described to primarily enter the constitutive pathway and is thus continuously secreted from the cell surface (294). A furin cleavage site was inserted between the signal peptide-HA tag and the minigene to release the minigene from the signal peptide. Furin is a ubiquitously expressed PC which is located in the TGN, instead of in secretory vesicles, and cycles back and forth to the plasma membrane (295, 296, 297).

We used the cDNA of AgRP₈₃₋₁₃₂, because this is the main secreted form of AgRP after processing by PC (267). AgRP is an inverse agonist for the MC3R and MC4R and stimulates food intake and reduces energy expenditure, while α -MSH is a peptide derived from the POMC gene and is able to activate the MC3R and MC4R to inhibit food intake and increase energy expenditure (162, 178, 187, 188, 248). AgRP and α -MSH compete to bind to the MC4R and the balance between these peptides determines the activity of the MC4R.

Material and methods

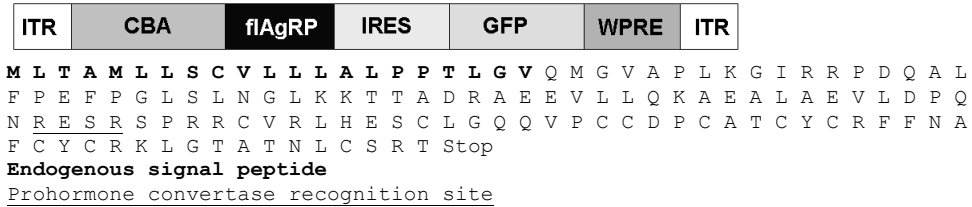
Cell lines and constructs

Human embryonic kidney (HEK) 293T cells were maintained at 37°C with 5% CO₂ in Dulbecco's modified Eagles medium (DMEM) supplemented with 10% fetal calf serum (FCS), 2mM glutamine, 100 units/ml penicillin, 100 units/ml streptomycin and non-essential amino acids.

pAAV-CBA-GFP with AAV2 inverted terminal resolutions sites, was previously described (207) and was a kind gift from M. Sena-Esteves. pAAV-CBA-flAgRP-ires-GFP (Fig. 1) was constructed by cloning the full length mouse Agouti-related protein (AgRP) cDNA in pIRES2-EGFP (Clontech). Subsequently, AgRP-ires-EGFP was isolated and ligated in pAAV-CBA-GFP-WPRE, after removing GFP from the AAV plasmid. Agel-furin-AgRP₈₃₋₁₃₂-EcoRI was made by PCR on AgRP-ires-GFP with the following primers: Agrp83f: 5' GATCCAACCGGTGCGAAGCGT CGTTCTCCGCGTCGCTGTGTAA and ires reverse long: 5' CGGCTTCGCCAG TAACGTTAGGGGGGGGGAGGGAGA. The PCR fragment was subsequently digested with Agel and EcoRI and ligated into Agel- EcoRI digested pCMV-VWF- α MSH4-ires-GFP resulting in pCMV-VWF-AgRP₈₃₋₁₃₂-ires-GFP. pCMV-VWF-

α MSH1-ires-GFP and pCMV-VWF- α MSH4-ires-GFP were described elsewhere (298).

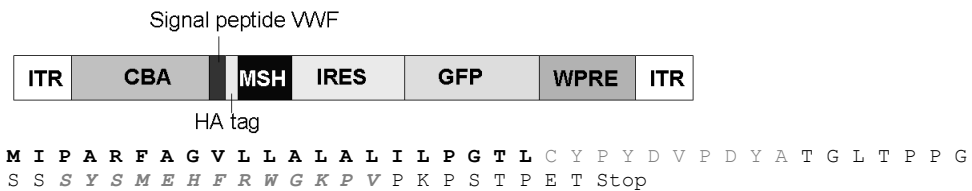
AAV-CBA-flAgRP-ires-gfp



AAV-CBA-VWF-AgRP₈₃₋₁₃₂-ires-gfp



AAV-CBA-VWF- α -MSH1



AAV-CBA-VWF- α -MSH4

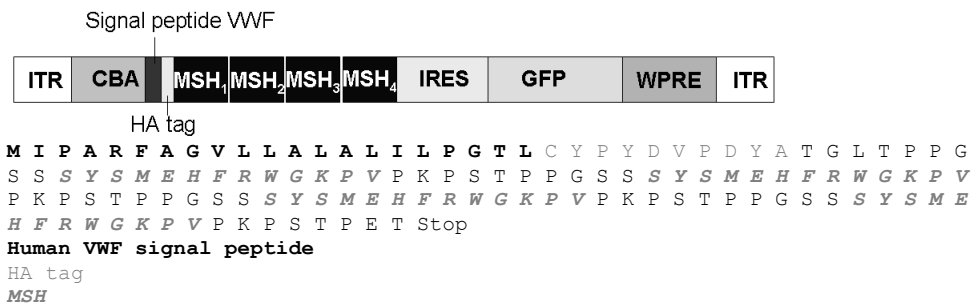


Figure 1 – Overview of the vectors used in this study

The three pCMV-VWF-neuropeptide-ires-GFP vectors were digested with Afel-BsrGI and the VWF-neuropeptide-ires-GFP parts were isolated and inserted in pAAV-CBA-GFP, resulting in pCBA-VWF-AgRP₈₃₋₁₃₂-ires-gfp, pCBA-VWF-

α MSH1-ires-GFP and pCBA-VWF- α MSH4-ires-GFP (Fig. 1). Sequences were verified by sequence analysis.

The pDP1 helper plasmid used to produce AAV vectors has been described (211) and was obtained from Plasmid factory (Bielefeld, Germany).

LacZ reporter gene assay

Activation of the MC4R was determined using LacZ as a reporter gene (299). DNA was transfected into cells with polyethylenimine (210). Fifty nanograms of human MC4R and 10 μ g of cAMP-responsive element (CRE)-LacZ were transfected into 293T cells on 10cm dishes. Another five 10cm dishes with 293T cells were transfected with 10 μ g of respectively pAAV-GFP, pAAV-flAgRP, pAAV-VWF-AgRP₈₃₋₁₃₂, pAAV-VWF- α MSH1 and pAAV-VWF- α MSH4. One day after transfection the MC4R_CRE-LacZ cells were transferred to poly-L-lysine coated 96-wells plates. Three days after transfection supernatant of 10cm dishes was removed and used for LacZ reporter assay. At this day the medium was removed from MC4R_CRE_LacZ transfected cells and replaced with assay buffer (DMEM containing 0.2% BSA, 25mM hepes and 30 μ g/ml aprotinin) supplemented with NDP-MSH alone or in combination with conditioned supernatants of cells transfected with flAgRP, VWF-AgRP₈₃₋₁₃₂ or GFP. In addition only forskolin was added to other wells as a positive control for CRE-LacZ transfection and the subsequent colometric reaction. The medium of another plate with MC4R_CRE-LacZ transfected cells was replaced with assay buffer containing serial dilutions of conditioned medium from cells transfected with α MSH1, α MSH4 or GFP. As assay controls only NDP-MSH or forskolin were added to other wells of this plate. After 5-6 hour incubation at 37°C the assay medium was removed and replaced by 40 μ l lysisbuffer (phosphate buffered saline (PBS) containing 0.1% Triton-X-100). The plates were stored at -20°C. After thawing of the plates, 80 μ l of substrate (0.1M phosphate buffer, pH7.4, containing 1.6 g/l o-nitrophenyl β -D-galactopyranoside (ONPG, Invitrogen, the Netherlands), 67.5 mM β -mercaptoethanol (Merck, Germany) and 1.5mM magnesium chloride) was added to each well. Absorbance at 405 nm was measured in a Victor² microplate reader (PerkinElmer, Brussels, Belgium).

Spot blot

To determine the amount of protein secreted into the medium of 293T cells transfected with flAgRP, VWF-AgRP₈₃₋₁₃₂ and GFP a spot blot was performed. A serial dilution of the medium was made in water. The first dilution was 20 times followed by 5 times dilutions. Subsequently 1 μ l of undiluted and diluted conditioned medium was spotted on Hybond-C extra. The blot was dried and blocked for 10 minutes in PBS containing 0.05% Tween-20 (PBS-T) and 5% milk. Afterwards the blot was incubated with a rabbit-AgRP antibody (1:1.000; a kind gift

of G. Barsh) in PBS-T for 90 minutes, washed three times 10 minutes with PBS-T and incubated for 60 minutes with goat-anti-rabbit horse-radish peroxidase (1:20.000) in PBS-T. After three washes with PBS-T and one wash with PBS the spots were developed with SuperSignal West Dura extended duration substrate (Thermo scientific) and exposed to a CL-film.

AAV production

Each AAV production was performed with 15 dishes of 80-90% confluent 293T cells at day of transfection. Two hours before transfection, the 10% FCS-DMEM was replaced with 2% FCS-DMEM. The transfections were performed with polyethylenimine (PEI) as described by Reed S.E. et al. (210). The pAAV plasmids were co-transfected helper plasmid pDp1 in a molar ratio of 1:1. The transfection mix remained on the cells until the next day, then the 2% FCS-DMEM was refreshed. The purification was performed as described by Zolotukhin et al. (212). The titer, in genomic copies per ml (g.c./ ml), was determined by qPCR with sybergreen mix in a LightCycler (Roche) (213). The qPCR primers were designed to detect BGHpolyA and were BGHpolyA_F: 5' CCTCGACTGTGCCTTCTAG; BGHpolyA_R: 5' CCCCAGAATAGAATGACACCTA. The titers were AAV-CBA-GFP 1×10^{13} g.c./ml; AAV-CBA-flAgRP 1.7×10^{14} g.c./ml AAV-CBA-VWF-AgRP₈₃₋₁₃₂ 3×10^{12} g.c./ml; AAV-CBA- α MSH4 2.7×10^{14} g.c./ml. To obtain titer matched AAV preps, preps were diluted in PBS.

Animals

All experimental procedures were approved by the Committee for Animal Experimentation of the University of Utrecht (Utrecht, The Netherlands). C57BL/6 mice were obtained from Charles River. Timed-pregnant mice were killed by means of cervical dislocation. The morning on which a vaginal plug was detected was considered embryonic day 0.5 (E0.5).

Male Wistar rats, weight ranging from 220–250 g, were purchased from Charles River. All rats were individually housed in filtertop cages with *ad libitum* access to food (CRM pellets; Special Diet Services, Whitham, Essex, UK) and water. Animals were kept in a temperature- and humidity-controlled room ($21 \pm 2^\circ\text{C}$) with a 12 h light/dark cycle (lights on at 7:00 A.M.).

Primary cortical neuron cultures

Cerebral cortices of E16.5 mouse embryos were dissected and dissociated by incubation with 0.25% trypsin at 37°C for 10-15 minutes, followed by tissue trituration with a fire-polished Pasteur pipet in DMEM containing 10% FCS and 20 $\mu\text{g}/\text{ml}$ DNaseI. After dissociation, the medium was removed and cells were resuspended in Neurobasal medium containing B27 supplement. Dissociated cells were plated at a density of 12.000 cells per well on poly-D-Lysin- (100 $\mu\text{g}/\text{ml}$;

Sigma, Zwijndrecht, The Netherlands) and laminin- (40 µg/ml; Invitrogen, Breda, The Netherlands) coated glass coverslips in 24 well plates. Neuronal cultures were maintained in a humidified incubator at 37°C and 5% CO₂. After two days in culture, half of the medium was replaced with fresh maintenance medium (Neurobasal medium with B27). Two hours later neurons were infected with the different AAV vectors at multiplicity of infection 10.000 (thus 1.2×10^8 g.c. of AAV vector added per well). Seventy-two hours after infection neurons were washed twice with PBS, fixed with 4% paraformaldehyde for 30 minutes and stored in PBS at 4°C.

Immunohistochemistry

Fixed neurons were washed twice with PBS. After 30 minutes incubation in block-t (PBS containing 1% FCS and 0.1% Triton-X-100) neurons were incubated overnight with block-t containing rabbit anti-AgRP antibody (1:1000, a kind gift from G. Barsh) and mouse anti-βIII-tubulin (1:3000, Sigma) at 4°C. The next day neurons were washed 3 times with PBS-t (PBS containing 0.1% Triton-X-100) and incubated for 60 minutes with secondary antibodies (goat-anti-mouse alexa555 (1:500) and goat-anti-rabbit alexa488 (1:500) (Invitrogen) in block buffer (PBS containing 1% FCS). Afterwards neurons were washed 3 times with PBS, incubated with DAPI (1:3000, Sigma) for 5 minutes, washed 3 times with PBS and mounted in 90% glycerol in PBS.

In vivo AAV injections

Six rats were anesthetized with 0.1 ml/100 g Hypnorm intramuscular (Janssen Pharmaceutica, Beerse, Belgium) and 0.05 ml/100 g Dormicum intraperitoneal (Hoffman-LaRoche, Mijdrecht, The Netherlands). Rimadyl (Pfizer animal health, Capelle a/d IJssel, the Netherlands) was administrated as pain medication before surgery and on day 1 and 2 after surgery. Subsequently, the rats were injected bilaterally in the paraventricular nucleus (PVN, coordinates AP -1.8, ML +1.7, DV -8.1, angle 10 degrees) with 1 µl of AAV-CBA-GFP or AAV-CBA-VWF-AgRP₈₃₋₁₃₂. The injected volume contained 1×10^9 g.c. of AAV vector and was delivered at a rate of 0.2 µl/ minute. After the injection the needle remained in the injection site for 10 minutes. Four weeks after injection the rats were decapitated, the brains were removed, quickly frozen on dry-ice and stored at -80°C until they were sectioned on a cryostat (Leica, The Netherlands) at 20 µm, in series of 10. Serie 1 was used for *in situ* hybridization with GFP-dig labeled mRNA probe to show the transduction area of the AAV vectors and serie 2 for a Nissl staining to show the overall morphology of the brain. Body weight and food intake data of animals with correct injection sites, as determined with GFP ISH, were used for behavioral analysis.

In situ hybridization

In situ hybridization was performed with a 720 basepair long digoxigenin (DIG)-labeled eGFP riboprobe (antisense to NCBI gene DQ768212) as described by Schaeren-Wiemers and Gerfin-Moser (244) with small modifications in the fixation procedure and hybridization temperature. Sections were fixed in 4% PFA for 20 minutes and hybridization was performed at 72°C.

Data analysis

Data were analyzed with GraphPad Prism (GraphPad Software Inc., California). Competition curves were fitted from duplicate data points using sigmoidal dose response curve with variable slope. Body weight gain and food intake were tested with two sided *t*-test.

Results

VWF-AgRP₈₃₋₁₃₂ and VWF-αMSH are secreted and biologically active

To investigate if peptides produced from constructs with a VWF signal peptide followed by a cleavage site and a neuropeptide are secreted and are biologically active, we tested whether the medium of cells transfected with the VWF-AgRP₈₃₋₁₃₂ constructs was able to antagonize the MC4R. The ability of the VWF-AgRP₈₃₋₁₃₂ to shift the NDP-MSH dose response curve to the right was compared to a construct encoding for full length AgRP, containing the normal AgRP signal peptide.

Activation of MC4R *in vitro* results in an increase in cyclic adenosine monophosphate (cAMP)(300). In our assay upregulation of cAMP increased LacZ expression through a cAMP responsive element.

Addition of NDP-MSH to MC4R and CRE-LacZ transfected cells resulted in a dose response curve with an EC₅₀ value of 0.1 nM (1×10^{-10}). Another control was the addition of forskolin to MC4R_Cre-LacZ transfected cells (Fig. 2A). Forskolin directly activates adenylyl cyclase, thereby increasing cAMP. When supernatants of GFP transfected cells were added together with different concentrations of NDP-MSH to MC4R_CRE-LacZ transfected cells, the dose response curve did not alter. However, addition of supernatants of fAgRP or VWF-AgRP₈₃₋₁₃₂ transfected cells shifted the NDP-MSH dose response curve to the right. The EC₅₀ decreased to 1.4 and 0.5 nM, respectively when 10% of the volume added was supernatant (Fig. 2B). When 50% of the volume added to the MC4R_CRE-LacZ cells was supernatant from fAgRP or VWF-AgRP₈₃₋₁₃₂ the NDP-MSH dose response curve shifted even further to the right (Fig. 2C). In order to determine the amount of secreted AgRP protein, supernatants were analyzed on a spot blot (data not shown). This blot showed that 18.2-fold less AgRP was secreted from the VWF-AgRP₈₃₋₁₃₂ transfected cells compared to fAgRP transfected cells, even though the transfection efficiencies were similar.

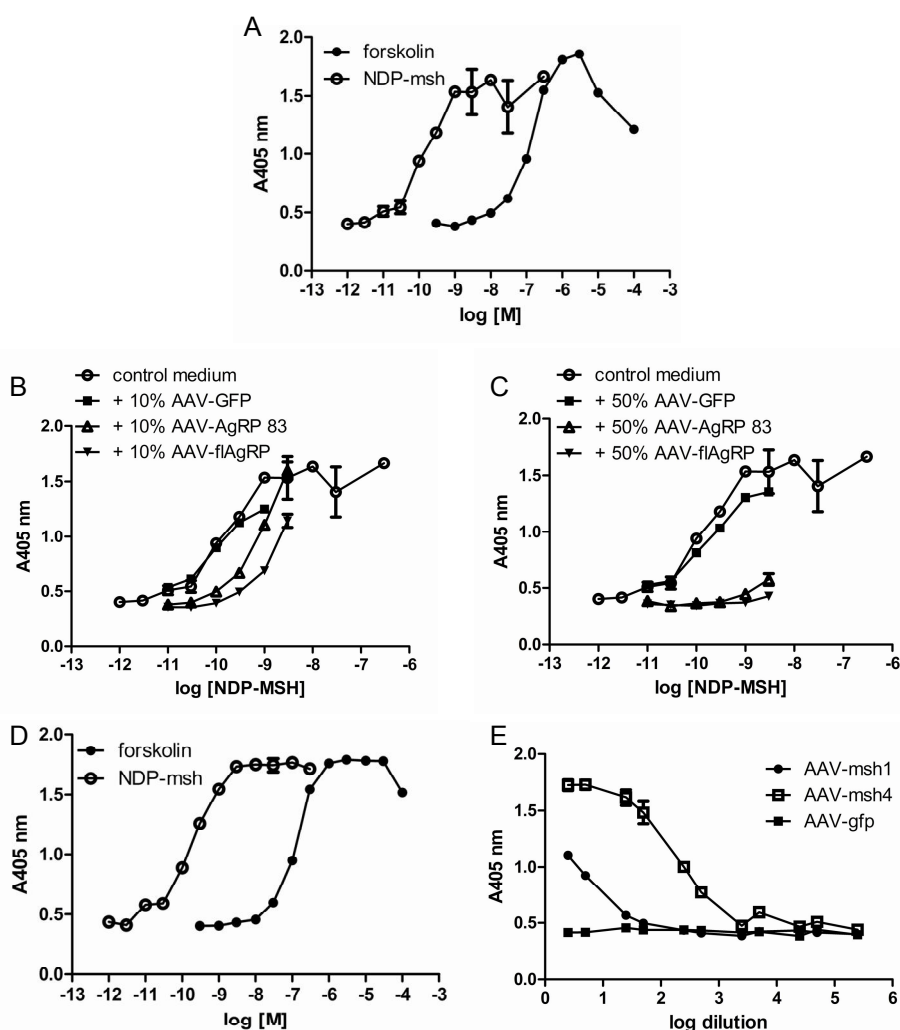


Figure 2 - VWF-proteins are secreted and biologically active

A: Dose-response curve of NDP-MSH and forskolin showing their ability to stimulate 293T cells transfected with MC4R and cAMP sensitive reporter gene. **B:** similar as 2A, but in the presence of 10% of conditioned medium from 293T cells transfected with AAV-CBA-GFP, AAV-CBA- Δ AgRP or AAV-CBA-VWF-AgRP₈₃₋₁₃₂. **C:** similar as 2B, but with 50% of conditioned medium. **D:** dose-response curve of NDP-MSH and forskolin as positive control for MC4R and CRE-LacZ transfection. **E:** response curve of cells transfected with MC4R and CRE-LacZ incubated with different dilutions of conditioned medium. Medium was taken from cells transfected with AAV-CBA-GFP, AAV-CBA-MSH1 or AAV-CBA-MSH4.

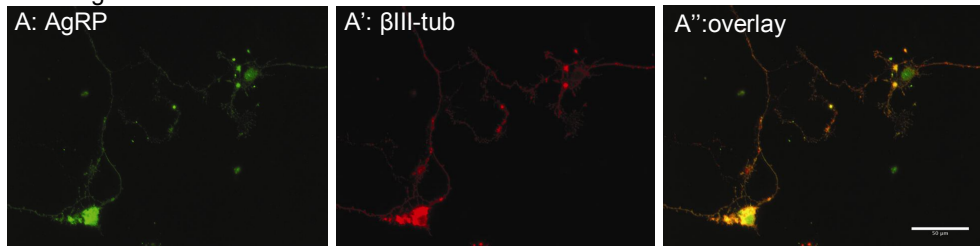
To check if monomeric VWF- α MSH1 and polymeric VWF- α MSH4 were able to activate the MC4R, different dilutions of supernatants from cells transfected with these constructs were added to MC4R_CRE-LacZ transfected cells. Supernatants of both constructs activated the MC4R, with the polymeric VWF- α MSH4 being more potent. The polymeric VWF- α MSH4 reached 50% of MC4R activation at a

dilution of 216 times, while VWF- α MSH1 already reached 50% activation of MC4-R after 10.7 times dilution. The supernatant of GFP transfected cells was not able to activate the MC4R (Fig 2E).

Localization of flAgRP and VWF-AgRP₈₃₋₁₃₂ in primary neurons.

We compared the localization of AgRP in primary cortical neurons which were infected with AAV-flAgRP or AAV-VWF-AgRP₈₃₋₁₃₂ to check if AAV-VWF-AgRP₈₃₋₁₃₂ entered the regulated secretion pathway. Three days after infection the primary cortical neurons were stained for AgRP. In addition, β -tubulin-III was used to stain the cytoskeleton of neurons and DAPI to identify the cell nucleus.

AAV-flAgRP



AAV-VWF-AgRP₈₃₋₁₃₂

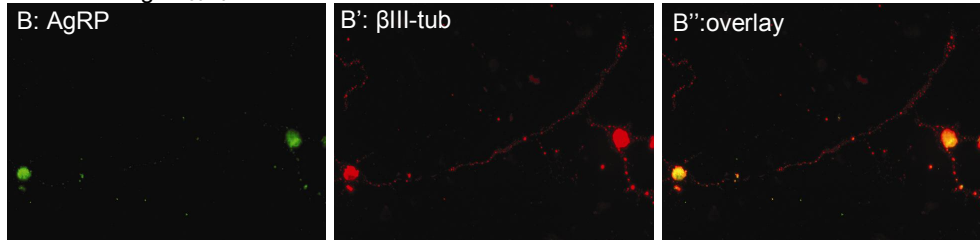


Figure 3 - Fluorescent immunostaining showing the localization of flAgRP versus VWF-AgRP₈₃₋₁₃₂.

132

Primary cortical neurons were infected with AAV-flAgRP-ires-gfp (**A**) or AAV-VWF-AgRP₈₃₋₁₃₂ (**B**) at a multiplicity of infection of 10.000. Seventy hours after infection neurons were fixed and immunostained for AgRP (green (**A** and **B**) and β III-tubulin (red (**A'** and **B'**)). "shows overlay of the green and red signal (**A''** and **B''**)).

Neurons transduced with AAV-CBA-flAgRP, which contained the endogenous signal peptide to target AgRP into the regulated secretory pathways, showed AgRP immunostaining in their cell bodies and their branches. In contrast, AAV-CBA-VWF-AgRP₈₃₋₁₃₂ transduced neurons only showed AgRP immunostaining in the cell bodies and almost no staining in the branches (Fig. 3).

Behavioral effects of AAV-VWF-AgRP₈₃₋₁₃₂

To further prove the functionality of AAV-VWF-AgRP₈₃₋₁₃₂, this virus was also injected in the PVN of rats. One μl containing 1×10^9 genomic copies of AAV-VWF-AgRP₈₃₋₁₃₂ or AAV-GFP was injected in the PVN. In situ hybridization against GFP showed that the PVN was transduced (unilaterally). Overexpression of AAV-VWF-AgRP₈₃₋₁₃₂ increased daily food intake when compared to titer matched AAV-GFP injected rats ($p=0.049$) (Fig. 4A). In addition, the AAV-VWF-AgRP₈₃₋₁₃₂ rats showed a significant increase in body weight gain compared to AAV-GFP rats ($p=0.0032$) from day 0 until day 28 post injection (Fig. 4B).

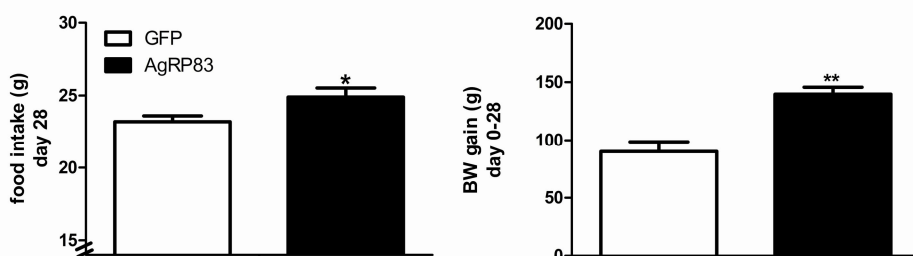


Figure 4 - In vivo effects of AAV-VWF-AgRP₈₃₋₁₃₂ on energy balance

AAV-VWF-AgRP₈₃₋₁₃₂ increased food intake (A, $p=0.049$) and BW gain (B, $p=0.0032$) compared to AAV-GFP. The PVN was unilateral transduced with $1\mu\text{l}$ containing 1×10^9 g.c. of AAV-VWF-AgRP₈₃₋₁₃₂. Data at 28 days post injection. * $p<0.05$, ** $p<0.01$ compared to AAV-GFP.

Discussion

We here successfully demonstrate a novel approach to locally overexpress a individual neuropeptide rather than a whole neuropeptide precursor. This was achieved by fusing a neuropeptide minigene to the VWF signal peptide in a rAAV vector. We demonstrated that the neuropeptide minigene was released from the cell body and did not enter the regulated secretory pathway *in vitro*. In addition, we showed that the delivery of the neuropeptide minigene, using AAV, to neurons of the PVN resulted in an increased food intake and body weight. This demonstrated that this method to deliver AgRP locally in the brain was effective.

Previous studies have shown that specific signal peptides could route a protein to the regulated pathway. Fusion of GFP to NPY or insulin signal sequence was sufficient to route GFP to regulated secretory granules and resulted in GFP secretion at axon terminals (301, 302). In this study we showed that it is also possible to route peptides into the constitutive secretion pathway resulting in secretion by the cell body, through the use of the VWF signal peptide. We replaced the endogenous signal peptide and cleavage site for a VWF signal peptide and a furin cleavage site. To obtain long term expression of the neuropeptide minigenes we embedded these DNA constructs in an rAAV vector. During our study a paper was published which described a method to deliver two gene products, GFP and

galanin, from one rAAV vector (303). They placed a furin sequence between the two genes and the first gene was fused to a fibronectin secretory signal peptide to cause the products to be constitutively secreted. This confirmed the feasibility of using furin as a cleavage site.

First we investigated if the vectors with the VWF signal peptide are secreted into the medium and compared this with a vector with its endogenous signal peptide. The MC4R_CRE-LacZ assay showed that VWF-AgRP₈₃₋₁₃₂ and VWF-αMSH1 and VWF-αMSH4 were secreted by 293T cells into the culture medium. The secreted peptides were also biologically active since the medium could, respectively, inhibit or activate the MC4R. The medium of cells transfected with fAgRP vector, containing the endogenous AgRP signal peptide, also inhibited the MC4R. However, the inhibition by fAgRP was stronger than the inhibition caused by medium from VWF-AgRP₈₃₋₁₃₂ transfected cells. After the MC4R assay we determined the amount of protein secreted in the medium of the cells. This revealed that there was 18.2 fold less AgRP immunoreactivity in the medium of VWF-AgRP₈₃₋₁₃₂ transfected cells than in the medium of fAgRP. The difference in potency between VWF-AgRP₈₃₋₁₃₂ and fAgRP to antagonize NDP-MSH, 0.5 versus 1.4 nM respectively, is in the range which we expected, since a study by Creemers et. al. showed that AgRP₈₃₋₁₃₂ was 6.1 fold more potent than fAgRP in inhibiting the MC4R (267). Thus, given the amount of peptide release (18.2 fold less secretion of VWF-AgRP₈₃₋₁₃₂ than fAgRP) and potencies (VWF-AgRP₈₃₋₁₃₂ approximately 3 times less potent than fAgRP) our results are in agreement with the study by Creemers et al that VWF-AgRP₈₃₋₁₃₂ is 6 times more potent than fAgRP.

Medium from cells transfected with AAV-VWF-αMSH4 was more potent in activating MC4R_CRE-LacZ than medium from AAV-VWF-αMSH1 transfected cells. Medium from GFP transfected cells was not able to stimulate MC4R_CRE-LacZ. These data are in agreement with previous data (298).

In addition, we compared the localization of fAgRP and VWF-AgRP₈₃₋₁₃₂ in primary neuronal cultures. These results showed that fAgRP was expressed in the cell body and in the projections and that VWF-AgRP₈₃₋₁₃₂ was only expressed in the cell body and not in the projections. These results were in agreement with the expectation: peptides coupled to the VWF signal peptide entered the constitutive secretion pathway and the one coupled to the endogenous AgRP signal peptide entered the regulated secretion pathway in the axons.

As a proof of principle we showed that unilateral overexpression with the VWF-AgRP₈₃₋₁₃₂ AAV vector in a target area of AgRP neurons, the PVN, increased food intake. This showed that the VWF-AgRP₈₃₋₁₃₂ is also functional *in vivo*.

This study showed that it is possible to overexpress a single neuropeptide derived from a large precursor and establish long term release, local to the transduced area, through the use of a VWF signal peptide.

Acknowledgements

We gratefully acknowledge dr. Tom Vink for his assistance in the design of the VWF-vector.

This work was supported by the Netherlands Organization for Scientific Research (NWO grant No. 90339175).

Chapter 6

Suppressor of cytokine signaling (Socs) 3 knockdown in the mediobasal hypothalamus: counterintuitive effects on energy balance

Marijke W.A. de Backer¹, Maïke A.D. Brans¹, Rea J. van Rozen¹, Esther M. van der Zwaal¹, Mienieke C.M. Luijendijk¹, Keith G. Garner¹, Mariken de Krom¹, Olivier van Beekum¹, Susanne E. la Fleur^{\$1,2}, R.A.H. Adan^{\$1}

\$ shared last authorship

¹ Rudolf Magnus Institute of Neuroscience, Department of Neuroscience and Pharmacology, University Medical Centre Utrecht, Utrecht, the Netherlands.

² Department of Endocrinology and Metabolism, Academic Medical Center, University of Amsterdam, Amsterdam, the Netherlands.

SUPPRESSOR OF CYTOKINE SIGNALIN (Socs) 3 KNOCKDOWN IN THE MADIOBASAL HYPOTHALAMUS: COUNTERINTUITIVE EFFECTS ON ENERGY BALANCE

Abstract

An increase in suppressor of cytokine signaling 3 (Socs3) has been implicated in the development of both leptin and insulin resistance. Furthermore, neuronal deletion of Socs3 has been shown to protect against diet-induced obesity. However, Socs3 mRNA is localized throughout the brain and it remains unclear which brain areas are involved in the effect of Socs3 levels on energy balance. Therefore, we determined the role of Socs3 expressed in the mediobasal hypothalamus (MBH) in the development of diet-induced obesity in adult rats. Socs3 mRNA was downregulated in the MBH, by local injection of adeno-associated viral (AAV) vectors expressing a short hairpin directed against Socs3, after which we determined the response to a high fat high sucrose choice diet. In contrast to neuronal Socs3 knockout mice, rats with Socs3 knockdown limited to the MBH showed increased body weight gain, larger amounts of white adipose tissue and higher leptin concentrations at the end of the experiment. These effects were partly due to the decrease in locomotor activity, as 24 hour food intake was comparable with controls. In addition, rats with Socs3 knockdown in the MBH showed altered meal patterns; an increase in average meal size in the light period that was accompanied by a compensatory decrease in meal frequency in the dark period. Finally, in situ hybridization revealed that NPY mRNA levels were significantly increased in the arcuate nucleus of Socs3 knockdown rats. Together these data suggest that knockdown of Socs3 mRNA limited to the MBH increases NPY mRNA levels, which subsequently decreases locomotor activity and alters feeding patterns.

Introduction

Obesity has been associated with leptin resistance in both humans and rodents. Although leptin normally reduces food intake, obese humans and rodents still overconsume calories despite their increased leptin levels (101, 107, 108). In addition, after injection of exogenous leptin, obese humans and rodents do not respond with the decrease in food intake, that is normally observed in lean subjects and rodents (109, 304, 305, 306). Several mechanisms have been proposed to mediate this leptin resistance e.g. impaired transport of leptin over the blood-brain barrier, impaired leptin receptor b (LEPRb) expression and impaired LEPRb signaling (see review (102)). When leptin binds to the LEPRb, one of the pathways activated is JAK2-STAT3 cascade (111). Phosphorylated STAT3 enters the nucleus and serves as a transcription factor, increasing the transcription of several genes including Socs3. In turn, Socs3 inhibits leptin signaling through binding to JAK2 and phosphorylated tyrosine 985 on the LEPRb (111, 112). Thus Socs3 appears to act as a negative feedback regulator to prevent overactivation of leptin signaling. It has been shown that administration of leptin increases Socs3 mRNA in lean animals and that Socs3 mRNA levels are elevated in hypothalami of obese animals (110, 113, 114, 115, 116, 117). Together this suggests that Socs3 plays an important role in the development of leptin resistance and obesity.

The importance of Socs3 in leptin resistance and diet-induced obesity is supported by studies examining the phenotype of mice with altered Socs3 alleles. Although Socs3 knockout mice die at midgestation because of placenta failure (307), heterozygous Socs3^{+/-} and neuronal Socs3-deficient animals are viable (119, 120). These studies showed that Socs3^{+/-} and neuronal Socs3^{-/-} mice had normal body weight gain on a chow-diet, but that they were more sensitive to leptin treatment than their wild type littermates. Moreover, Socs3^{+/-} and neuronal Socs3^{-/-} mice were resistant to diet-induced obesity when placed on a high-fat diet (119, 120).

Although deletion of genes by homologous recombination in mice has greatly contributed to understand how genes affect energy balance, there are also limitations to what extent full deletion of a gene can teach us about the role of this gene in physiology. There may occur compensation for the loss of gene expression by redundant genes, interference by selection markers, effects due to background strain and development defects. Therefore, we performed complementary experiments to investigate the role of Socs3 levels in the mediobasal hypothalamus (MBH) in the susceptibility to diet-induced obesity, via adeno-associated viral (AAV) vector-mediated knockdown of Socs3.

Material and Methods

Cell lines and plasmids

Human embryonic kidney (HEK) 293T cells were maintained at 37°C with 5% CO₂ in Dulbecco's modified Eagles medium (DMEM) supplemented with 10% fetal calf serum (FCS), 2mM glutamine, 100 units/ml penicillin, 100 units/ml streptomycin and non-essential amino acids.

pAAV-shCTRL (sh-c) and pAAV-shbase were a kind gift from R.J. Dileone (308). We used bioinformatics tools on the website of Biopredsi and Invitrogen to identify possible functional siRNA/shRNA sequences against Socs3 gene of the rat. We ordered four sets of two oligonucleotides (Stratagene) with SapI and XbaI overhangs (sh-1 to sh-4). These oligonucleotides were annealed and ligated into SapI and XbaI restricted pAAV-shbase (Fig. 1). The shRNA was driven by a mouse U6 promotor and after the shRNA sequence there was a terminator sequence. In addition, this plasmid also expressed GFP under a CMV promoter hybridized to a β -actin intron. The GFP gene was followed by an independent terminator sequence.

The Socs3 rat cDNA was obtained through PCR with *Pfu* on hypothalamic rat cDNA with the following primers: Socs3-g-F-2: 5' AGACACAGTCTTCAGCGGG T and Socs3-g-R-2: 5' AGAGTCCGCTTGTCATGCT. The Socs3 PCR product was ligated in PCR-script. Subsequently the Socs3 gene was flanked with BamHI sites and inserted in BamHI restricted p3xflag-renilla (p3xflag-renilla was a kind gift from M. Vooijs), this resulted in Socs3-renilla fusion plasmid. pcDNA4/TO-luc (luciferase) was a kind gift from M. van der Wetering.

All constructs were verified by sequencing.

Luciferase assay

HEK293T cells in 24 wells plate were transfected using polyethylenimine (Polysciences). Per well 5 ng pcDNA4/TO-luc, 250 ng Socs3-renilla and 812 ng pAAV-shRNA were transfected (molar ratio Socs3-renilla: pAAV-shRNA was 1:4). Three days after transfection the cells were lysed in passive lysis buffer (Promega) according to manufacturer's protocol. Samples were assayed with a dual luciferase kit (Promega) and measured using a Viktor 96-well plate reader (PerkinElmer). All values were normalized to luciferase (to correct for transfection efficiencies). Subsequently the different pAAV-shRNA's were normalized to pAAV-shbase, which contains no shRNA insert. Experiments were performed three times in duplicate.

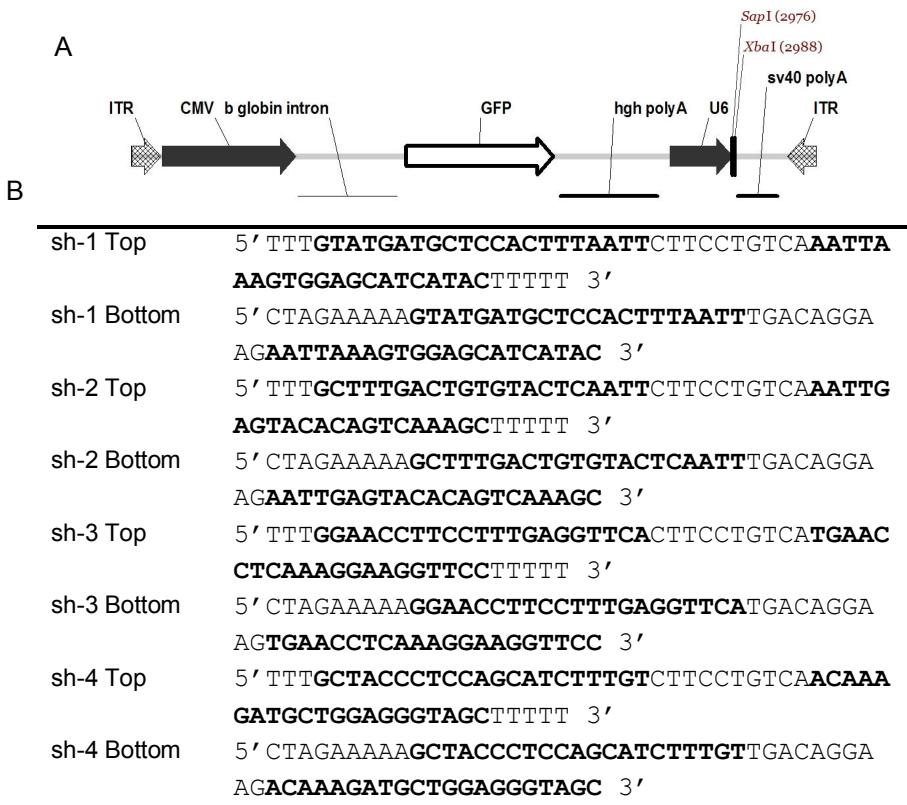


Figure 1 - Constructs

Map of the AAV vector used. The shRNAs were cloned between SapI and XbaI (**A**). Overview of the Socs3 oligonucleotides used. The bold font indicates the Socs3 sequence, with in between a miR-23 loop (**B**). The oligonucleotides were extended with SapI and XbaI overhangs (Top and Bottom, respectively).

Virus production and purification

AAV production was performed with 15x15 cm dishes 293T cells, of 80-90% confluent on the day of transfection. Two hours before transfection, the 10% FCS-DMEM was replaced with 2% FCS-DMEM. The transfections were performed with polyethylenimine (PEI) as described by Reed S.E. et al. (210). pAAV-sh-1, pAAV-sh-2 or pAAV-sh-c were co-transfected with the helper plasmid pDP1 (211) (Plasmid factory, Germany) in a molar ratio of 1:1. The transfection mix remained on the cells until the next day, and then the medium was refreshed with 2% FCS-DMEM. AAV production and purification were essentially performed as described by Zolotukhin et al. (212). Briefly, sixty hours after transfection, the cells were harvested in their medium, centrifuged and washed with PBS containing 5mM ethylenediaminetetraacetic acid (EDTA). Finally, the cells were collected in 12 ml ice cold buffer (150 mM sodium chloride (NaCl), 50 mM 2-amino-(hydroxymethyl)-1,3-propanediol (Tris), pH 8.4) and stored at -20°C until further use. After at least

three days the cells were freeze-thawed twice, incubated for 30 minutes with 50units/ml Benzonase (Sigma, The Netherlands) at 37°C and centrifuged. After centrifugation, the supernatant was loaded onto an iodixanol gradient (60%, 40%, 25%, 15%, supernatant (Optiprep, Lucron bioproducts, Belgium)) in Quick-seal tubes (Beckman Coulter, The Netherlands). After 1 hour of ultracentrifugation (70.000 rpm at 20°C) in Ti70 rotor (Beckman Coulter, The Netherlands), the 40% layer was extracted. This 40% layer was used for ion-exchange chromatography with 5ml Hitrap Q HP columns (GE Healthcare, The Netherlands). The AAV positive fractions, determined by PCR, were pooled and concentrated on Centricon Plus-20 Biomax-100 concentrator columns (Millipore, The Netherlands). The titer, in genomic copies per ml (g.c./ ml), was determined by qPCR with sybergreen mix in a LightCycler (Roche) (213). The qPCR primers were designed to detect GFP and were GFP-F: 5' CACATGAAGCAGCACGACTT and GFP-R: 5' GAAGTTCACCTTGATGCCGT. The titer obtained was in the range of 6×10^{12} to 2×10^{13} g.c./ml.

Animals

Male Wistar rats, weight ranging from 220–250 g, were purchased from Charles River (CrI-Wu, Germany). All rats were individually housed in filter top cages in a temperature- and humidity-controlled room (temperature $21 \pm 2^\circ\text{C}$ and humidity $55 \pm 5\%$) with a 12 h light/dark cycle (lights on at 7:00 A.M.). All experimental procedures were approved by the Committee for Animal Experimentation of the University of Utrecht (Utrecht, the Netherlands). From the moment of arrival the rats received *ad libitum* chow (CRM pellets (3.31 calories/gram), Special Diet Service, Whitham, Essex, UK) and water. Three weeks after injection of AAV-particles into the MBH, animals were switched from chow to a high fat high sucrose choice (HFHS) diet. During this diet the rats had *ad libitum* access to a 30% sucrose solution (30 grams sugar in 100 ml water; 1.2 calories/gram) and saturated fat (Blanc de boeuf, ossewit (9 calories/gram)) in addition to their normal chow and water. Following viral injections rats were monitored for 50 days for effects on body weight, food intake, body core temperature and locomotor activity. Body weight gain and food intake were measured three times a week at 10.00 A.M. (on Monday, Wednesday and Friday). Core temperature and activity were automatically recorded via transmitters that sent digitized data to a nearby receiver. These data were recorded every 10 minutes using DSI software (DSI, St. Paul, MN). Food hoppers were automatically weighed using scales (Dept. Biomedical Engineering, UMCU, Utrecht, the Netherlands) which sent data to a computer every 12s. The data of day 18-20 (last week chow), 27-29 (after 1 wk of HFHS) and day 48-50 (after 4 weeks of HFHS) were used to analyze meal patterns. A meal was defined as an episode of food intake with a minimal consumption of 0.3 g of chow or 0.1 g of lard and an intermeal interval of 5 minutes.

Surgical procedures

After 1½ week of acclimatization surgery was performed under fentanyl/fluanisone (Hypnorm®, Janssen Pharmaceutica, Beerse, Belgium, 0.1 ml/100 g intramuscular) and midazolam (Dormicum®, Roche, Woerden, The Netherlands, 0.05 ml/100 g intraperitoneal) anesthesia. Carprofen (Rimadyl®, Pfizer Animal Health, Capelle a/d IJssel, The Netherlands, 0.01 ml/100 g s.c.) was administered as pain medication, before surgery and for 2 days after. During surgery the rats received an abdominal transmitter (TA10TA-F40; Data Science International, St. Paul, MN), to measure temperature and activity. This was immediately followed by a bilateral injection (AAV-sh-1, AAV-sh-2 or AAV-sh-c, n=16 per group) at the border of the arcuate nucleus (ARC) and ventromedial hypothalamic nucleus (VMH) (coordinates anterior posterior (AP) -2.6 mm from bregma; mediolateral (ML) ±1.2 mm from bregma; dorsoventral (DV) -9.9 mm below the skull; with angle of 5 degrees. Per site 1 µl of virus containing 6×10^9 g.c. of AAV-shRNA was injected at a rate of 0.2 µl/ minute. Following the injection needles remained in place for 10 minutes before removal.

Collection of blood and tissues

On day 51 chow, fat and sucrose were removed at 7.00 A.M... In the afternoon the rats were decapitated, the brains were immediately removed, quickly frozen on dry ice and stored at -80°C. Trunk blood was collected in heparinized tubes containing 83µmol EDTA and 1 mg aprotinin and immediately placed on ice. After centrifugation blood plasma was stored at -20°C until further additional analysis. Retroperitoneal, epididymal, mesenteric and subcutaneous white adipose tissue, thymus and adrenals were isolated and weighed.

DIG in situ hybridization

To verify injection sites, brains were sectioned on a cryostat at 20 µm thickness in series of 10. One series was used for *in situ* hybridization (ISH) with a 720 basepair long digoxigenin (DIG)-labeled eGFP riboprobe (antisense to NCBI gene DQ768212). The ISH was performed as described by Schaeren-Wiemers and Gerfin-Moser (244) with small modifications in the fixation procedure and hybridization temperature. Briefly, sections were fixed in 4% PFA for 20 minutes and washed in PBS. After acetylation for 10 minutes (0.25% acetic anhydride in 0.1 M triethanolamine), sections were washed in PBS and prehybridized at RT in hybridization solution, containing 50% deionized formamide, 5xSSC, 5xDenhardt's solution, 250 µg/ml tRNA Baker's yeast and 500 µg/ml sonicated salmon sperm DNA. After 2 hours, 150µl of hybridization mixture containing 400 ng/ml DIG-labeled riboprobe was applied per slide, slides were covered with Nescofilm and hybridized overnight at 72°C. The next morning, slides were quickly washed in 2xSSC followed by 0.2xSSC for 2 hours. Both wash steps were performed at 72°C.

DIG was detected with an alkaline phosphatase labeled antibody (1:5000, Roche, Mannheim) using nitroblue tetrazolium and bromochloroindolylphosphate (NBT/BCIP) as a substrate. After overnight incubation at RT with NBT/BCIP mixture, sections were quickly dehydrated in ethanol, cleared in xylene and mounted using Entellan.

Radioactive in situ hybridization

Adjacent cryostat brain sections were used for radioactive ISH with ^{33}P -labeled antisense RNA probes for agouti-related peptide (AgRP, 396-bp mouse AgRP cDNA (256)), neuropeptide Y (NPY, 287-bp rat NPY cDNA), pro-opiomelanocortin (POMC, 350-bp rat POMC cDNA fragment (256)), suppressor of cytokine signaling 3 (Socs3, 1200-bp Socs3 cDNA in PCR-script described above in *cell lines and plasmids*). The procedure for radioactive ISH and analysis has been described previously (257).

Plasma analysis

Plasma leptin and insulin were measured in duplicate using rat radioimmunoassay kits (Millipore, Billerica, MA, USA). Plasma glucose was analyzed in triplicate using a glucose/GOD- perid method (Boehringer Mannheim, Mannheim, Germany).

Statistical analysis

Data are presented as group means \pm SEM. All tissues weights are expressed as percentage of total body weight. Differences in body weight and food intake were assessed using repeated measure analysis with post-hoc Bonferroni tests to correct for multiple comparisons. Additional statistical analysis was performed using two-sided t tests. Differences were considered significant at $p < 0.05$.

Results

Knockdown efficiency of Socs3 shRNA's *in vitro*

To determine the efficiency of the different shRNA against Socs3 *in vitro*, we fused genes encoding renilla and Socs3 and performed renilla-luciferase assays. Socs3-renilla was co-transfected in a 1:4 molar ratio with the different pAAV-shRNA constructs against Socs3 (sh-1 to sh-4), an AAV plasmid with control shRNA (sh-c) and an AAV plasmid without a shRNA insert (empty). In addition, a luciferase construct was co-transfected to correct for the transfection efficiencies. The renilla-luciferase assays showed that sh-1 resulted in the lowest levels of Socs3-renilla, thus the highest level of knockdown, namely 81% (Fig. 2A). Sh-2 was the second best with 74% knockdown and sh-4 resulted in 68% knockdown. However, sh-3 did not result in any knockdown of the Socs3-renilla construct. As expected, sh-c did not reduce Socs3-renilla expression.

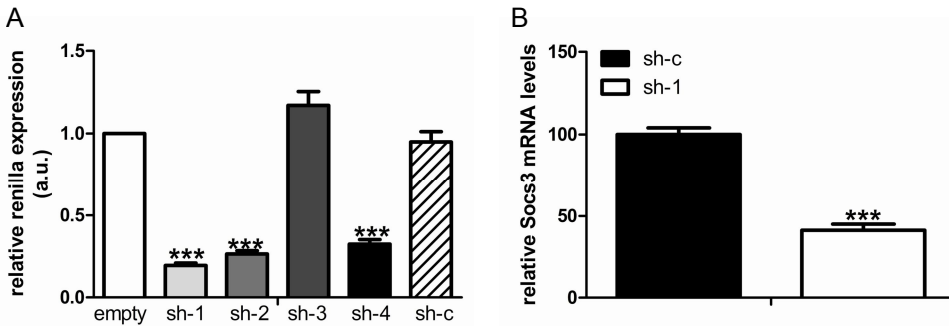


Figure 2 - Knockdown of Socs3 *in vitro* and *in vivo*

Graphical representation showing the *in vitro* knock down of Socs3-renilla construct by pAAV-sh-1 to sh-4 and sh-c relative to pAAV without an shRNA insert (empty) (A). *In vivo* knockdown of Socs3 in the Arc by AAV-sh-1 (relative to AAV-sh-c) (B). *** $p < 0.0001$ compared to empty vector (A) or sh-c (B).

Localization of AAV-shRNA injections and knockdown *in vivo*

Based on the renilla-luciferase assay we decided to use AAV-sh-1 and AAV-sh-2 to knockdown Socs3 mRNA in the rat MBH *in vivo*, using AAV-sh-c as a control. Each group consisted of 15 to 16 rats. At the end of the experiment we performed dig-labeled GFP ISH to determine the injection site in each rat (GFP was a marker in each AAV-shRNA vector). The MBH was considered to be transduced if GFP signal was observed bilaterally in the arcuate nucleus (ARC) or ARC and the ventromedial hypothalamus (VMH) (AP between -2.1 and -3.6 mm; ML between 0 and 1 mm from Bregma). Four out of 16 rats that received AAV-sh-1 were bilaterally transduced in the MBH and 5 rats were transduced unilaterally. The MBH was missed on both sides in 5 rats (GFP signal too far lateral) and in 2 rats no GFP signal could be detected anywhere. In the AAV-sh-2 group none of the 15 rats were transduced bilaterally, but 7 rats were transduced unilaterally. In 5 rats the MBH was not hit and in 3 rats no GFP signal could be detected at all. In the AAV-sh-c group, correct bilaterally placed injections were observed in 3 out of 16 and unilateral injections in 9 rats. In 2 rats the GFP signal was observed lateral to the MBH and in 2 rats no GFP signal could be detected. In all rats with GFP expression, we noticed that AAV-shRNA did not transduce all cells at the site of injection.

For analysis all controls (rats injected with AAV-sh-c vector) were pooled together, excluding one rat, which had hydronephrosis. In addition, only rats with bilateral AAV-sh-1 rat transduction of the MBH were analyzed.

To quantify the knockdown of Socs3 mRNA by AAV-sh-1 *in vivo*, we performed a radioactive ISH with a ^{33}P -labeled Socs3 RNA probe. For each rat coronal sections throughout the ARC (200 μm apart) were analyzed. Knockdown of Socs3 mRNA in the ARC was $59\% \pm 4\%$ with AAV-sh-1 compared to Socs3 mRNA in controls (Fig. 2B).

Effect of Socs3 knockdown on body weight

After injection of the AAV-shRNA, rats received *ad libitum* access to chow and water for the first 3 weeks (day 0 to 21 post injection (p.i.)). Subsequently, rats were switched to a high fat high sucrose choice (HFHS) diet for 4 weeks (day 22 to 50 p.i.) to determine sensitivity to diet-induced obesity. During these 4 weeks the rats had *ad libitum* access to chow, water, a 30% sucrose solution and saturated fat. Surprisingly, bilateral knockdown of Socs3 mRNA in the MBH increased body weight gain significantly compared to AAV-sh-c from day 38 onwards (Fig. 3A). Unilateral Socs3 knockdown in the MBH or other regions (missed injections) by AAV-sh-1 did not affect body weight gain significantly when compared to AAV-sh-c during the experiment (Fig. 3B).

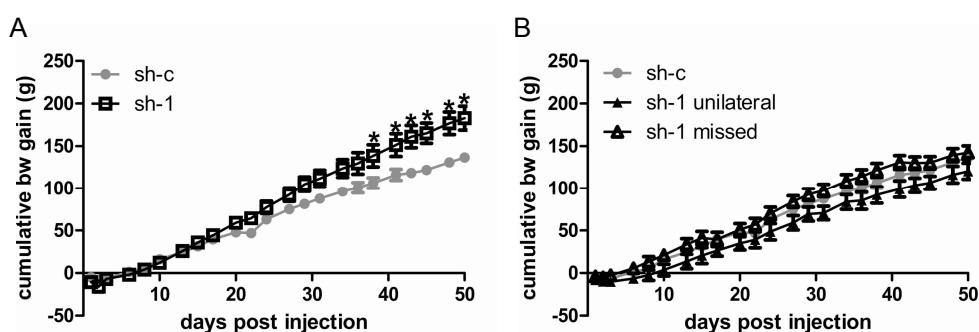


Figure 3 - Effect of Socs3 knockdown on cumulative body weight gain

Body weight gain of bilaterally transduced sh-1 rats was increased compared to sh-c rats (A). In contrast, rats with unilateral or more lateral expression of sh-1 did not differ in body weight from sh-c (B). * $p < 0.05$ compared to sh-c.

Effects of Socs3 knockdown on food intake

In the bilateral AAV-sh-1 group, total caloric intake during the experiment was not significantly increased, except for the first measuring point on HFHS diet (day 24 p.i.) (Fig. 4A). Furthermore, there were no apparent differences in choice of food between AAV-sh-1 and AAV-sh-c rats exposed to the HFHS diet. Chow, fat, sucrose and water intake were not significantly different between the groups (Fig. 4B-E).

To investigate whether knockdown of Socs3 mRNA in the MBH affects feeding behavior independently of total food intake, we analyzed meal patterns at 3 different time points: after 3 weeks of chow diet (day 18-20 p.i.), after 1 week of HFHS (day 27-29 p.i.) and after 4 weeks of HFHS diet (day 48-50 p.i.). On day 18-20 p.i. the AAV-sh-1 rats ate significantly more chow than AAV-sh-c rats in the light phase (Table 1). This was due to a significant increase in average meal size. After 1 and 4 weeks of HFHS diet the AAV-sh-1 rats did not significantly differ in 24h chow or lard intake compared to controls; however, the increased meal size

remained after 1 week on HFHS diet, but did not reach significance after 4 weeks on HFHS diet compared to AAV-sh-c (Table 1).

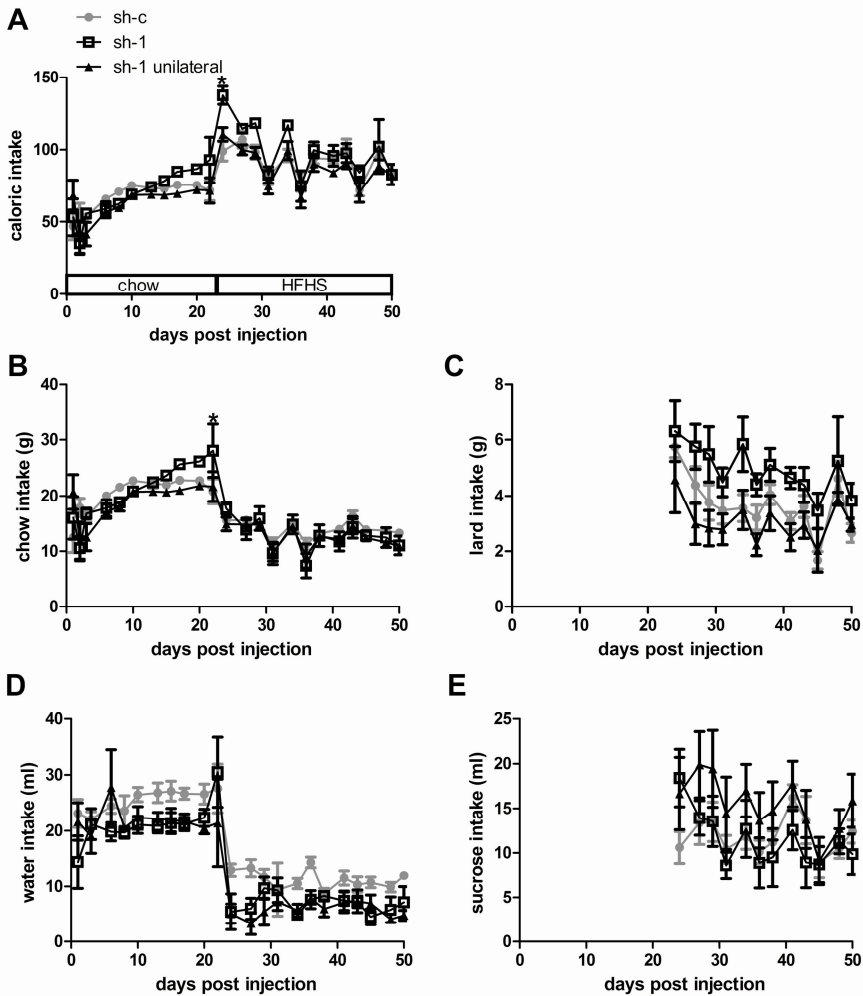


Figure 4 - Effects of Socs3 knockdown on food and water intake

Rats received chow and water for the first 21 days. Subsequently, saturated fat and a sucrose solution were added to the diet. Total caloric intake (A) was calculated by adding calories derived from chow (B), fat (C) and sucrose (E) intake. Water intake (D) did not add any caloric value. * $p < 0.05$ compared to sh-c.

Normally, rats do not eat much during the light period and eat most of their food in the dark period. To investigate if this circadian pattern was affected by MBH Socs3 mRNA knockdown, we performed an additional analysis for both the light and dark period separately. On day 18-20 AAV-sh-1 rats ate significantly more calories in

the light period, while in the dark period food intake was similar to the AAV-sh-c rats (Table 2).

Table 1- Effects of MBH Socs3 knockdown on average 24h food intake, meal size and frequency in grams

	sh-c	sh-1
Day 18-20 (3rd wk chow)		
Chow		
total intake	20.0 ± 0.50	25.9 ± 0.038***
av. size	1.43 ± 0.11	2.00 ± 0.09*
av. frequency	14.3 ± 0.92	13.0 ± 0.76
Day 27-29 (1st wk HFHS)		
Chow		
total intake	14.1 ± 0.80	13.2 ± 2.42
av. size	1.29 ± 0.08	1.67 ± 0.05*
av. frequency	11.2 ± 0.88	8.0 ± 1.76
Lard		
total intake	3.5 ± 0.78	4.9 ± 1.18
av. size	0.56 ± 0.10	1.37 ± 0.49*
av. frequency	5.9 ± 0.96	4.2 ± 0.88
Day 48-50 (4th wk HFHS)		
Chow		
total intake	13.4 ± 0.79	10.1 ± 2.01
av. size	1.31 ± 0.06	1.48 ± 0.11
av. frequency	10.4 ± 0.84	7.0 ± 1.53
Lard		
total intake	3.0 ± 0.46	3.5 ± 0.54
av. size	0.65 ± 0.10	1.24 ± 0.51
av. frequency	4.7 ± 0.17	3.5 ± 0.87

* $p < 0.05$, *** $p < 0.001$ compared to sh-c

This increase in caloric intake in the light period was also observed on day 27-29 and 48-50. However, on these days, AAV-sh-1 rats compensated by significantly decreasing their caloric intake in the dark period. AAV-sh-1 rats ate approximately the same amount of calories in the light period as in the dark period, while AAV-sh-c showed a normal feeding rhythm, with higher caloric intake in the dark period than in the light period (Table 2).

Table 2 – Effects of MBH Socs3 knockdown on caloric intake in light and dark phase

	sh-c	sh-1
Day 18-20		
Light	13.8 ± 1.49	33.4 ± 0.96***
Dark	52.3 ± 1.16	52.3 ± 1.72
Day 27-29		
Light	21.1 ± 4.87	47.6 ± 7.60*
Dark	61.1 ± 3.45	39.9 ± 3.99**
Day 48-50		
Light	12.9 ± 1.23	34.4 ± 2.99***
Dark	57.2 ± 2.24	31.2 ± 2.96***

* $p < 0.05$, ** $p < 0.01$, *** $p < 0.001$ compared to sh-c

The increase in caloric intake of AAV-sh-1 in rats in the light period of day 18-20 was due to a significant increase in both meal size and frequency, while there were no significant effects in the dark period (Fig. 5 A, D). On day 27-29 and 48-50 the average frequency of chow meals was significantly decreased in the dark period in AAV-sh-1 rats, while in the light period the average size of chow meals was significantly increased compared to AAV-sh-c rats (Fig. 5 B, C, E, F). In addition, the average size of fat meals was significantly larger in the light phase of the first week of exposure to the HFHS diet (day 27-29), however this effect did not reach significance when measured at day 48-50 (Fig. 5 G, H, I, J).

Table 3 – Effects of MBH Socs3 knockdown on locomotor activity and body core temperature

		sh-c	sh-1
Activity (a.u.)			
Day 18-20	Light	89.6 ± 9.2	93.2 ± 8.7
	Dark	325.1 ± 39.2	218.4 ± 57.6
Day 27-29	Light	174.8 ± 34.7	132.9 ± 17.5
	Dark	523.3 ± 40.9	290.1 ± 60.4*
Day 48-50	Light	150.3 ± 15.5	150.5 ± 21.5
	Dark	463.7 ± 38.2	289.0 ± 66.8*
Body temperature (°C)			
Day 18-20	Light	37.07 ± 0.05	37.19 ± 0.04
	Dark	37.72 ± 0.06	37.53 ± 0.06
Day 27-29	Light	37.17 ± 0.03	37.28 ± 0.03
	Dark	37.73 ± 0.06	37.50 ± 0.02
Day 48-50	Light	37.15 ± 0.04	37.12 ± 0.03
	Dark	37.60 ± 0.05	37.34 ± 0.03*

* $p < 0.05$ compared to sh-c

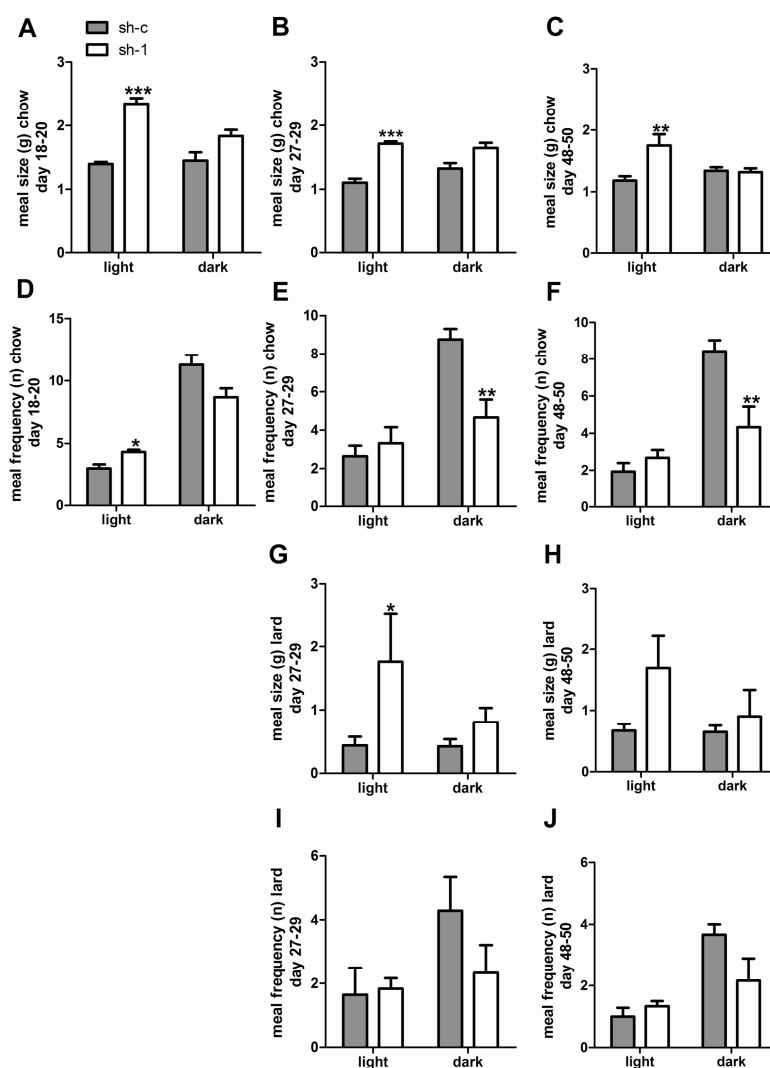


Figure 5 - Effect of Socs3 knockdown on meal patterns

Average size of chow meals in light and dark period on day 18-10 (A), 27-29 (B) and day 48-50 (C), and average meal frequency for these days (D-F). Average size and frequency of fat meals in light and dark period on day 27-29 (G, I) or 48-50 (H, J). * $p < 0.05$, ** $p < 0.01$, *** $p < 0.001$ compared to sh-c.

Effects of Socs3 knockdown on locomotor activity and body temperature

Knockdown of Socs3 mRNA in the MBH did not significantly alter locomotor activity and body core temperature during the third week (day 18-20 p.i.) on chow (Table 3). However, after 1 (day 27-29 p.i.) and 4 weeks (day 48-50 p.i.) on HFHS diet, locomotor activity in the dark period was reduced in AAV-sh-1 rats compared to control rats. This decrease in locomotor activity was accompanied by a trend

towards lower body core temperature in the dark period in week 1 of the HFHS diet and a significant decrease in temperature in week 4 of the HFHS diet (Table 3).

Effects of Socs3 knockdown on endocrine parameters and body composition

The increase in body weight gain due to knockdown of Socs3 mRNA in the MBH was accompanied by a significant increase in subcutaneous and abdominal white adipose tissue in AAV-sh-1 rats compared to AAV-sh-c rats (Table 4). AAV-sh-1 rats also showed significantly elevated plasma leptin concentrations and a trend to increased plasma concentrations of insulin and glucose (Table 4). Furthermore, thymus and adrenal weights did not differ between AAV-sh-1 and AAV-sh-c rats, suggesting that the obesity due to knockdown of Socs3 mRNA in the MBH was not due to activation of the HPA-axis.

Table 4 – Effects of Socs3 knockdown on body composition and endocrine parameters

	sh-c	sh-1
Leptin (ng/ml)	15.75 ± 1.69	32.79 ± 5.64***
Insulin (ng/ml)	3.63 ± 0.38	4.73 ± 1.10
Glucose (mmol/l)	7.71 ± 0.30	8.57 ± 0.09
SWAT (%bw)	1.34 ± 0.05	2.15 ± 0.17***
AWAT (%bw)	3.81 ± 0.18	5.30 ± 0.14***
Adrenals (%bw)	0.11 ± 0.007	0.09 ± 0.005
Thymus (%bw)	1.14 ± 0.06	0.97 ± 0.18

*** $p < 0.001$ compared to sh-c

Effect of Socs3 knockdown on AgRP, NPY and POMC mRNA in the ARC

Since leptin signaling is implicated in regulating the levels of transcription of genes encoding AgRP, NPY and POMC, we investigated if knockdown of Socs3 mRNA in the MBH had any effects on mRNA expression levels of these neuropeptides. Radioactive ISH showed that AAV-sh-1 rats had significantly increased levels of NPY in the ARC compared to AAV-sh-c (Fig. 6 A). mRNA levels of AgRP and POMC were comparable between AAV-sh-c and AAV-sh-1 rats.

Effects of unilateral Socs3 knockdown

In unilaterally transduced AAV-sh-1 rats we compared NPY mRNA levels between the side of the ARC that showed knockdown of Socs3 mRNA to the side that did not.

This revealed an upregulation of NPY levels on the side where Socs3 mRNA was down-regulated (Fig. 6 B, C). The Socs3 mRNA was down-regulated on the side where GFP was expressed (data not shown). Rats with unilateral expression of AAV-sh-1 or AAV-sh-2 in the MBH showed a significant up-regulation of NPY mRNA ($39\% \pm 12.2$) compared to controls ($p=0.0194$) on the side of transduction.

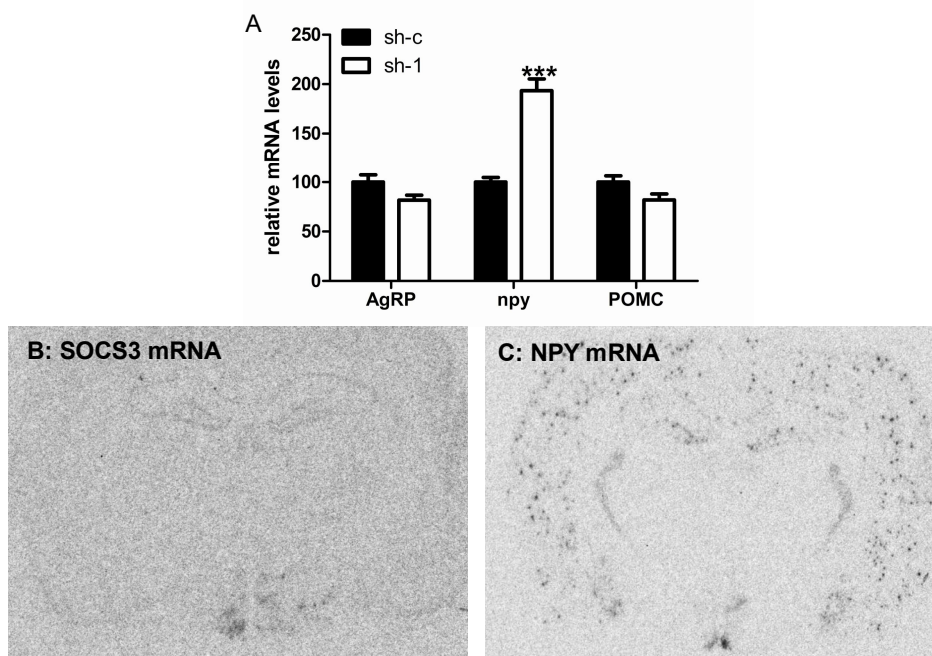


Figure 6 - Effect of Socs3 knock down on mRNA expression levels in the arcuate nucleus
mRNA expression levels of AgRP, NPY and POMC in the ARC of sh-c and sh-1 rats (**A**). For each mRNA the sh-c values were set to 100% and the sh-1 values were correlated to this. Socs3 mRNA expression in a unilaterally transduced rat (**B**) shows that the Socs3 signal on the right side is lower than the left side. NPY mRNA (**C**) on an adjacent section of the same rat shows that the NPY signal is higher on the right side than on the left side. *** $p < 0.001$ compared to sh-c.

Since bilateral Socs3 mRNA knockdown clearly affected SWAT, leptin concentrations and locomotor activity, we also examined these parameters in rats with unilateral Socs3 mRNA knockdown in the MBH. This revealed an increase in % SWAT and leptin concentrations, while locomotor activity was decreased compared to controls. Interestingly, the values of these parameters in unilaterally transduced rats were in between those of bilaterally transduced AAV-sh-1 and control rats (Table 5).

Discussion

In contrast to the current hypothesis that Socs3 levels are correlated with the susceptibility to diet-induced weight gain, we here show that knockdown of Socs3 mRNA limited to the MBH increased body weight, fat mass and leptin levels. This was at least partly due to a decrease in locomotor activity during the dark period in MBH Socs3 knockdown rats compared to control rats. Moreover, MBH Socs3 knockdown increased meal size in the light phase throughout the experiment, but only transiently increased total daily food intake. Interestingly, NPY mRNA levels in

the ARC were increased significantly in rats which received the Socs3 shRNA in the MBH compared to control rats.

Table 5 – Effects of unilateral Socs3 knockdown in the MBH with two shRNAs

		sh-c	sh-1 unilateral	sh-2 unilateral
Leptin (ng/ml)		15.75 ± 1.69	22.19 ± 3.02**	26.51 ± 4.75***
SWAT (% bw)		1.34 ± 0.05	1.63 ± 0.08***	1.83 ± 0.20***
Activity (a.u.)				
Day 18-20	Light	89.6 ± 9.2	78.8 ± 12.9	80.1 ± 10.7
	Dark	325.1 ± 39.2	270.7 ± 59.8	218.1 ± 61.8*
Day 27-29	Light	174.8 ± 34.7	142.0 ± 25.3	130.9 ± 17.1
	Dark	523.3 ± 40.9	360.4 ± 35.5***	362.9 ± 63.8***
Day 48-50	Light	150.3 ± 15.5	96.2 ± 17.8	131.3 ± 19.3
	Dark	463.7 ± 38.2	304.2 ± 63.4***	304.0 ± 46.5***

* $p < 0.05$, ** $p < 0.01$, *** $p < 0.001$ compared to sh-c

The results obtained in this study are in contrast with previous Socs3 deletion studies in the mouse brain (120, 309, 310). In these studies, neuronal Socs3 deletion prevented diet-induced obesity (120). However, Socs3 specifically deleted in POMC neurons or in SF-1 neurons had only modest effects on body weight upon exposure to a high fat diet, although glucose homeostasis did markedly improve. When Socs3 was deleted in POMC neurons, these effects were due to increased energy expenditure without any change in food intake (310). Conversely, when Socs3 was deleted in SF-1 neurons, a decrease in food intake was observed combined with decreased energy expenditure (309). In the present study, knockdown of Socs3 mRNA in the MBH resulted in an unexpected increase in body weight and fat mass, accompanied by a decrease in locomotor activity. There are several possible explanations for the differences with the previous studies. Firstly, we knocked down Socs3 in the MBH of adult rats that had normal Socs3 expression during development. In contrast, neuronal Socs3 knockout mice lack Socs3 mRNA in (specific) neurons throughout development and we can therefore not exclude that developmental compensation may have occurred in these mice. Secondly, our viral vector did not transduce all neurons in the MBH allowing some neurons to continue expressing normal levels of Socs3 mRNA. Nevertheless, at least part of the cells transduced in our experiment, were likely to be AgRP/NPY neurons that increased their NPY expression due to the decrease in Socs3 mRNA. Finally, Socs3 mRNA levels were only reduced partially, whereas Socs3 is completely absent in knockout mice.

The marked increase in NPY mRNA levels (+ 93.4%) that we observed in the ARC of MBH Socs3 mRNA knockdown rats is in line with several *in vitro* studies (311,

312). These have shown that, in the absence of Socs3, leptin activates the NPY promoter via STAT3. However, if Socs3 is present in cells, leptin suppresses NPY transcription (312). In addition, Socs3 also decreases basal NPY transcription. Taken together this suggests that Socs3 may act as a negative regulator of NPY transcription (312). In our experiment, Socs3 levels in the MBH were decreased by viral mediated knockdown, similar to the *in vitro* experiment by Higuchi et al., allowing leptin to stimulate NPY transcription by STAT3 binding to its promoter and simultaneously reducing Socs3-mediated suppression of basal NPY transcription. Thus, in cells with reduced levels of Socs3 mRNA, leptin could no longer inhibit NPY expression and leptin could even increase NPY expression and this may contribute to the development of obesity.

The increased levels of NPY mRNA that we observed may explain the unexpected effects on body weight, food intake, fat mass and locomotor activity after Socs3 knockdown in the MBH. Viral vector-mediated NPY overexpression in several hypothalamic regions results in increased food intake, especially in the light period, increased body weight and decreased locomotor activity in the dark period (201, 255). In addition, acute intracerebroventricular (ICV) injections with NPY increase food intake and when NPY is infused for longer periods it also reduces energy expenditure (313, 314, 315, 316). In rats with MBH Socs3 knockdown we observed an increase in chow intake in the light period of day 18-20. This increase in food intake may be due to the increased NPY levels in the ARC at this time. Once the rats were switched to the HFHS diet, hyperphagia was no longer observed, which may be due to counter-regulatory mechanisms. Similarly, overexpression of NPY in the PVN (a target area for NPY neurons located in the ARC) was reported to only temporarily increase food intake due to compensatory mechanisms (199, 255). The reduced locomotor activity that we observed in the dark period of day 27-29 and 48-50 is also in agreement with both NPY overexpression studies and ICV administration studies that show a long term decrease in locomotor activity (255, 317, 318). Because we expected that rats with unilateral knockdown of Socs3 in the MBH would show similar features as those with bilateral knockdown we also examined the effects on locomotor activity, fat mass and leptin concentration in these rats. Despite the fact that rats with unilateral knockdown of Socs3 in the MBH did not show increased total body weight gain, these rats did show reduced locomotor activity, increased fat mass and leptin concentrations compared to controls. This underscores the role of MBH Socs3 in regulating locomotor activity, body composition and endocrine parameters.

Although knockdown of Socs3 mRNA in the MBH did not clearly affect total food intake, it persistently altered meal patterns. Meal size in the light period was increased in rats with MBH Socs3 knockdown, while there were no effects on the

number of meals. On the HFHS diet, rats with MBH Socs3 knockdown appeared to compensate for the increase in meal size during the light phase by decreasing the number of meals in the dark period. An increase in meal size and decrease in frequency was also observed in diet-induced obese rats when they are placed on a HF diet (319). Similarly, meal size has been reported to increase when rats are placed on a cafeteria-style diet. The first weeks on cafeteria diet the meal frequency is also increased, but after several weeks frequency returns to levels even slightly below the frequency of chow fed rats (320). Taken together, this suggests that in rats on a chow diet, knockdown of Socs3 in the MBH seems to simulate some of the effects of a high fat diet on meal patterns. Furthermore, when placed on HFHS diet, susceptibility to the alterations that normally accompany high-fat feeding seems to increase. However the compensatory decrease in meal frequency, that normally accompanies increased meal size in DIO rats, only occurs in the dark phase, but not in the light phase.

In conclusion, knockdown of Socs3 mRNA in the mediobasal hypothalamus increased NPY levels in the ARC and this most likely explains the effects observed on energy balance, such as the decreased locomotor activity, the small increase in food intake on chow and the alterations in meal patterns. These results described here, underscore what was observed *in vitro* by Higuchi et al.(312), namely that regulation of gene expression by STAT3 and Socs3 depends on an intricate balance of signal transduction molecules that together modulate transcriptional activity of genes such as NPY.

Acknowledgements

Moniek Veltman is gratefully acknowledged for her help in cloning the Socs3-PCR-script plasmid.

This work was supported by the Netherlands Organization for Scientific Research (NWO grant No. 90339175).

Chapter 7

General discussion and summary

GENERAL DISCUSSION AND SUMMARY

Viral vectors: tools for gene transfer

Viral vectors are great tools to alter gene expression locally or systemically to investigate gene function. In addition, they can be used as therapeutic gene delivery vehicles for various diseases (321). As described in chapter 1, different viral vectors all have their own advantages and disadvantages e.g. limited packaging size, neutralization by host immune responses or poor transduction efficiencies of therapeutic cells. Depending on the aim of the study specific viral vectors can be chosen to mediate gene transfer.

Local gene transfer: AAV versus LV in rat brain

To investigate the role of a gene in a tissue, viral vectors can be injected in this specific tissue to overexpress or silence gene expression. Local gene transfer has several advantages: first, the viral vectors can be injected at any moment during life, which may reduce developmental compensation; second, the vectors can be injected in other species than rodents; third, several vectors can be used to affect different genes simultaneously or one vector can carry different genes (303, 322). When the tissue of interest contains non-dividing cells, integrating and non-integrating vectors can be used, because the transduced cells are not replaced. To reduce the risk of insertional mutagenesis induced by lentiviral (LV) vectors, non-integrative LV vectors may be used (323, 324). In chapter 2, the efficiency of LV and AAV vectors to transduce the rat lateral hypothalamus (LH) or amygdala (AM) were compared. This study showed that an AAV vector was more efficient in transducing the LH or AM of the rat brain. The difference in transduction efficiency may be due to the use of different cell entry receptors or uncoating routes. Therefore pseudotyping of AAV or LV with other capsids or envelopes may improve the transduction efficiency.

There appears to be a threshold to achieve consistent transgene expression from viral vectors in the rat brain. For AAV vectors the minimum amount to be injected appears to be 5×10^7 genomic particles (230), for LV vectors the minimal threshold is 1×10^4 transducing units (325). In chapter 2 the injected amounts of AAV and LV vectors were higher than the minimal amounts. In addition, AAV production yields much higher titers than LV production; thus the number of injected AAV particles can be increased much further than those of LV to increase the number of transduced cells.

Chapter 2 indicated that AAV vectors are more feasible tools to transduce the rat hypothalamus than LV vectors, therefore the transduction patterns of AAV were further investigated in chapter 3. The study in chapter 3 revealed that an AAV vector pseudotyped with AAV1 capsid was significantly more efficient than the one

encapsidated with the “golden standard”, an AAV2 capsid. In addition, transduction efficiencies after pseudotyping with AAV8 or mosaic capsids 1/2 or 2/8 were comparable to the AAV2 coated vector. This difference between AAV1 and the other serotypes may be due to the use of different entry receptors. In addition, expression of the transgene depends on the uncoating rate. If a virion is uncoated slowly, antigenic epitopes may be presented long enough to be recognized by T cells (40, 326, 327, 328). However, the uncoating rate of AAV1 is still unknown, but may be different from AAV2 encapsidated vectors. Transgene expression may be reduced by proteasomal degradation of AAV vectors (329, 330, 331). All these properties contribute to the fact that an AAV serotype which efficiently transduces a specific brain area is not necessarily efficient in other brain areas (62, 65, 66, 231, 332). In addition, the transduction efficiency of one serotype in a specific brain area may be different at different ages, e.g. neonate versus adult (216, 333) or species (chapter 2).

An important barrier to efficient transduction with AAV vector is the conversion of single stranded DNA into double stranded DNA, this conversion is necessary for transgene expression (258, 259). One solution to circumvent this conversion is the use of self-complementary/double stranded AAV vectors (334, 335). These AAV vectors mediate 10 to 100 fold higher levels of transgene expression, but they can only package 2.4 kb (334, 335, 336, 337). The packaging limitations may be addressed by splitting the expression cassette across two vectors, when both vectors are in the same cell, concatamerization can occur and the whole cassette is expressed (338, 339, 340, 341). In the future double stranded AAV vectors may be used to improve transduction efficiencies and increase transgene expression when this is necessary.

In this thesis we did not test all available serotypes, thus it would be interesting to study if other serotypes are even better in transduction of the hypothalamus. In addition, when the appropriate markers are available it would be fascinating to determine if different serotypes transduce specific neuronal populations.

Regulation of transgene expression

Viral vector mediated gene transfer in this thesis was performed with constructs which contained constitutive promoters, namely CBA, CMV and U6, to drive transgene expression. In the future more specific expression may be established by the use of cell type-specific and/or inducible promoters. However, the packaging capacity of the viral vectors has to be kept mind; AAV vectors can only package up to 5.7 kb (342), whereas LV vectors can package 8-10 kb (343) without a dramatic decrease in vector titers. Table 1 shows an overview of some (tissue) specific promoters which may be used to establish more specific gene expression. Most of

these promoters have been shown to establish specific expression. However, an AAV vector with a GFAP promoter driven transgene was reported to show transgene expression mainly in neurons instead of in astrocytes, after injections in hippocampus and striatum and spinal cord (342, 344). This is in contrast with the specific expression in astrocytes in transgenic mice or AAV-GFAP-EAAT2 expression in rat hippocampal slice culture (345, 346). The more generalized expression of GFAP in neurons may be due to transcriptional activity in the terminal repeats of AAV (347).

Table 1 - examples of commonly used cell type-specific promoters

Promoters	Size	References
<u>Neuron specific</u>		
Neuron specific enolase (NSE)	1.8 kb	(342, 348, 349)
Human synapsin (hSYN)	0.48 kb	(348, 350)
Rat tubulin α 1 (Ta1)	1.1 kb	(348, 351)
<u>Glial specific</u>		
<i>astrocytes</i>		
Glial fibrillary acidic protein (GFAP)	0.6-2.2 kb	(345, 352)
<i>oligodendrocytes</i>		
Myelin basic protein (MBP)	1.9 kb	(353)
<u>Brain nucleus specific</u>		
Single minded 1 (SIM1; PVN neurons)	0.67 kb	(354, 355)
Steroidogenic factor 1 (SF-1; VMH neurons)	0.85 kb	(356)
POMC (POMC neurons in ARC)	0.38-0.39 kb	(357)
AgRP (AgRP neurons in ARC)	0.48 kb	(227, 358)

ShRNA mediated knockdown of a gene is often regulated by ubiquitous RNA polymerase III promoters, such as U6 or H1. However, by using microRNA-based hairpins tissue specific RNA polymerase II promoters can be used, like synapsin or AgRP promoters, to increase tissue specificity (359). In addition, microRNA-based hairpins may have increased efficiency and reduced toxicity due to shRNA dependent saturation of the endogenous microRNA pathway (360, 361, 362, 363). Thus to obtain more specific and efficient knockdown microRNA-based hairpins may be used in the future.

An overexpression transgene and microRNA-based hairpin can be located on one construct to autoregulate overexpression of a specific gene. Recently, such an approach was used by Cao et al. (227). Continuous overexpression of BDNF led to starvation and was accompanied by upregulation of AgRP mRNA *in vivo*. The starvation could be prevented by inserting a microRNA targeting BDNF under transcriptional control of AgRP promoter in the same construct; as a result the BDNF overexpression was downregulated, when AgRP was upregulated by starvation. Thus BDNF overexpression lowered body weight temporarily until

overexpression was reduced by microRNA expression; thereby a new, lower body weight set point was achieved.

In some studies time specific expression may be preferred. Time specific expression may be achieved with the tetracycline-regulatable systems with dual AAV vectors or a single autoregulatory AAV vector (reviewed in (364, 365)).

Thus in the future more specific and/or regulatable gene expression can be used to identify the role of a gene in a specific cell type.

The studies in chapter 3 showed that AAV1 mediated gene transfer to the hypothalamus was most optimal with a titer of 1×10^9 g.c. in a volume of 1 μ l. These parameters were used in the subsequent studies to overexpress AgRP and to knockdown Socs3 in the rat hypothalamus (chapter 4, 5 and 6).

In chapter 4 the effects of reduced MC receptor signaling in the PVN, LH or VMH on energy balance were investigated. Overexpression of AgRP in these areas increased body weight and food intake. The increase in food intake was mainly due to an increase in meal size. However, reduction of MC signaling in the Acc did not have any effect on food intake or body weight.

Melanocortin versus NPY signaling

AgRP and NPY have similarities, they are both produced in the same neurons in the ARC and released in the same projection areas (74). AgRP and NPY increase food intake and reduce energy expenditure when they are administered ICV for 1 week (184, 248, 315). This suggests that they may have similar functions, but there are clear differences between AgRP and NPY systems. Acute ICV administration of NPY instantly increases food intake but only for approximately 4 hours, whereas the effects of AgRP start somewhat later, but they can last up to 7 days (188, 189, 313, 314). The effects of overexpression of AgRP and NPY are compared below.

Energy intake

Chapter 4 indicated the differences in meal patterns which were seen after AAV mediated overexpression of AgRP compared with AAV mediated overexpression of NPY in the PVN or LH (255). NPY in PVN transiently increases meal frequency during the light phase, while AgRP increases meal size in both the dark and light phase. In the LH NPY increases frequency in the light phase and meal size irrespective of the time of the day, however, AgRP only increases meal size. This suggests that NPY, especially in the PVN, is involved in the initiation of feeding (hunger), while the MC system alters the consummatory phase of meals that are normally eaten (satiation). The motivation (and initiation) to eat involves many brain regions, including the dopaminergic reward pathways (67) and probably NPY, whereas the consummatory phase involves the hindbrain that can function

independently of forebrain structures (366). As described in chapter 1, the PVN, LH and VMH have projections to the hindbrain and melanocortins can alter satiation by interfering with sensitivity for CCK. Thus inhibition of MC signaling in neurons of the PVN, LH or VMH may decrease satiation in the hindbrain via these projections. The PVN has direct projections to the hindbrain which contain oxytocin and CRH (129). It is interesting to study if oxytocin or CRH expression is altered after inhibition of MC signaling in the PVN, this to confirm a direct link which can influence meal size in the hindbrain. In addition it would be interesting to investigate if inhibition of MC signaling in the LH or VMH alters oxytocin or CRH expression in the PVN via hypothalamic interconnections or if they directly modulate satiation in the hindbrain.

Inhibition of MC signaling in the Acc, on chow diet, did not alter any of the measured parameters of energy balance. The Acc is implicated in non-homeostatic control of food intake and may perhaps play a role when rats are exposed to high fat high sucrose diet; however this remains to be investigated.

Energy expenditure and endocrine parameters

Overexpression of NPY in the PVN or LH reduced body temperature, while AgRP overexpression in the LH had no effects on body temperature or locomotor activity. However, aged AgRP^{-/-} mice do show an increase in locomotor activity, body temperature and metabolic rate. In addition, chronic AgRP infusion reduces oxygen consumption (184, 248). These data suggest that the energy expenditure effects exerted by MC signaling may be located in brain regions other than the PVN, LH, VMH and Acc. We can not exclude that these brain areas are involved in reductions in metabolic rate, because the rats with AAV-mediated AgRP overexpression were not analyzed in metabolic cages. In contrast, the PVN and LH are involved in the effects of NPY on energy expenditure.

It would be interesting to study if overexpression of an agonist of MC signaling, e.g. α -MSH, results in the exact opposite effects as AgRP overexpression. In addition, overexpression of γ -MSH, a MC3R specific agonist, may help to dissociate between MC3R and MC4R specific effects.

AgRP overexpression in the PVN, LH or VMH did not alter the expression of AgRP, NPY or POMC in the ARC (chapter 4). This is in agreement with a study which overexpressed Agouti in the PVN or LH and that did not find any changes in NPY, POMC or AgRP mRNA compared to controls (249). In addition, mice with MC4R^{-/-}, AgRP^{-/-} or ectopic expression of agouti have normal NPY and POMC mRNA levels in the ARC (1). NPY signaling is not altered in MC4R^{-/-} mice, since they show a normal feeding response when exposed to NPY (173). These data suggest that altered MC signaling can not be compensated by NPY. In contrast, the MC system is suggested to be able to compensate altered NPY signaling. Viral mediated

overexpression of NPY in the LH or PVN, reduced AgRP mRNA in the ARC, while it did not alter POMC mRNA (255). In addition, NPY^{-/-} mice show an increase in AgRP mRNA (no changes in POMC mRNA) and these mice are more sensitive for effects of AgRP (175, 367). These data implicate that increase in NPY signaling may be (partially) compensated by an increase in MC signaling.

An endogenous neuropeptide has a signal peptide which directs the neuropeptide to axon terminals to be secreted. When a neuropeptide is overexpressed in its target area, most peptide secretion probably remains local, since there are many interneurons which project within the same nucleus. However, it can not be excluded that a projection neuron is transduced and that the peptide is secreted in another brain area. In chapter 5 a new construct was created and tested which prevents secretion from axon terminals, but results in secretion from the cell body; this was established by removing the endogenous signal peptide and replacing it with a Von Willebrand signal peptide with a furin site. VWF-AgRP₈₃₋₁₃₂ was secreted by the cell body, was biologically active and could increase food intake. This new method ensures that secretion of the overexpressed neuropeptide remains local to the transduced area. Since it is unknown to what extent the phenotypes observed after overexpression of full-length AgRP in the PVN, LH and VMH were due to effects of AgRP in other brain areas, it will be interesting to study if this new construct with local secretion will result in similar phenotypes.

Leptin-melanocortin signaling

Leptin reduces food intake and body weight, it is suggested that this is due to the influence of leptin on MC signaling and NPY signaling; leptin can upregulate POMC mRNA and reduce AgRP and NPY mRNA levels in ARC neurons. Thus interference with the leptin signaling may alter melanocortin and NPY signaling. In chapter 6 the expression of a negative regulator of leptin signaling, Socs3, was reduced via AAV-mediated knockdown. It was expected that rats with a decrease in MBH Socs3 mRNA would be resistant for diet-induced obesity, due to improved leptin signaling in the mediobasal hypothalamus. However, knockdown of Socs3 in the MBH increased body weight, fat mass and leptin levels, significantly. This was accompanied by a decrease in locomotor activity and an increase in NPY mRNA in the ARC. The increase in NPY mRNA levels may explain some of the phenotypes observed, e.g. the decrease in locomotor activity and the feeding effects (shift to light phase feeding). It would be interesting to study if NPY mRNA is already increased after 3 weeks, when knockdown of Socs3 has reached a plateau and food intake in the light phase is increased. This in order to study if the phenotypes we observed were really due to a continuous increase in NPY mRNA levels. In addition, it would be helpful to increase Socs3 mRNA via AAV-mediated overexpression and determine if NPY mRNA can not be induced during a fast.

AAV mediated overexpression of NPY in the PVN (a target area for NPY produced in the ARC) started to be compensated after 3 weeks (resulting in normal food intake after 5-6 weeks of NPY overexpression (199, 255)). Therefore, it would be intriguing to study if rats with MBH Socs3 knockdown also compensate food intake when they remain on chow, instead of switching to the high fat high sucrose diet after 3 weeks.

These data suggest that the leptin signaling has a larger effect on NPY transcription than on AgRP transcription when rats are exposed to an HFHS diet. The increase in NPY mRNA suggests that at least NPY/AgRP neurons were transduced, however the data on POMC mRNA levels has to be interpreted carefully, because not all cells in the MBH were transduced.

The obese phenotype after Socs3 knockdown resembles obese leptin deficient rats; leptin deficient rats also show increased NPY levels compared to lean controls and normal AgRP mRNA levels (100, 368). It is possible that other brain regions compensated the local improved leptin sensitivity, by reducing their leptin sensitivity, thereby causing leptin resistance (369, 370). To study if other brain regions become leptin resistant after improving leptin sensitivity in the mediobasal hypothalamus, it would be interesting to investigate the levels of phosphorylated STAT3 protein levels or Socs3 mRNA levels in other brain areas; a reduction in phosphorylated STAT3 or an increase in Socs3 mRNA may indicate leptin resistance. Also the contribution of other Socs3 regulated signaling pathways, such as insulin or IL-6, to obesity remain to be investigated.

Conclusions

Viral vector mediated gene transfer is a great tool to investigate the functions of genes in specific brain areas. In addition, recent studies are investigating the possibilities of using viral vectors to treat genetic diseases in humans, such as diabetes type 1. It will be exciting to see if gene therapy will become an accepted technique to treat diseases in humans.

In this thesis a relatively “simple” behavior as feeding behavior was modified by AAV mediated overexpression or silencing. Feeding behavior is present in all animals, but it already involves many brain circuits and signaling molecules. In this thesis the focus was on leptin, melanocortin and NPY signaling and the role of the hypothalamus. Nevertheless, other pathways may be involved in regulation of energy balance, for example endocannabinoid system and dopamine system (reviewed in (371, 372)). In addition, peripheral signals may regulate neural systems (373). When a “simple” behavior, such as feeding, is already quite complex, it will probably be difficult to fully understand a disorder, such as autism, in which many genes contribute to the susceptibility for this disorder. However, local overexpression or knockdown of genes in certain brain areas at certain

developmental stages may help to unravel the functions of genes, which are involved in certain aspects of “complex” disorders.

REFERENCES

1. Qian S, Chen H, Weingarth D, Trumbauer ME, Novi DE, Guan XM, Yu H, Shen Z, Feng Y, Frazier E, Chen AR, Camacho RE, Shearman LP, Gopal-Truter S, MacNeil DJ, Van der Ploeg LHT, Marsh DJ. 2002. Neither agouti-related protein nor neuropeptide Y is critically required for the regulation of energy homeostasis in mice. *Molecular and Cellular Biology* 22:5027-35
2. Rossi M, Kim MS, Morgan DG, Small CJ, Edwards CM, Sunter D, Abusnana S, Goldstone AP, Russell SH, Stanley SA, Smith DM, Yagaloff K, Gbatei MA, Bloom SR. 1998. A C-terminal fragment of Agouti-related protein increases feeding and antagonizes the effect of alpha-melanocyte stimulating hormone in vivo. *Endocrinology* 139:4428-31
3. Kay MA, Glorioso JC, Naldini L. 2001. Viral vectors for gene therapy: the art of turning infectious agents into vehicles of therapeutics. *Nat. Med.* 7:33-40
4. Matzke MA, Birchler JA. 2005. RNAi-mediated pathways in the nucleus. *Nat. Rev. Genet.* 6:24-35
5. Fire A, Xu SQ, Montgomery MK, Kostas SA, Driver SE, Mello CC. 1998. Potent and specific genetic interference by double-stranded RNA in *Caenorhabditis elegans*. *Nature* 391:806-11
6. Yu JY, DeRuiter SL, Turner DL. 2002. RNA interference by expression of short-interfering RNAs and hairpin RNAs in mammalian cells. *Proc. Natl. Acad. Sci. U. S. A* 99:6047-52
7. Miyagishi M, Taira K. 2002. U6 promoter-driven siRNAs with four uridine 3' overhangs efficiently suppress targeted gene expression in mammalian cells. *Nat. Biotechnol.* 20:497-500
8. Rao DD, Vorhies JS, Senzer N, Nemunaitis J. 2009. siRNA vs. shRNA: similarities and differences. *Adv. Drug Deliv. Rev.* 61:746-59
9. Thomas CE, Ehrhardt A, Kay MA. 2003. Progress and problems with the use of viral vectors for gene therapy. *Nat. Rev. Genet.* 4:346-58
10. Barquinero J, Eixarch H, Perez-Melgosa M. 2004. Retroviral vectors: new applications for an old tool. *Gene Therapy* 11:S3-S9

11. Wong LF. 2006. Lentivirus-mediated gene transfer to the central nervous system: Therapeutic and research applications (vol 17, pg 1, 2006). *Human Gene Therapy* 17:376
12. Pannell D, Ellis J. 2001. Silencing of gene expression: implications for design of retrovirus vectors. *Rev. Med. Virol.* 11:205-17
13. Mok HP, Lever AM. 2007. Chromatin, gene silencing and HIV latency. *Genome Biol.* 8:228
14. Kaplitt MG, Pfaus JG, Kleopoulos SP, Hanlon BA, Rabkin SD, Pfaff DW. 1991. Expression of a functional foreign gene in adult mammalian brain following in Vivo transfer via a herpes simplex virus type 1 defective viral vector. *Mol. Cell Neurosci.* 2:320-30
15. Epstein AL. 2009. HSV-1-derived amplicon vectors: recent technological improvements and remaining difficulties--a review. *Mem. Inst. Oswaldo Cruz* 104:399-410
16. Parks R, Eveleigh C, Graham F. 1999. Use of helper-dependent adenoviral vectors of alternative serotypes permits repeat vector administration. *Gene Ther.* 6:1565-73
17. Morsy MA, Caskey CT. 1999. Expanded-capacity adenoviral vectors--the helper-dependent vectors. *Mol. Med. Today* 5:18-24
18. Zennou V, Serguera C, Sarkis C, Colin P, Perret E, Mallet J, Charneau P. 2001. The HIV-1 DNA flap stimulates HIV vector-mediated cell transduction in the brain. *Nat. Biotechnol.* 19:446-50
19. Follenzi A, Ailles LE, Bakovic S, Geuna M, Naldini L. 2000. Gene transfer by lentiviral vectors is limited by nuclear translocation and rescued by HIV-1 pol sequences. *Nat. Genet.* 25:217-22
20. Dvorin JD, Bell P, Maul GG, Yamashita M, Emerman M, Malim MH. 2002. Reassessment of the roles of integrase and the central DNA flap in human immunodeficiency virus type 1 nuclear import. *J. Virol.* 76:12087-96
21. Lever AM, Strappe PM, Zhao J. 2004. Lentiviral vectors. *J. Biomed. Sci.* 11:439-49
22. Zufferey R, Dull T, Mandel RJ, Bukovsky A, Quiroz D, Naldini L, Trono D. 1998. Self-inactivating lentivirus vector for safe and efficient in vivo gene delivery. *J. Virol.* 72:9873-80

23. Akkina RK, Walton RM, Chen ML, Li QX, Planelles V, Chen IS. 1996. High-efficiency gene transfer into CD34+ cells with a human immunodeficiency virus type 1-based retroviral vector pseudotyped with vesicular stomatitis virus envelope glycoprotein G. *J. Virol.* 70:2581-5
24. Naldini L, Blomer U, Gally P, Ory D, Mulligan R, Gage FH, Verma IM, Trono D. 1996. In vivo gene delivery and stable transduction of nondividing cells by a lentiviral vector. *Science* 272:263-7
25. Schlegel R, Tralka TS, Willingham MC, Pastan I. 1983. Inhibition of VSV binding and infectivity by phosphatidylserine: is phosphatidylserine a VSV-binding site? *Cell* 32:639-46
26. Coil DA, Miller AD. 2004. Phosphatidylserine is not the cell surface receptor for vesicular stomatitis virus. *J. Virol.* 78:10920-6
27. Burns JC, Friedmann T, Driever W, Burrascano M, Yee JK. 1993. Vesicular stomatitis virus G glycoprotein pseudotyped retroviral vectors: concentration to very high titer and efficient gene transfer into mammalian and nonmammalian cells. *Proc. Natl. Acad. Sci. U. S. A* 90:8033-7
28. Cronin J, Zhang XY, Reiser J. 2005. Altering the tropism of lentiviral vectors through pseudotyping. *Curr. Gene Ther.* 5:387-98
29. Baekelandt V, Claeys A, Eggermont K, Lauwers E, De Strooper B, Nuttin B, Debyser Z. 2002. Characterization of lentiviral vector-mediated gene transfer in adult mouse brain. *Hum. Gene Ther.* 13:841-53
30. Nielsen TT, Marion I, Hasholt L, Lundberg C. 2009. Neuron-specific RNA interference using lentiviral vectors. *J. Gene Med.* 11:559-69
31. Naldini L, Blomer U, Gage FH, Trono D, Verma IM. 1996. Efficient transfer, integration, and sustained long-term expression of the transgene in adult rat brains injected with a lentiviral vector. *Proc. Natl. Acad. Sci. U. S. A* 93:11382-8
32. Lois C, Hong EJ, Pease S, Brown EJ, Baltimore D. 2002. Germline transmission and tissue-specific expression of transgenes delivered by lentiviral vectors. *Science* 295:868-72
33. Robinson DA, Dillon CP, Kwiatkowski AV, Sievers C, Yang L, Kopinja J, Rooney DL, Zhang M, Ihrig MM, McManus MT, Gertler FB, Scott ML, Van Parijs L. 2003. A lentivirus-based system to functionally silence genes in

- primary mammalian cells, stem cells and transgenic mice by RNA interference. *Nat. Genet.* 33:401-6
34. Weindler FW, Heilbronn R. 1991. A subset of herpes simplex virus replication genes provides helper functions for productive adeno-associated virus replication. *J. Virol.* 65:2476-83
35. Schlehofer JR, Ehrbar M, zur HH. 1986. Vaccinia virus, herpes simplex virus, and carcinogens induce DNA amplification in a human cell line and support replication of a helpervirus dependent parvovirus. *Virology* 152:110-7
36. Lu Y. 2004. Recombinant adeno-associated virus as delivery vector for gene therapy - A review. *Stem Cells and Development* 13:133-45
37. McCarty DM, Young SM, Samulski RJ. 2004. Integration of adeno-associated virus (AAV) and recombinant AAV vectors. *Annual Review of Genetics* 38:819-45
38. Bartlett JS, Samulski RJ, Mccown TJ. 1998. Selective and rapid uptake of adeno-associated virus type 2 in brain. *Human Gene Therapy* 9:1181-6
39. Ding W, Zhang L, Yan Z, Engelhardt JF. 2005. Intracellular trafficking of adeno-associated viral vectors. *Gene Therapy* 12:873-80
40. Thomas CE, Storm TA, Huang Z, Kay MA. 2004. Rapid uncoating of vector genomes is the key to efficient liver transduction with pseudotyped adeno-associated virus vectors. *Journal of Virology* 78:3110-22
41. Gao GP, Alvira MR, Wang L, Calcedo R, Johnston J, Wilson JM. 2002. Novel adeno-associated viruses from rhesus monkeys as vectors for human gene therapy. *Proc. Natl. Acad. Sci. U. S A* 99:11854-9
42. Hoggan MD, Blacklow NR, Rowe WP. 1966. Studies of small DNA viruses found in various adenovirus preparations: physical, biological, and immunological characteristics. *Proc. Natl. Acad. Sci. U. S A* 55:1467-74
43. ATCHISON RW, CASTO BC, HAMMON WM. 1965. ADENOVIRUS-ASSOCIATED DEFECTIVE VIRUS PARTICLES. *Science* 149:754-6
44. Parks WP, Green M, Pina M, Melnick JL. 1967. Physicochemical characterization of adeno-associated satellite virus type 4 and its nucleic acid. *J. Virol.* 1:980-7

45. Bantel-Schaal U, zur HH. 1984. Characterization of the DNA of a defective human parvovirus isolated from a genital site. *Virology* 134:52-63
46. Georg-Fries B, Biederlack S, Wolf J, zur HH. 1984. Analysis of proteins, helper dependence, and seroepidemiology of a new human parvovirus. *Virology* 134:64-71
47. Rutledge EA, Halbert CL, Russell DW. 1998. Infectious clones and vectors derived from adeno-associated virus (AAV) serotypes other than AAV type 2. *J. Virol.* 72:309-19
48. Gao G, Vandenberghe LH, Alvira MR, Lu Y, Calcedo R, Zhou X, Wilson JM. 2004. Clades of Adeno-associated viruses are widely disseminated in human tissues. *J. Virol.* 78:6381-8
49. Mori S, Wang L, Takeuchi T, Kanda T. 2004. Two novel adeno-associated viruses from cynomolgus monkey: pseudotyping characterization of capsid protein. *Virology* 330:375-83
50. Schmidt M, Voutetakis A, Afione S, Zheng C, Mandikian D, Chiorini JA. 2008. Adeno-associated virus Type 12 (AAV12): A novel AAV serotype with sialic acid- and heparan sulfate proteoglycan-independent transduction activity. *Journal of Virology* 82:1399-406
51. Summerford C, Samulski RJ. 1998. Membrane-associated heparan sulfate proteoglycan is a receptor for adeno-associated virus type 2 virions. *Journal of Virology* 72:1438-45
52. Summerford C, Bartlett JS, Samulski RJ. 1999. alpha V beta 5 integrin: a co-receptor for adeno-associated virus type 2 infection. *Nature Medicine* 5:78-82
53. Qing K, Mah C, Hansen J, Zhou SZ, Dwarki V, Srivastava A. 1999. Human fibroblast growth factor receptor 1 is a co-receptor for infection by adeno-associated virus 2. *Nature Medicine* 5:71-7
54. Kashiwakura Y, Tamayose K, Iwabuchi K, Hirai Y, Shimada T, Matsumoto K, Nakamura T, Watanabe M, Oshimi K, Daida H. 2005. Hepatocyte growth factor receptor is a coreceptor for adeno-associated virus type 2 infection. *Journal of Virology* 79:609-14
55. Rabinowitz JE, Rolling F, Li CW, Conrath H, Xiao WD, Xiao X, Samulski RJ. 2002. Cross-packaging of a single adeno-associated virus (AAV) type

- 2 vector genome into multiple AAV serotypes enables transduction with broad specificity. *Journal of Virology* 76:791-801
56. Wu ZJ, Miller E, Agbandje-McKenna M, Samulski RJ. 2006. alpha 2,3 and alpha 2,6 N-linked sialic acids facilitate efficient binding and transduction by adeno-associated virus types 1 and 6. *Journal of Virology* 80:9093-103
57. Kaludov N, Brown KE, Walters RW, Zabner J, Chiorini JA. 2001. Adeno-associated virus serotype 4 (AAV4) and AAV5 both require sialic acid binding for hemagglutination and efficient transduction but differ in sialic acid linkage specificity. *Journal of Virology* 75:6884-93
58. Di Pasquale G, Davidson BL, Stein CS, Martins IS, Scudiero D, Monks A, Chiorini JA. 2003. Identification of PDGFR as a receptor for AAV-5 transduction. *Nature Medicine* 9:1306-12
59. Rabinowitz JE, Bowles DE, Faust SM, Ledford JG, Cunningham SE, Samulski RJ. 2004. Cross-dressing the virion: the transcapsidation of adeno-associated virus serotypes functionally defines subgroups. *J. Virol.* 78:4421-32
60. Trepel M, Grifman M, Weitzman MD, Pasqualini R. 2000. Molecular adaptors for vascular-targeted adenoviral gene delivery. *Human Gene Therapy* 11:1971-81
61. Michelfelder S, Trepel M. 2009. Adeno-associated viral vectors and their redirection to cell-type specific receptors. *Adv. Genet.* 67:29-60
62. Burger C, Gorbatyuk OS, Velardo MJ, Peden CS, Williams P, Zolotukhin S, Reier PJ, Mandel RJ, Muzyczka N. 2004. Recombinant AAV viral vectors pseudotyped with viral capsids from serotypes 1, 2, and 5 display differential efficiency and cell tropism after delivery to different regions of the central nervous system. *Mol. Ther.* 10:302-17
63. Klein RL, Dayton RD, Leidenheimer NJ, Jansen K, Golde TE, Zweig RM. 2006. Efficient neuronal gene transfer with AAV8 leads to neurotoxic levels of tau or green fluorescent proteins. *Mol. Ther.* 13:517-27
64. Reimsnider S, Manfredsson FP, Muzyczka N, Mandel RJ. 2007. Time course of transgene expression after intrastriatal pseudotyped rAAV2/1, rAAV2/2, rAAV2/5, and rAAV2/8 transduction in the rat. *Mol. Ther.* 15:1504-11

65. McFarland NR, Lee JS, Hyman BT, McLean PJ. 2009. Comparison of transduction efficiency of recombinant AAV serotypes 1, 2, 5, and 8 in the rat nigrostriatal system. *J. Neurochem.* 109:838-45
66. Blits B, Derks S, Twisk J, Ehler E, Prins J, Verhaagen J. 2009. Adeno-associated viral vector (AAV)-mediated gene transfer in the red nucleus of the adult rat brain: Comparative analysis of the transduction properties of seven AAV serotypes and lentiviral vectors. *J. Neurosci. Methods*
67. Berthoud HR. 2002. Multiple neural systems controlling food intake and body weight. *Neurosci. Biobehav. Rev.* 26:393-428
68. ANAND BK, BROBECK JR. 1951. Hypothalamic control of food intake in rats and cats. *Yale J. Biol. Med.* 24:123-40
69. STELLAR E. 1954. The physiology of motivation. *Psychol. Rev.* 61:5-22
70. Norsted E, Gomuc B, Meister B. 2008. Protein components of the blood-brain barrier (BBB) in the mediobasal hypothalamus. *J. Chem. Neuroanat.* 36:107-21
71. Tang-Christensen M, Holst JJ, Hartmann B, Vrang N. 1999. The arcuate nucleus is pivotal in mediating the anorectic effects of centrally administered leptin. *Neuroreport* 10:1183-7
72. Dawson R, Pellemounter MA, Millard WJ, Liu S, Eppler B. 1997. Attenuation of leptin-mediated effects by monosodium glutamate-induced arcuate nucleus damage. *American Journal of Physiology-Endocrinology and Metabolism* 36:E202-E206
73. Vrang N, Larsen PJ, Clausen JT, Kristensen P. 1999. Neurochemical characterization of hypothalamic cocaine- amphetamine-regulated transcript neurons. *J. Neurosci.* 19:RC5
74. Hahn TM, Breininger JF, Baskin DG, Schwartz MW. 1998. Coexpression of Agrp and NPY in fasting-activated hypothalamic neurons. *Nat. Neurosci.* 1:271-2
75. Cowley MA, Smart JL, Rubinstein M, Cerdan MG, Diano S, Horvath TL, Cone RD, Low MJ. 2001. Leptin activates anorexigenic POMC neurons through a neural network in the arcuate nucleus. *Nature* 411:480-4
76. Schwartz MW, Woods SC, Porte D, Jr., Seeley RJ, Baskin DG. 2000. Central nervous system control of food intake. *Nature* 404:661-71

77. Grill HJ. 2009. Leptin and the systems neuroscience of meal size control. *Front Neuroendocrinol.*
78. Adan RA, Tiesjema B, Hillebrand JJ, la Fleur SE, Kas MJ, de Krom M. 2006. The MC4 receptor and control of appetite. *Br. J. Pharmacol.* 149:815-27
79. Blouet C, Schwartz GJ. 2009. Hypothalamic nutrient sensing in the control of energy homeostasis. *Behav. Brain Res.*
80. Tokunaga K, Fukushima M, Kemnitz JW, Bray GA. 1986. Comparison of ventromedial and paraventricular lesions in rats that become obese. *Am. J. Physiol* 251:R1221-R1227
81. King BM. 2006. The rise, fall, and resurrection of the ventromedial hypothalamus in the regulation of feeding behavior and body weight. *Physiol Behav.* 87:221-44
82. Miki T, Liss B, Minami K, Shiuchi T, Saraya A, Kashima Y, Horiuchi M, Ashcroft F, Minokoshi Y, Roeper J, Seino S. 2001. ATP-sensitive K⁺ channels in the hypothalamus are essential for the maintenance of glucose homeostasis. *Nat. Neurosci.* 4:507-12
83. Murphy BA, Fakira KA, Song Z, Beuve A, Routh VH. 2009. AMP-activated protein kinase and nitric oxide regulate the glucose sensitivity of ventromedial hypothalamic glucose-inhibited neurons. *Am. J. Physiol Cell Physiol* 297:C750-C758
84. Bamshad M, Aoki VT, Adkison MG, Warren WS, Bartness TJ. 1998. Central nervous system origins of the sympathetic nervous system outflow to white adipose tissue. *Am. J. Physiol* 275:R291-R299
85. Bamshad M, Song CK, Bartness TJ. 1999. CNS origins of the sympathetic nervous system outflow to brown adipose tissue. *Am. J. Physiol* 276:R1569-R1578
86. Ter Horst GJ, Luiten PG, Kuipers F. 1984. Descending pathways from hypothalamus to dorsal motor vagus and ambiguous nuclei in the rat. *J. Auton. Nerv. Syst.* 11:59-75
87. Oltmans GA, Harvey JA. 1976. Lateral hypothalamic syndrome in rats: a comparison of the behavioral and neurochemical effects of lesions placed

- in the lateral hypothalamus and nigrostriatal bundle. *J. Comp Physiol Psychol.* 90:1051-62
88. Herberg LJ, Blundell JE. 1967. Lateral hypothalamus: hoarding behavior elicited by electrical stimulation. *Science* 155:349-50
 89. Qu D, Ludwig DS, Gammeltoft S, Piper M, Pelleymounter MA, Cullen MJ, Mathes WF, Przypek R, Kanarek R, Maratos-Flier E. 1996. A role for melanin-concentrating hormone in the central regulation of feeding behaviour. *Nature* 380:243-7
 90. Ludwig DS, Tritos NA, Mastaitis JW, Kulkarni R, Kokkotou E, Elmquist J, Lowell B, Flier JS, Maratos-Flier E. 2001. Melanin-concentrating hormone overexpression in transgenic mice leads to obesity and insulin resistance. *J. Clin. Invest* 107:379-86
 91. Sakurai T, Amemiya A, Ishii M, Matsuzaki I, Chemelli RM, Tanaka H, Williams SC, Richardson JA, Kozlowski GP, Wilson S, Arch JR, Buckingham RE, Haynes AC, Carr SA, Annan RS, McNulty DE, Liu WS, Terrett JA, Elshourbagy NA, Bergsma DJ, Yanagisawa M. 1998. Orexins and orexin receptors: a family of hypothalamic neuropeptides and G protein-coupled receptors that regulate feeding behavior. *Cell* 92:1
 92. Sakurai T. 2002. Roles of orexins in regulation of feeding and wakefulness. *Neuroreport* 13:987-95
 93. Peyron C, Tighe DK, van Den Pol AN, de Lecea L, Heller HC, Sutcliffe JG, Kilduff TS. 1998. Neurons containing hypocretin (orexin) project to multiple neuronal systems. *J. Neurosci.* 18:9996-10015
 94. Kaplan JM, Seeley RJ, Grill HJ. 1993. Daily Caloric-Intake in Intact and Chronic Decerebrate Rats. *Behavioral Neuroscience* 107:876-81
 95. Seeley RJ, Grill HJ, Kaplan JM. 1994. Neurological Dissociation of Gastrointestinal and Metabolic Contributions to Meal Size Control. *Behavioral Neuroscience* 108:347-52
 96. Hayes MR, Skibicka KP, Lechner TM, Guarnieri DJ, Dileone RJ, Bence KK, Grill HJ. 2010. Endogenous leptin signaling in the caudal nucleus tractus solitarius and area postrema is required for energy balance regulation. *Cell Metab* 11:77-83

97. Kelley AE, Baldo BA, Pratt WE, Will MJ. 2005. Corticostriatal-hypothalamic circuitry and food motivation: Integration of energy, action and reward. *Physiology & Behavior* 86:773-95
98. Elias CF, Aschkenasi C, Lee C, Kelly J, Ahima RS, Bjorbaek C, Flier JS, Saper CB, Elmquist JK. 1999. Leptin differentially regulates NPY and POMC neurons projecting to the lateral hypothalamic area. *Neuron* 23:775-86
99. van den TM, Lee K, Whyment AD, Blanks AM, Spanswick D. 2004. Orexigen-sensitive NPY/AgRP pacemaker neurons in the hypothalamic arcuate nucleus. *Nat. Neurosci.* 7:493-4
100. Korner J, Savontaus E, Chua SC, Jr., Leibel RL, Wardlaw SL. 2001. Leptin regulation of *AgRP* and *Npy* mRNA in the rat hypothalamus. *J. Neuroendocrinol.* 13:959-66
101. Considine RV, Sinha MK, Heiman ML, Kriauciunas A, Stephens TW, Nyce MR, Ohannesian JP, Marco CC, McKee LJ, Bauer TL, . 1996. Serum immunoreactive-leptin concentrations in normal-weight and obese humans. *N. Engl. J. Med.* 334:292-5
102. Morris DL, Rui L. 2009. Recent advances in understanding leptin signaling and leptin resistance. *Am. J. Physiol Endocrinol. Metab* 297:E1247-E1259
103. Zhang Y, Proenca R, Maffei M, Barone M, Leopold L, Friedman JM. 1994. Positional cloning of the mouse obese gene and its human homologue. *Nature* 372:425-32
104. Bahary N, Leibel RL, Joseph L, Friedman JM. 1990. Molecular mapping of the mouse *db* mutation. *Proc. Natl. Acad. Sci. U. S. A* 87:8642-6
105. Phillips MS, Liu QY, Hammond HA, Dugan V, Hey PJ, Caskey CT, Hess JF. 1996. Leptin receptor missense mutation in the fatty Zucker rat. *Nature Genetics* 13:18-9
106. Takaya K, Ogawa Y, Hiraoka J, Hosoda K, Yamori Y, Nakao K, Koletsky RJ. 1996. Nonsense mutation of leptin receptor in the obese spontaneously hypertensive Koletsky rat. *Nature Genetics* 14:130-1
107. Maffei M, Halaas J, Ravussin E, Pratley RE, Lee GH, Zhang Y, Fei H, Kim S, Lallone R, Ranganathan S, . 1995. Leptin levels in human and rodent:

- measurement of plasma leptin and ob RNA in obese and weight-reduced subjects. *Nat. Med.* 1:1155-61
108. Frederich RC, Hamann A, Anderson S, Lollmann B, Lowell BB, Flier JS. 1995. Leptin levels reflect body lipid content in mice: evidence for diet-induced resistance to leptin action. *Nat. Med.* 1:1311-4
109. Heymsfield SB, Greenberg AS, Fujioka K, Dixon RM, Kushner R, Hunt T, Lubina JA, Patane J, Self B, Hunt P, McCamish M. 1999. Recombinant leptin for weight loss in obese and lean adults: a randomized, controlled, dose-escalation trial. *JAMA* 282:1568-75
110. Bjorbaek C, Elmquist JK, Frantz JD, Shoelson SE, Flier JS. 1998. Identification of SOCS-3 as a potential mediator of central leptin resistance. *Mol. Cell* 1:619-25
111. Bjorbaek C, El Haschimi K, Frantz JD, Flier JS. 1999. The role of SOCS-3 in leptin signaling and leptin resistance. *J. Biol. Chem.* 274:30059-65
112. Bjorbak C, Lavery HJ, Bates SH, Olson RK, Davis SM, Flier JS, Myers MG, Jr. 2000. SOCS3 mediates feedback inhibition of the leptin receptor via Tyr985. *J. Biol. Chem.* 275:40649-57
113. Peiser C, McGregor GP, Lang RE. 2000. Leptin receptor expression and suppressor of cytokine signaling transcript levels in high-fat-fed rats. *Life Sci.* 67:2971-81
114. Emilsson V, Arch JR, de Groot RP, Lister CA, Cawthorne MA. 1999. Leptin treatment increases suppressors of cytokine signaling in central and peripheral tissues. *FEBS Lett.* 455:170-4
115. Munzberg H, Flier JS, Bjorbaek C. 2004. Region-specific leptin resistance within the hypothalamus of diet-induced obese mice. *Endocrinology* 145:4880-9
116. Tups A, Ellis C, Moar KM, Logie TJ, Adam CL, Mercer JG, Klingenspor M. 2004. Photoperiodic regulation of leptin sensitivity in the Siberian hamster, *Phodopus sungorus*, is reflected in arcuate nucleus SOCS-3 (suppressor of cytokine signaling) gene expression. *Endocrinology* 145:1185-93
117. Krol E, Tups A, Archer ZA, Ross AW, Moar KM, Bell LM, Duncan JS, Mayer C, Morgan PJ, Mercer JG, Speakman JR. 2007. Altered expression of SOCS3 in the hypothalamic arcuate nucleus during seasonal body mass

- changes in the field vole, *Microtus agrestis*. *Journal of Neuroendocrinology* 19:83-94
118. Baker BJ, Akhtar LN, Benveniste EN. 2009. SOCS1 and SOCS3 in the control of CNS immunity. *Trends in Immunology* 30:392-400
 119. Howard JK, Cave BJ, Oksanen LJ, Tzamelis I, Bjorbaek C, Flier JS. 2004. Enhanced leptin sensitivity and attenuation of diet-induced obesity in mice with haploinsufficiency of Socs3. *Nat. Med.* 10:734-8
 120. Mori H, Hanada R, Hanada T, Aki D, Mashima R, Nishinakamura H, Torisu T, Chien KR, Yasukawa H, Yoshimura A. 2004. Socs3 deficiency in the brain elevates leptin sensitivity and confers resistance to diet-induced obesity. *Nat. Med.* 10:739-43
 121. Druce M, Bloom SR. 2006. The regulation of appetite. *Archives of Disease in Childhood* 91:183-7
 122. de Krom M, Bauer F, Collier D, Adan RA, la Fleur SE. 2009. Genetic Variation and Effects on Human Eating Behavior. *Annu. Rev. Nutr.*
 123. Flynn MC, Scott TR, Pritchard TC, Plata-Salaman CR. 1998. Mode of action of OB protein (leptin) on feeding. *Am. J. Physiol* 275:R174-R179
 124. Eckel LA, Langhans W, Kahler A, Campfield LA, Smith FJ, Geary N. 1998. Chronic administration of OB protein decreases food intake by selectively reducing meal size in female rats. *Am. J. Physiol* 275:R186-R193
 125. Kahler A, Geary N, Eckel LA, Campfield LA, Smith FJ, Langhans W. 1998. Chronic administration of OB protein decreases food intake by selectively reducing meal size in male rats. *Am. J. Physiol* 275:R180-R185
 126. Elmquist JK, Bjorbaek C, Ahima RS, Flier JS, Saper CB. 1998. Distributions of leptin receptor mRNA isoforms in the rat brain. *J. Comp Neurol.* 395:535-47
 127. Mercer JG, Hoggard N, Williams LM, Lawrence CB, Hannah LT, Trayhurn P. 1996. Localization of leptin receptor mRNA and the long form splice variant (Ob-Rb) in mouse hypothalamus and adjacent brain regions by in situ hybridization. *FEBS Lett.* 387:113-6
 128. Morton GJ, Niswender KD, Rhodes CJ, Myers MG, Jr., Blevins JE, Baskin DG, Schwartz MW. 2003. Arcuate nucleus-specific leptin receptor gene

- therapy attenuates the obesity phenotype of Koletsky (fa(k)/fa(k)) rats. *Endocrinology* 144:2016-24
129. Blevins JE, Morton GJ, Williams DL, Caldwell DW, Bastian LS, Wisse BE, Schwartz MW, Baskin DG. 2009. Forebrain melanocortin signaling enhances the hindbrain satiety response to CCK-8. *Am. J. Physiol Regul. Integr. Comp Physiol* 296:R476-R484
130. Moran TH, Aja S, Ladenheim EE. 2006. Leptin modulation of peripheral controls of meal size. *Physiol Behav.* 89:511-6
131. Gautron L, Lee C, Funahashi H, Friedman J, Lee S, Elmquist J. 2010. Melanocortin-4 receptor expression in a vago-vagal circuitry involved in postprandial functions. *J. Comp Neurol.* 518:6-24
132. Grill HJ, Ginsberg AB, Seeley RJ, Kaplan JM. 1998. Brainstem application of melanocortin receptor ligands produces long-lasting effects on feeding and body weight. *J. Neurosci.* 18:10128-35
133. Williams DL, Kaplan JM, Grill HJ. 2000. The role of the dorsal vagal complex and the vagus nerve in feeding effects of melanocortin-3/4 receptor stimulation. *Endocrinology* 141:1332-7
134. Zheng H, Patterson LM, Phifer CB, Berthoud HR. 2005. Brain stem melanocortinerbic modulation of meal size and identification of hypothalamic POMC projections. *Am. J. Physiol Regul. Integr. Comp Physiol* 289:R247-R258
135. Bagnol D, Lu XY, Kaelin CB, Day HE, Ollmann M, Gantz I, Akil H, Barsh GS, Watson SJ. 1999. Anatomy of an endogenous antagonist: relationship between Agouti-related protein and proopiomelanocortin in brain. *J. Neurosci.* 19:RC26
136. Mezey E, Kiss JZ, Mueller GP, Eskay R, O'Donohue TL, Palkovits M. 1985. Distribution of the pro-opiomelanocortin derived peptides, adrenocorticotrope hormone, alpha-melanocyte-stimulating hormone and beta-endorphin (ACTH, alpha-MSH, beta-END) in the rat hypothalamus. *Brain Res.* 328:341-7
137. Haskell-Luevano C, Chen P, Li C, Chang K, Smith MS, Cameron JL, Cone RD. 1999. Characterization of the neuroanatomical distribution of agouti-

- related protein immunoreactivity in the rhesus monkey and the rat. *Endocrinology* 140:1408-15
138. Wilson BD, Bagnol D, Kaelin CB, Ollmann MM, Gantz I, Watson SJ, Barsh GS. 1999. Physiological and anatomical circuitry between Agouti-related protein and leptin signaling. *Endocrinology* 140:2387-97
139. Kishi T, Aschkenasi CJ, Lee CE, Mountjoy KG, Saper CB, Elmquist JK. 2003. Expression of melanocortin 4 receptor mRNA in the central nervous system of the rat. *J. Comp Neurol.* 457:213-35
140. Elmquist JK. 2001. Hypothalamic pathways underlying the endocrine, autonomic, and behavioral effects of leptin. *Int. J. Obes. Relat Metab Disord.* 25 Suppl 5:S78-S82
141. MacNeil DJ, Howard AD, Guan X, Fong TM, Nargund RP, Bednarek MA, Goulet MT, Weinberg DH, Strack AM, Marsh DJ, Chen HY, Shen CP, Chen AS, Rosenblum CI, MacNeil T, Tota M, MacIntyre ED, Van der Ploeg LH. 2002. The role of melanocortins in body weight regulation: opportunities for the treatment of obesity. *Eur. J. Pharmacol.* 450:93-109
142. Bertolini A, Tacchi R, Vergoni AV. 2009. Brain effects of melanocortins. *Pharmacol. Res.* 59:13-47
143. Schioth HB, Chhajlani V, Muceniece R, Klusa V, Wikberg JE. 1996. Major pharmacological distinction of the ACTH receptor from other melanocortin receptors. *Life Sci.* 59:797-801
144. Adan RA, Gispen WH. 1997. Brain melanocortin receptors: from cloning to function. *Peptides* 18:1279-87
145. Ollmann MM, Wilson BD, Yang YK, Kerns JA, Chen Y, Gantz I, Barsh GS. 1997. Antagonism of central melanocortin receptors in vitro and in vivo by agouti-related protein. *Science* 278:135-8
146. Roselli-Reh fuss L, Mountjoy KG, Robbins LS, Mortrud MT, Low MJ, Tatro JB, Entwistle ML, Simerly RB, Cone RD. 1993. Identification of a receptor for gamma melanotropin and other proopiomelanocortin peptides in the hypothalamus and limbic system. *Proc. Natl. Acad. Sci. U. S. A* 90:8856-60

147. Mountjoy KG, Mortrud MT, Low MJ, Simerly RB, Cone RD. 1994. Localization of the melanocortin-4 receptor (MC4-R) in neuroendocrine and autonomic control circuits in the brain. *Mol. Endocrinol.* 8:1298-308
148. Fathi Z, Iben LG, Parker EM. 1995. Cloning, expression, and tissue distribution of a fifth melanocortin receptor subtype. *Neurochem. Res.* 20:107-13
149. Griffon N, Mignon V, Facchinetti P, Diaz J, Schwartz JC, Sokoloff P. 1994. Molecular cloning and characterization of the rat fifth melanocortin receptor. *Biochem. Biophys. Res. Commun.* 200:1007-14
150. Xia Y, Wikberg JE, Chhajlani V. 1995. Expression of melanocortin 1 receptor in periaqueductal gray matter. *Neuroreport* 6:2193-6
151. Wikberg JE. 1999. Melanocortin receptors: perspectives for novel drugs. *Eur. J. Pharmacol.* 375:295-310
152. Wikberg JE, Muceniece R, Mandrika I, Prusis P, Lindblom J, Post C, Skottner A. 2000. New aspects on the melanocortins and their receptors. *Pharmacol. Res.* 42:393-420
153. Boston BA. 1999. The role of melanocortins in adipocyte function. *Ann. N. Y. Acad. Sci.* 885:75-84
154. Gantz I, Fong TM. 2003. The melanocortin system. *Am. J. Physiol Endocrinol. Metab* 284:E468-E474
155. Lipton JM, Catania A. 1998. Mechanisms of antiinflammatory action of the neuroimmunomodulatory peptide alpha-MSH. *Ann. N. Y. Acad. Sci.* 840:373-80
156. Huszar D, Lynch CA, Fairchild-Huntress V, Dunmore JH, Fang Q, Berkemeier LR, Gu W, Kesterson RA, Boston BA, Cone RD, Smith FJ, Campfield LA, Burn P, Lee F. 1997. Targeted disruption of the melanocortin-4 receptor results in obesity in mice. *Cell* 88:131-41
157. Chen AS, Marsh DJ, Trumbauer ME, Frazier EG, Guan XM, Yu H, Rosenblum CI, Vongs A, Feng Y, Cao L, Metzger JM, Strack AM, Camacho RE, Mellin TN, Nunes CN, Min W, Fisher J, Gopal-Truter S, MacIntyre DE, Chen HY, Van der Ploeg LH. 2000. Inactivation of the mouse melanocortin-3 receptor results in increased fat mass and reduced lean body mass. *Nat. Genet.* 26:97-102

158. Butler AA, Kesterson RA, Khong K, Cullen MJ, Pellemounter MA, Dekoning J, Baetscher M, Cone RD. 2000. A unique metabolic syndrome causes obesity in the melanocortin-3 receptor-deficient mouse. *Endocrinology* 141:3518-21
159. Liu H, Kishi T, Roseberry AG, Cai X, Lee CE, Montez JM, Friedman JM, Elmquist JK. 2003. Transgenic mice expressing green fluorescent protein under the control of the melanocortin-4 receptor promoter. *J. Neurosci.* 23:7143-54
160. Bultman SJ, Michaud EJ, Woychik RP. 1992. Molecular characterization of the mouse agouti locus. *Cell* 71:1195-204
161. Mountjoy KG, Willard DH, Wilkison WO. 1999. Agouti antagonism of melanocortin-4 receptor: greater effect with desacetyl-alpha-melanocyte-stimulating hormone (MSH) than with alpha-MSH. *Endocrinology* 140:2167-72
162. Nijenhuis WA, Oosterom J, Adan RA. 2001. AgRP(83-132) acts as an inverse agonist on the human-melanocortin-4 receptor. *Mol. Endocrinol.* 15:164-71
163. Graham M, Shutter JR, Sarmiento U, Sarosi I, Stark KL. 1997. Overexpression of Agrt leads to obesity in transgenic mice. *Nat. Genet.* 17:273-4
164. Yaswen L, Diehl N, Brennan MB, Hochgeschwender U. 1999. Obesity in the mouse model of pro-opiomelanocortin deficiency responds to peripheral melanocortin. *Nat. Med.* 5:1066-70
165. Challis BG, Coll AP, Yeo GS, Pinnock SB, Dickson SL, Thresher RR, Dixon J, Zahn D, Rochford JJ, White A, Oliver RL, Millington G, Aparicio SA, Colledge WH, Russ AP, Carlton MB, O'Rahilly S. 2004. Mice lacking pro-opiomelanocortin are sensitive to high-fat feeding but respond normally to the acute anorectic effects of peptide-YY(3-36). *Proc. Natl. Acad. Sci. U. S. A* 101:4695-700
166. Savontaus E, Breen TL, Kim A, Yang LM, Chua SC, Jr., Wardlaw SL. 2004. Metabolic effects of transgenic melanocyte-stimulating hormone overexpression in lean and obese mice. *Endocrinology* 145:3881-91

167. Mizuno TM, Kelley KA, Pasinetti GM, Roberts JL, Mobbs CV. 2003. Transgenic neuronal expression of proopiomelanocortin attenuates hyperphagic response to fasting and reverses metabolic impairments in leptin-deficient obese mice. *Diabetes* 52:2675-83
168. Li G, Zhang Y, Cheng KY, Scarpance PJ. 2007. Lean rats with hypothalamic pro-opiomelanocortin overexpression exhibit greater diet-induced obesity and impaired central melanocortin responsiveness. *Diabetologia* 50:1490-9
169. Li G, Zhang Y, Wilsey JT, Scarpance PJ. 2005. Hypothalamic pro-opiomelanocortin gene delivery ameliorates obesity and glucose intolerance in aged rats. *Diabetologia* 48:2376-85
170. Wortley KE, Anderson KD, Yasenchak J, Murphy A, Valenzuela D, Diano S, Yancopoulos GD, Wiegand SJ, Sleeman MW. 2005. Agouti-related protein-deficient mice display an age-related lean phenotype. *Cell Metab* 2:421-7
171. Ste ML, Miura GI, Marsh DJ, Yagaloff K, Palmiter RD. 2000. A metabolic defect promotes obesity in mice lacking melanocortin-4 receptors. *Proc. Natl. Acad. Sci. U. S. A* 97:12339-44
172. Chen AS, Metzger JM, Trumbauer ME, Guan XM, Yu H, Frazier EG, Marsh DJ, Forrest MJ, Gopal-Truter S, Fisher J, Camacho RE, Strack AM, Mellin TN, MacIntyre DE, Chen HY, Van der Ploeg LH. 2000. Role of the melanocortin-4 receptor in metabolic rate and food intake in mice. *Transgenic Res.* 9:145-54
173. Marsh DJ, Hollopeter G, Huszar D, Laufer R, Yagaloff KA, Fisher SL, Burn P, Palmiter RD. 1999. Response of melanocortin-4 receptor-deficient mice to anorectic and orexigenic peptides. *Nat. Genet.* 21:119-22
174. Fekete C, Marks DL, Sarkar S, Emerson CH, Rand WM, Cone RD, Lechan RM. 2004. Effect of Agouti-related protein in regulation of the hypothalamic-pituitary-thyroid axis in the melanocortin 4 receptor knockout mouse. *Endocrinology* 145:4816-21
175. Marsh DJ, Miura GI, Yagaloff KA, Schwartz MW, Barsh GS, Palmiter RD. 1999. Effects of neuropeptide Y deficiency on hypothalamic agouti-related

- p>protein expression and responsiveness to melanocortin analogues.
- Brain Res.*
- 848:66-77
176. Balthasar N, Dalgaard LT, Lee CE, Yu J, Funahashi H, Williams T, Ferreira M, Tang V, McGovern RA, Kenny CD, Christiansen LM, Edelstein E, Choi B, Boss O, Aschkenasi C, Zhang CY, Mountjoy K, Kishi T, Elmquist JK, Lowell BB. 2005. Divergence of melanocortin pathways in the control of food intake and energy expenditure. *Cell* 123:493-505
 177. Poggioli R, Vergoni AV, Bertolini A. 1986. ACTH-(1-24) and alpha-MSH antagonize feeding behavior stimulated by kappa opiate agonists. *Peptides* 7:843-8
 178. Kask A, Rago L, Wikberg JE, Schioth HB. 2000. Differential effects of melanocortin peptides on ingestive behaviour in rats: evidence against the involvement of MC(3) receptor in the regulation of food intake. *Neurosci. Lett.* 283:1-4
 179. Abbott CR, Rossi M, Kim M, AlAhmed SH, Taylor GM, Ghatei MA, Smith DM, Bloom SR. 2000. Investigation of the melanocyte stimulating hormones on food intake. Lack Of evidence to support a role for the melanocortin-3-receptor. *Brain Res.* 869:203-10
 180. McKay LD, Kenney NJ, Edens NK, Williams RH, Woods SC. 1981. Intracerebroventricular beta-endorphin increases food intake of rats. *Life Sci.* 29:1429-34
 181. Fan W, Boston BA, Kesterson RA, Hruby VJ, Cone RD. 1997. Role of melanocortinerbic neurons in feeding and the agouti obesity syndrome. *Nature* 385:165-8
 182. Giraudo SQ, Billington CJ, Levine AS. 1998. Feeding effects of hypothalamic injection of melanocortin 4 receptor ligands. *Brain Res.* 809:302-6
 183. Jonsson L, Skarphedinsson JO, Skuladottir GV, Watanobe H, Schioth HB. 2002. Food conversion is transiently affected during 4-week chronic administration of melanocortin agonist and antagonist in rats. *J. Endocrinol.* 173:517-23
 184. Small CJ, Kim MS, Stanley SA, Mitchell JR, Murphy K, Morgan DG, Ghatei MA, Bloom SR. 2001. Effects of chronic central nervous system

- administration of agouti-related protein in pair-fed animals. *Diabetes* 50:248-54
185. Brito MN, Brito NA, Baro DJ, Song CK, Bartness TJ. 2007. Differential activation of the sympathetic innervation of adipose tissues by melanocortin receptor stimulation. *Endocrinology* 148:5339-47
186. Murphy B, Nunes CN, Ronan JJ, Hanaway M, Fairhurst AM, Mellin TN. 2000. Centrally administered MTII affects feeding, drinking, temperature, and activity in the Sprague-Dawley rat. *J. Appl. Physiol* 89:273-82
187. Pierroz DD, Ziotopoulou M, Ungsuan L, Moschos S, Flier JS, Mantzoros CS. 2002. Effects of acute and chronic administration of the melanocortin agonist MTII in mice with diet-induced obesity. *Diabetes* 51:1337-45
188. Hagan MM, Rushing PA, Pritchard LM, Schwartz MW, Strack AM, Van der Ploeg LH, Woods SC, Seeley RJ. 2000. Long-term orexigenic effects of AgRP-(83---132) involve mechanisms other than melanocortin receptor blockade. *Am. J. Physiol Regul. Integr. Comp Physiol* 279:R47-R52
189. Lu XY, Nicholson JR, Akil H, Watson SJ. 2001. Time course of short-term and long-term orexigenic effects of Agouti-related protein (86-132). *Neuroreport* 12:1281-4
190. Wirth MM, Giraudo SQ. 2000. Agouti-related protein in the hypothalamic paraventricular nucleus: effect on feeding. *Peptides* 21:1369-75
191. Kask A, Schioth HB. 2000. Tonic inhibition of food intake during inactive phase is reversed by the injection of the melanocortin receptor antagonist into the paraventricular nucleus of the hypothalamus and central amygdala of the rat. *Brain Res.* 887:460-4
192. Wirth MM, Olszewski PK, Yu C, Levine AS, Giraudo SQ. 2001. Paraventricular hypothalamic alpha-melanocyte-stimulating hormone and MTII reduce feeding without causing aversive effects. *Peptides* 22:129-34
193. Skibicka KP, Grill HJ. 2009. Hypothalamic and hindbrain melanocortin receptors contribute to the feeding, thermogenic, and cardiovascular action of melanocortins. *Endocrinology* 150:5351-61
194. Kim MS, Rossi M, Abusnana S, Sunter D, Morgan DG, Small CJ, Edwards CM, Heath MM, Stanley SA, Seal LJ, Bhatti JR, Smith DM, Ghatei MA, Bloom SR. 2000. Hypothalamic localization of the feeding effect of agouti-

- related peptide and alpha-melanocyte-stimulating hormone. *Diabetes* 49:177-82
195. Terzi D, Zachariou V. 2008. Adeno-associated virus-mediated gene delivery approaches for the treatment of CNS disorders. *Biotechnol. J.* 3:1555-63
196. Lundberg C, Bjorklund T, Carlsson T, Jakobsson J, Hantraye P, Deglon N, Kirik D. 2008. Applications of lentiviral vectors for biology and gene therapy of neurological disorders. *Curr. Gene Ther.* 8:461-73
197. Segura MM, Alba R, Bosch A, Chillon M. 2008. Advances in helper-dependent adenoviral vector research. *Curr. Gene Ther.* 8:222-35
198. Berges BK, Wolfe JH, Fraser NW. 2007. Transduction of brain by herpes simplex virus vectors. *Mol. Ther.* 15:20-9
199. Tiesjema B, la Fleur SE, Luijendijk MC, Adan RA. 2009. Sustained NPY overexpression in the PVN results in obesity via temporarily increasing food intake. *Obesity. (Silver. Spring)* 17:1448-50
200. Liu M, Thankachan S, Kaur S, Begum S, Blanco-Centurion C, Sakurai T, Yanagisawa M, Neve R, Shiromani PJ. 2008. Orexin (hypocretin) gene transfer diminishes narcoleptic sleep behavior in mice. *Eur. J. Neurosci.* 28:1382-93
201. Yang L, Scott KA, Hyun J, Tamashiro KL, Tray N, Moran TH, Bi S. 2009. Role of dorsomedial hypothalamic neuropeptide Y in modulating food intake and energy balance. *J. Neurosci.* 29:179-90
202. Couturier C, Sarkis C, Seron K, Belouzard S, Chen P, Lenain A, Corset L, Dam J, Vauthier V, Dubart A, Mallet J, Froguel P, Rouille Y, Jockers R. 2007. Silencing of OB-RGRP in mouse hypothalamic arcuate nucleus increases leptin receptor signaling and prevents diet-induced obesity. *Proc. Natl. Acad. Sci. U. S. A* 104:19476-81
203. Spiteri T, Musatov S, Ogawa S, Ribeiro A, Pfaff DW, Agmo A. 2009. Estrogen-Induced Sexual Incentive Motivation, Proceptivity and Receptivity Depend on a Functional Estrogen Receptor alpha in the Ventromedial Nucleus of the Hypothalamus but Not in the Amygdala. *Neuroendocrinology*

204. Liu YF, Chen HI, Wu CL, Kuo YM, Yu L, Huang AM, Wu FS, Chuang JI, Jen CJ. 2009. Differential effects of treadmill running and wheel running on spatial or aversive learning and memory: roles of amygdalar brain-derived neurotrophic factor and synaptotagmin I. *J. Physiol* 587:3221-31
205. Shin AC, Zheng H, Berthoud HR. 2009. An expanded view of energy homeostasis: neural integration of metabolic, cognitive, and emotional drives to eat. *Physiol Behav.* 97:572-80
206. Eaton MJ, Blits B, Ruitenberg MJ, Verhaagen J, Oudega M. 2002. Amelioration of chronic neuropathic pain after partial nerve injury by adeno-associated viral (AAV) vector-mediated over-expression of BDNF in the rat spinal cord. *Gene Ther.* 9:1387-95
207. Broekman MLD, Comer LA, Hyman BT, Siena-Esteves M. 2006. Adeno-associated virus vectors serotyped with AAV8 capsid are more efficient than AAV-1 or-2 serotypes for widespread gene delivery to the neonatal mouse brain. *Neuroscience* 138:501-10
208. Fitzsimons CP, Ahmed S, Wittevrongel CF, Schouten TG, Dijkmans TF, Scheenen WJ, Schaaf MJ, de Kloet ER, Vreugdenhil E. 2008. The microtubule-associated protein doublecortin-like regulates the transport of the glucocorticoid receptor in neuronal progenitor cells. *Mol. Endocrinol.* 22:248-62
209. Stegmeier F, Hu G, Rickles RJ, Hannon GJ, Elledge SJ. 2005. A lentiviral microRNA-based system for single-copy polymerase II-regulated RNA interference in mammalian cells. *Proc. Natl. Acad. Sci. U. S A* 102:13212-7
210. Reed SE, Staley EM, Mayginnes JP, Pintel DJ, Tullis GE. 2006. Transfection of mammalian cells using linear polyethylenimine is a simple and effective means of producing recombinant adeno-associated virus vectors. *Journal of Virological Methods* 138:85-98
211. Grimm D, Kay MA, Kleinschmidt JA. 2003. Helper virus-free, optically controllable, and two-plasmid-based production of adeno-associated virus vectors of serotypes 1 to 6. *Mol. Ther.* 7:839-50
212. Zolotukhin S, Potter M, Zolotukhin I, Sakai Y, Loiler S, Fraitjes TJ, Jr., Chiodo VA, Phillipsberg T, Muzyczka N, Hauswirth WW, Flotte TR, Byrne

- BJ, Snyder RO. 2002. Production and purification of serotype 1, 2, and 5 recombinant adeno-associated viral vectors. *Methods* 28:158-67
213. Veldwijk MR, Topaly J, Laufs S, Hengge UR, Wenz F, Zeller WJ, Fruehauf S. 2002. Development and optimization of a real-time quantitative PCR-based method for the titration of AAV-2 vector stocks. *Mol. Ther.* 6:272-8
214. Scherr M, Battmer K, Blomer U, Ganser A, Grez M. 2001. Quantitative determination of lentiviral vector particle numbers by real-time PCR. *Biotechniques* 31:520, 522, 524, passim
215. de Backer M, Brans M, Luijendijk M, Garner K, Adan R. 2010. Optimization of adeno-associated viral vector mediated gene delivery to the hypothalamus. *Hum. Gene Ther.*
216. Harvey AR, Kamphuis W, Eggers R, Symons NA, Blits B, Niclou S, Boer GJ, Verhaagen J. 2002. Intravitreal injection of adeno-associated viral vectors results in the transduction of different types of retinal neurons in neonatal and adult rats: a comparison with lentiviral vectors. *Mol. Cell Neurosci.* 21:141-57
217. Blomer U, Naldini L, Kafri T, Trono D, Verma IM, Gage FH. 1997. Highly efficient and sustained gene transfer in adult neurons with a lentivirus vector. *Journal of Virology* 71:6641-9
218. van Hooijdonk LW, Ichwan M, Dijkmans TF, Schouten TG, de Backer MW, Adan RA, Verbeek FJ, Vreugdenhil E, Fitzsimons CP. 2009. Lentivirus-mediated transgene delivery to the hippocampus reveals sub-field specific differences in expression. *BMC. Neurosci.* 10:2
219. Ahmed BY, Chakravarthy S, Eggers R, Hermens WT, Zhang JY, Niclou SP, Levelt C, Sablitzky F, Anderson PN, Lieberman AR, Verhaagen J. 2004. Efficient delivery of Cre-recombinase to neurons in vivo and stable transduction of neurons using adeno-associated and lentiviral vectors. *BMC. Neurosci.* 5:4
220. Ehrengreuber MU, Hennou S, Bueler H, Naim HY, Deglon N, Lundstrom K. 2001. Gene transfer into neurons from hippocampal slices: comparison of recombinant Semliki Forest Virus, adenovirus, adeno-associated virus, lentivirus, and measles virus. *Mol. Cell Neurosci.* 17:855-71

221. Nathanson JL, Yanagawa Y, Obata K, Callaway EM. 2009. Preferential labeling of inhibitory and excitatory cortical neurons by endogenous tropism of adeno-associated virus and lentivirus vectors. *Neuroscience* 161:441-50
222. Wu Z, Miller E, Agbandje-McKenna M, Samulski RJ. 2006. Alpha2,3 and alpha2,6 N-linked sialic acids facilitate efficient binding and transduction by adeno-associated virus types 1 and 6. *J. Virol.* 80:9093-103
223. Willer CJ, Speliotes EK, Loos RJ, Li S, Lindgren CM, Heid IM, Berndt SI, Elliott AL, Jackson AU, Lamina C, Lettre G, Lim N, Lyon HN, McCarroll SA, Papadakis K, Qi L, Randall JC, Roccascaccia RM, Sanna S, Scheet P, Weedon MN, Wheeler E, Zhao JH, Jacobs LC, Prokopenko I, Soranzo N, Tanaka T, Timpson NJ, Almgren P, Bennett A, Bergman RN, Bingham SA, Bonnycastle LL, Brown M, Burtt NP, Chines P, Coin L, Collins FS, Connell JM, Cooper C, Smith GD, Dennison EM, Deodhar P, Elliott P, Erdos MR, Estrada K, Evans DM, Gianniny L, Gieger C, Gillson CJ, Guiducci C, Hackett R, Hadley D, Hall AS, Havulinna AS, Hebebrand J, Hofman A, Isomaa B, Jacobs KB, Johnson T, Jousilahti P, Jovanovic Z, Khaw KT, Kraft P, Kuokkanen M, Kuusisto J, Laitinen J, Lakatta EG, Luan J, Luben RN, Mangino M, McArdle WL, Meitinger T, Mulas A, Munroe PB, Narisu N, Ness AR, Northstone K, O'Rahilly S, Purmann C, Rees MG, Ridderstrale M, Ring SM, Rivadeneira F, Ruokonen A, Sandhu MS, Saramies J, Scott LJ, Scuteri A, Silander K, Sims MA, Song K, Stephens J, Stevens S, Stringham HM, Tung YC, Valle TT, Van Duijn CM, Vimalaswaran KS, Vollenweider P, Waeber G, Wallace C, Watanabe RM, Waterworth DM, Watkins N, Witterman JC, Zeggini E, Zhai G, Zillikens MC, Altshuler D, Caulfield MJ, Chanock SJ, Farooqi IS, Ferrucci L, Guralnik JM, Hattersley AT, Hu FB, Jarvelin MR, Laakso M, Mooser V, Ong KK, Ouwehand WH, Salomaa V, Samani NJ, Spector TD, Tuomi T, Tuomilehto J, Uda M, Uitterlinden AG, Wareham NJ, Deloukas P, Frayling TM, Groop LC, Hayes RB, Hunter DJ, Mohlke KL, Peltonen L, Schlessinger D, Strachan DP, Wichmann HE, McCarthy MI, Boehnke M, Barroso I, Abecasis GR, Hirschhorn JN. 2009. Six new loci associated with body mass index

- p>highlight a neuronal influence on body weight regulation.
- Nat. Genet.*
- 41:25-34
224. Renstrom F, Payne F, Nordstrom A, Brito EC, Rolandsson O, Hallmans G, Barroso I, Nordstrom P, Franks PW. 2009. Replication and extension of genome-wide association study results for obesity in 4923 adults from northern Sweden. *Hum. Mol. Genet.* 18:1489-96
 225. Bolze F, Klingenspor M. 2009. Mouse models for the central melanocortin system. *Genes Nutr.* 4:129-34
 226. Shafrir E, Ziv E. 2009. A useful list of spontaneously arising animal models of obesity and diabetes. *Am. J. Physiol Endocrinol. Metab* 296:E1450-E1452
 227. Cao L, Lin EJ, Cahill MC, Wang C, Liu X, During MJ. 2009. Molecular therapy of obesity and diabetes by a physiological autoregulatory approach. *Nat. Med.* 15:447-54
 228. Broberger C, Johansen J, Johansson C, Schalling M, Hokfelt T. 1998. The neuropeptide Y/agouti gene-related protein (AGRP) brain circuitry in normal, anorectic, and monosodium glutamate-treated mice. *Proc. Natl. Acad. Sci. U. S. A* 95:15043-8
 229. Farooqi S, O'Rahilly S. 2006. Genetics of obesity in humans. *Endocr. Rev.* 27:710-8
 230. Klein RL, Hamby ME, Gong Y, Hirko AC, Wang S, Hughes JA, King MA, Meyer EM. 2002. Dose and promoter effects of adeno-associated viral vector for green fluorescent protein expression in the rat brain. *Experimental Neurology* 176:66-74
 231. Cearley CN, Vandenberghe LH, Parente MK, Carnish ER, Wilson JM, Wolfe JH. 2008. Expanded repertoire of AAV vector serotypes mediate unique patterns of transduction in mouse brain. *Mol. Ther.* 16:1710-8
 232. Howard DB, Powers K, Wang Y, Harvey BK. 2008. Tropism and toxicity of adeno-associated viral vector serotypes 1, 2, 5, 6, 7, 8, and 9 in rat neurons and glia in vitro. *Virology* 372:24-34
 233. Shevtsova Z, Malik JM, Michel U, Bahr M, Kugler S. 2005. Promoters and serotypes: targeting of adeno-associated virus vectors for gene transfer in the rat central nervous system in vitro and in vivo. *Exp. Physiol* 90:53-9

234. Buning H, Perabo L, Coutelle O, Quadt-Humme S, Hallek M. 2008. Recent developments in adeno-associated virus vector technology. *J. Gene Med.* 10:717-33
235. Kwon I, Schaffer DV. 2008. Designer gene delivery vectors: molecular engineering and evolution of adeno-associated viral vectors for enhanced gene transfer. *Pharm. Res.* 25:489-99
236. Hermonat PL, Muzyczka N. 1984. Use of adeno-associated virus as a mammalian DNA cloning vector: transduction of neomycin resistance into mammalian tissue culture cells. *Proc. Natl. Acad. Sci. U. S. A* 81:6466-70
237. Garza JC, Kim CS, Liu J, Zhang W, Lu XY. 2008. Adeno-associated virus-mediated knockdown of melanocortin-4 receptor in the paraventricular nucleus of the hypothalamus promotes high-fat diet-induced hyperphagia and obesity. *J. Endocrinol.* 197:471-82
238. McCrimmon RJ, Shaw M, Fan X, Cheng H, Ding Y, Vella MC, Zhou L, McNay EC, Sherwin RS. 2008. Key role for AMP-activated protein kinase in the ventromedial hypothalamus in regulating counterregulatory hormone responses to acute hypoglycemia. *Diabetes* 57:444-50
239. Royo NC, Vandenberghe LH, Ma JY, Hauspurg A, Yu L, Maronski M, Johnston J, Dichter MA, Wilson JM, Watson DJ. 2008. Specific AAV serotypes stably transduce primary hippocampal and cortical cultures with high efficiency and low toxicity. *Brain Res.* 1190:15-22
240. Klein RL, Dayton RD, Tatom JB, Henderson KM, Henning PP. 2008. AAV8, 9, Rh10, Rh43 vector gene transfer in the rat brain: effects of serotype, promoter and purification method. *Mol. Ther.* 16:89-96
241. Rabinowitz JE, Bowles DE, Faust SM, Ledford JG, Cunningham SE, Samulski RJ. 2004. Cross-dressing the virion: the transcapsidation of adeno-associated virus serotypes functionally defines subgroups. *Journal of Virology* 78:4421-32
242. Hauck B, Chen L, Xiao W. 2003. Generation and characterization of chimeric recombinant AAV vectors. *Mol. Ther.* 7:419-25
243. Xiao X, Li J, Samulski RJ. 1998. Production of high-titer recombinant adeno-associated virus vectors in the absence of helper adenovirus. *J. Virol.* 72:2224-32

244. Schaeren-Wiemers N, Gerfin-Moser A. 1993. A single protocol to detect transcripts of various types and expression levels in neural tissue and cultured cells: in situ hybridization using digoxigenin-labelled cRNA probes. *Histochemistry* 100:431-40
245. Vihinen-Ranta M, Suikkanen S, Parrish CR. 2004. Pathways of cell infection by parvoviruses and adeno-associated viruses. *J. Virol.* 78:6709-14
246. Akache B, Grimm D, Pandey K, Yant SR, Xu H, Kay MA. 2006. The 37/67-kilodalton laminin receptor is a receptor for adeno-associated virus serotypes 8, 2, 3, and 9. *J. Virol.* 80:9831-6
247. Semjonous NM, Smith KL, Parkinson JR, Gunner DJ, Liu YL, Murphy KG, Ghatei MA, Bloom SR, Small CJ. 2009. Coordinated changes in energy intake and expenditure following hypothalamic administration of neuropeptides involved in energy balance. *Int. J. Obes. (Lond)* 33:775-85
248. Small CJ, Liu YL, Stanley SA, Connoley IP, Kennedy A, Stock MJ, Bloom SR. 2003. Chronic CNS administration of Agouti-related protein (Agrp) reduces energy expenditure. *Int. J. Obes. Relat Metab Disord.* 27:530-3
249. Kas MJ, Tiesjema B, van Dijk G, Garner KM, Barsh GS, ter Brake O, Verhaagen J, Adan RA. 2004. Induction of brain-region-specific forms of obesity by agouti. *J. Neurosci.* 24:10176-81
250. Tice JA, Karliner L, Walsh J, Petersen AJ, Feldman MD. 2008. Gastric banding or bypass? A systematic review comparing the two most popular bariatric procedures. *Am. J. Med.* 121:885-93
251. Haskell-Luevano C, Monck EK. 2001. Agouti-related protein functions as an inverse agonist at a constitutively active brain melanocortin-4 receptor. *Regulatory Peptides* 99:1-7
252. Klebig ML, Wilkinson JE, Geisler JG, Woychik RP. 1995. Ectopic expression of the agouti gene in transgenic mice causes obesity, features of type II diabetes, and yellow fur. *Proc. Natl. Acad. Sci. U. S. A* 92:4728-32
253. Butler AA, Marks DL, Fan W, Kuhn CM, Bartolome M, Cone RD. 2001. Melanocortin-4 receptor is required for acute homeostatic responses to increased dietary fat. *Nat. Neurosci.* 4:605-11

254. Shrestha YB, Wickwire K, Giraudo SQ. 2006. Role of AgRP on Ghrelin-induced feeding in the hypothalamic paraventricular nucleus. *Regul. Pept.* 133:68-73
255. Tiesjema B, Adan RA, Luijendijk MC, Kalsbeek A, la Fleur SE. 2007. Differential effects of recombinant adeno-associated virus-mediated neuropeptide Y overexpression in the hypothalamic paraventricular nucleus and lateral hypothalamus on feeding behavior. *J. Neurosci.* 27:14139-46
256. Kas MJH, van Dijk G, Scheurink AJW, Adan RAH. 2003. Agouti-related protein prevents self-starvation. *Molecular Psychiatry* 8:235-40
257. la Fleur SE, van Rozen AJ, Luijendijk MC, Groeneweg F, Adan RA. 2009. A free-choice high-fat high-sugar diet induces changes in arcuate neuropeptide expression that support hyperphagia. *Int. J. Obes. (Lond)*
258. Fisher KJ, Gao GP, Weitzman MD, DeMatteo R, Burda JF, Wilson JM. 1996. Transduction with recombinant adeno-associated virus for gene therapy is limited by leading-strand synthesis. *Journal of Virology* 70:520-32
259. Ferrari FK, Samulski T, Shenk T, Samulski RJ. 1996. Second-strand synthesis is a rate-limiting step for efficient transduction by recombinant adeno-associated virus vectors. *Journal of Virology* 70:3227-34
260. Woods SC. 2009. The Control of Food Intake: Behavioral versus Molecular Perspectives. *Cell Metabolism* 9:489-98
261. Erlanson-Albertsson C. 2005. Appetite regulation and energy balance. *Acta Paediatrica* 94:40-1
262. Tang-Christensen M, Vrang N, Ortmann S, Bidlingmaier M, Horvath TL, Tschop M. 2004. Central administration of ghrelin and agouti-related protein (83-132) increases food intake and decreases spontaneous locomotor activity in rats. *Endocrinology* 145:4645-52
263. Santollo J, Eckel LA. 2008. Estradiol decreases the orexigenic effect of neuropeptide Y, but not agouti-related protein, in ovariectomized rats. *Behav. Brain Res.* 191:173-7
264. Azzara AV, Sokolnicki JP, Schwartz GJ. 2002. Central melanocortin receptor agonist reduces spontaneous and scheduled meal size but does

- not augment duodenal preload-induced feeding inhibition. *Physiol Behav.* 77:411-6
265. Williams DL, Grill HJ, Weiss SM, Baird JP, Kaplan JM. 2002. Behavioral processes underlying the intake suppressive effects of melanocortin 3/4 receptor activation in the rat. *Psychopharmacology (Berl)* 161:47-53
266. Farooqi IS, Keogh JM, Yeo GS, Lank EJ, Cheetham T, O'Rahilly S. 2003. Clinical spectrum of obesity and mutations in the melanocortin 4 receptor gene. *N. Engl. J. Med.* 348:1085-95
267. Creemers JW, Pritchard LE, Gyte A, Le Rouzic P, Meulemans S, Wardlaw SL, Zhu X, Steiner DF, Davies N, Armstrong D, Lawrence CB, Luckman SM, Schmitz CA, Davies RA, Brennand JC, White A. 2006. Agouti-related protein is posttranslationally cleaved by proprotein convertase 1 to generate agouti-related protein (AGRP)83-132: interaction between AGRP83-132 and melanocortin receptors cannot be influenced by syndecan-3. *Endocrinology* 147:1621-31
268. Kreier F, Kap YS, Mettenleiter TC, van Heijningen C, van d, V, Kalsbeek A, Sauerwein HP, Fliers E, Romijn JA, Buijs RM. 2006. Tracing from fat tissue, liver, and pancreas: a neuroanatomical framework for the role of the brain in type 2 diabetes. *Endocrinology* 147:1140-7
269. Song CK, Jackson RM, Harris RB, Richard D, Bartness TJ. 2005. Melanocortin-4 receptor mRNA is expressed in sympathetic nervous system outflow neurons to white adipose tissue. *Am. J. Physiol Regul. Integr. Comp Physiol* 289:R1467-R1476
270. Song CK, Vaughan CH, Keen-Rhinehart E, Harris RB, Richard D, Bartness TJ. 2008. Melanocortin-4 receptor mRNA expressed in sympathetic outflow neurons to brown adipose tissue: neuroanatomical and functional evidence. *Am. J. Physiol Regul. Integr. Comp Physiol* 295:R417-R428
271. Tallam LS, Stec DE, Willis MA, da Silva AA, Hall JE. 2005. Melanocortin-4 receptor-deficient mice are not hypertensive or salt-sensitive despite obesity, hyperinsulinemia, and hyperleptinemia. *Hypertension* 46:326-32
272. Greenfield JR, Miller JW, Keogh JM, Henning E, Satterwhite JH, Cameron GS, Astruc B, Mayer JP, Brage S, See TC, Lomas DJ, O'Rahilly S, Farooqi

- IS. 2009. Modulation of blood pressure by central melanocortinergic pathways. *N. Engl. J. Med.* 360:44-52
273. Nogueiras R, Wiedmer P, Perez-Tilve D, Veyrat-Durebex C, Keogh JM, Sutton GM, Pfluger PT, Castaneda TR, Neschen S, Hofmann SM, Howles PN, Morgan DA, Benoit SC, Szanto I, Schrott B, Schurmann A, Joost HG, Hammond C, Hui DY, Woods SC, Rahmouni K, Butler AA, Farooqi IS, O'Rahilly S, Rohner-Jeanrenaud F, Tschop MH. 2007. The central melanocortin system directly controls peripheral lipid metabolism. *J. Clin. Invest* 117:3475-88
274. Arase K, Sakaguchi T, Bray GA. 1987. Lateral hypothalamic lesions and activity of the sympathetic nervous system. *Life Sci.* 41:657-62
275. Yoshida T, Kemnitz JW, Bray GA. 1983. Lateral hypothalamic lesions and norepinephrine turnover in rats. *J. Clin. Invest* 72:919-27
276. Sakaguchi T, Arase K, Bray GA. 1988. Sympathetic activity and food intake of rats with ventromedial hypothalamic lesions. *Int. J. Obes.* 12:285-91
277. Takahashi A, Shimazu T. 1981. Hypothalamic regulation of lipid metabolism in the rat: effect of hypothalamic stimulation on lipolysis. *J. Auton. Nerv. Syst.* 4:195-205
278. Zhong MK, Duan YC, Chen AD, Xu B, Gao XY, De W, Zhu GQ. 2008. Paraventricular nucleus is involved in the central pathway of cardiac sympathetic afferent reflex in rats. *Exp. Physiol* 93:746-53
279. Gettys TW, Harkness PJ, Watson PM. 1996. The beta 3-adrenergic receptor inhibits insulin-stimulated leptin secretion from isolated rat adipocytes. *Endocrinology* 137:4054-7
280. Cong L, Chen K, Li J, Gao P, Li Q, Mi S, Wu X, Zhao AZ. 2007. Regulation of adiponectin and leptin secretion and expression by insulin through a PI3K-PDE3B dependent mechanism in rat primary adipocytes. *Biochem. J.* 403:519-25
281. Kishi T, Aschkenasi CJ, Choi BJ, Lopez ME, Lee CE, Liu H, Hollenberg AN, Friedman JM, Elmquist JK. 2005. Neuropeptide Y Y1 receptor mRNA in rodent brain: distribution and colocalization with melanocortin-4 receptor. *J. Comp Neurol.* 482:217-43

282. Gerald C, Walker MW, Criscione L, Gustafson EL, Batzl-Hartmann C, Smith KE, Vaysse P, Durkin MM, Laz TM, Linemeyer DL, Schaffhauser AO, Whitebread S, Hofbauer KG, Taber RI, Branchek TA, Weinshank RL. 1996. A receptor subtype involved in neuropeptide-Y-induced food intake. *Nature* 382:168-71
283. Lu D, Willard D, Patel IR, Kadwell S, Overton L, Kost T, Luther M, Chen W, Woychik RP, Wilkison WO, . 1994. Agouti protein is an antagonist of the melanocyte-stimulating-hormone receptor. *Nature* 371:799-802
284. Nilni EA. 2007. Regulation of prohormone convertases in hypothalamic neurons: implications for prothyrotropin-releasing hormone and proopiomelanocortin. *Endocrinology* 148:4191-200
285. Pritchard LE, White A. 2007. Neuropeptide processing and its impact on melanocortin pathways. *Endocrinology* 148:4201-7
286. Winsky-Sommerer R, Benjannet S, Rovere C, Barbero P, Seidah NG, Epelbaum J, Dournaud P. 2000. Regional and cellular localization of the neuroendocrine prohormone convertases PC1 and PC2 in the rat central nervous system. *J. Comp Neurol.* 424:439-60
287. Fernandez CJ, Haugwitz M, Eaton B, Moore HP. 1997. Distinct molecular events during secretory granule biogenesis revealed by sensitivities to brefeldin A. *Mol. Biol. Cell* 8:2171-85
288. Smith ML, Prall B, Nandar W, Cline MA. 2008. Beta-melanocyte-stimulating hormone potently reduces appetite via the hypothalamus in chicks. *J. Neuroendocrinol.* 20:220-6
289. McMinn JE, Wilkinson CW, Havel PJ, Woods SC, Schwartz MW. 2000. Effect of intracerebroventricular alpha-MSH on food intake, adiposity, c-Fos induction, and neuropeptide expression. *Am. J. Physiol Regul. Integr. Comp Physiol* 279:R695-R703
290. Silva RM, Hadjimarkou MM, Rossi GC, Pasternak GW, Bodnar RJ. 2001. Beta-endorphin-induced feeding: pharmacological characterization using selective opioid antagonists and antisense probes in rats. *J. Pharmacol. Exp. Ther.* 297:590-6
291. Grandison L, Guidotti A. 1977. Stimulation of food intake by muscimol and beta endorphin. *Neuropharmacology* 16:533-6

292. Appleyard SM, Hayward M, Young JI, Butler AA, Cone RD, Rubinstein M, Low MJ. 2003. A role for the endogenous opioid beta-endorphin in energy homeostasis. *Endocrinology* 144:1753-60
293. Zhang JV, Ren PG, Avsian-Kretchmer O, Luo CW, Rauch R, Klein C, Hsueh AJ. 2005. Obestatin, a peptide encoded by the ghrelin gene, opposes ghrelin's effects on food intake. *Science* 310:996-9
294. Sporn LA, Marder VJ, Wagner DD. 1986. Inducible secretion of large, biologically potent von Willebrand factor multimers. *Cell* 46:185-90
295. Takahashi S, Nakagawa T, Banno T, Watanabe T, Murakami K, Nakayama K. 1995. Localization of furin to the trans-Golgi network and recycling from the cell surface involves Ser and Tyr residues within the cytoplasmic domain. *J. Biol. Chem.* 270:28397-401
296. Thomas G. 2002. Furin at the cutting edge: from protein traffic to embryogenesis and disease. *Nat. Rev. Mol. Cell Biol.* 3:753-66
297. Schafer MK, Day R, Cullinan WE, Chretien M, Seidah NG, Watson SJ. 1993. Gene expression of prohormone and proprotein convertases in the rat CNS: a comparative in situ hybridization analysis. *J. Neurosci.* 13:1258-79
298. Tiesjema B, Merkestein M, Garner KM, de Krom M, Adan RA. 2008. Multimeric alpha-MSH has increased efficacy to activate the melanocortin MC4 receptor. *Eur. J. Pharmacol.* 585:24-30
299. Chen W, Shields TS, Stork PJ, Cone RD. 1995. A colorimetric assay for measuring activation of Gs- and Gq-coupled signaling pathways. *Anal. Biochem.* 226:349-54
300. Lee EJ, Lee SH, Jung JW, Lee W, Kim BJ, Park KW, Lim SK, Yoon CJ, Baik JH. 2001. Differential regulation of cAMP-mediated gene transcription and ligand selectivity by MC3R and MC4R melanocortin receptors. *Eur. J. Biochem.* 268:582-91
301. El Meskini R, Jin L, Marx R, Bruzzaniti A, Lee J, Emeson R, Mains R. 2001. A signal sequence is sufficient for green fluorescent protein to be routed to regulated secretory granules. *Endocrinology* 142:864-73

302. Pouli AE, Kennedy HJ, Schofield JG, Rutter GA. 1998. Insulin targeting to the regulated secretory pathway after fusion with green fluorescent protein and firefly luciferase. *Biochem. J.* 331 (Pt 2):669-75
303. Foti SB, Samulski RJ, McCown TJ. 2009. Delivering multiple gene products in the brain from a single adeno-associated virus vector. *Gene Ther.* 16:1314-9
304. Cusin I, Rohnerjeanrenaud F, StrickerKrongrad A, Jeanrenaud B. 1996. The weight-reducing effect of an intracerebroventricular bolus injection of leptin in genetically Obese falfa rats - Reduced sensitivity compared with lean animals. *Diabetes* 45:1446-51
305. Seeley RJ, vanDijk G, Campfield LA, Smith FJ, Burn P, Nelligan JA, Bell SM, Baskin DG, Woods SC, Schwartz MW. 1996. Intraventricular leptin reduces food intake and body weight of lean rats but not obese Zucker rats. *Hormone and Metabolic Research* 28:664-8
306. Halaas JL, Boozer C, BlairWest J, Fidahusein N, Denton DA, Friedman JM. 1997. Physiological response to long-term peripheral and central leptin infusion in lean and obese mice. *Proceedings of the National Academy of Sciences of the United States of America* 94:8878-83
307. Roberts AW, Robb L, Rakar S, Hartley L, Cluse L, Nicola NA, Metcalf D, Hilton DJ, Alexander WS. 2001. Placental defects and embryonic lethality in mice lacking suppressor of cytokine signaling 3. *Proc. Natl. Acad. Sci. U. S. A* 98:9324-9
308. Hommel JD, Trinko R, Sears RM, Georgescu D, Liu ZW, Gao XB, Thurmon JJ, Marinelli M, DiLeone RJ. 2006. Leptin receptor signaling in midbrain dopamine neurons regulates feeding. *Neuron* 51:801-10
309. Zhang R, Dhillon H, Yin H, Yoshimura A, Lowell BB, Maratos-Flier E, Flier JS. 2008. Selective inactivation of Socs3 in SF1 neurons improves glucose homeostasis without affecting body weight. *Endocrinology* 149:5654-61
310. Kievit P, Howard JK, Badman MK, Balthasar N, Coppari R, Mori H, Lee CE, Elmquist JK, Yoshimura A, Flier JS. 2006. Enhanced leptin sensitivity and improved glucose homeostasis in mice lacking suppressor of cytokine signaling-3 in POMC-expressing cells. *Cell Metab* 4:123-32

311. Muraoka O, Xu B, Tsurumaki T, Akira S, Yamaguchi T, Higuchi H. 2003. Leptin-induced transactivation of NPY gene promoter mediated by JAK1, JAK2 and STAT3 in the neural cell lines. *Neurochem. Int.* 42:591-601
312. Higuchi H, Hasegawa A, Yamaguchi T. 2005. Transcriptional regulation of neuronal genes and its effect on neural functions: transcriptional regulation of neuropeptide Y gene by leptin and its effect on feeding. *J. Pharmacol. Sci.* 98:225-31
313. Clark JT, Kalra PS, Crowley WR, Kalra SP. 1984. Neuropeptide-y and Human Pancreatic-Polypeptide Stimulate Feeding-Behavior in Rats. *Endocrinology* 115:427-9
314. Morley JE, Levine AS, Gosnell BA, Kneip J, Grace M. 1987. Effect of Neuropeptide-y on Ingestive Behaviors in the Rat. *American Journal of Physiology* 252:R599-R609
315. Baran K, Preston E, Wilks D, Cooney GJ, Kraegen EW, Sainsbury A. 2002. Chronic central melanocortin-4 receptor antagonism and central neuropeptide-Y infusion in rats produce increased adiposity by divergent pathways. *Diabetes* 51:152-8
316. Zarjevski N, Cusin I, Vettor R, Rohnerjeanrenaud F, Jeanrenaud B. 1993. Chronic Intracerebroventricular Neuropeptide-y Administration to Normal Rats Mimics Hormonal and Metabolic Changes of Obesity. *Endocrinology* 133:1753-8
317. Heilig M, Murison R. 1987. Intracerebroventricular Neuropeptide-y Suppresses Open-Field and Home Cage Activity in the Rat. *Regulatory Peptides* 19:221-31
318. Heilig M, Vecsei L, Widerlov E. 1989. Opposite effects of centrally administered neuropeptide Y (NPY) on locomotor activity of spontaneously hypertensive (SH) and normal rats. *Acta Physiol Scand.* 137:243-8
319. Farley C, Cook JA, Spar BD, Austin TM, Kowalski TJ. 2003. Meal pattern analysis of diet-induced obesity in susceptible and resistant rats. *Obesity Research* 11:845-51
320. Rogers PJ, Blundell JE. 1984. Meal Patterns and Food Selection During the Development of Obesity in Rats Fed A Cafeteria Diet. *Neuroscience and Biobehavioral Reviews* 8:441-53

321. Schaffer DV, Koerber JT, Lim KI. 2008. Molecular engineering of viral gene delivery vehicles. *Annual Review of Biomedical Engineering* 10:169-94
322. Rendahl KG, Leff SE, Otten GR, Spratt SK, Bohl D, Van Roey M, Donahue BA, Cohen LK, Mandel RJ, Danos O, Snyder RO. 1998. Regulation of gene expression in vivo following transduction by two separate rAAV vectors. *Nature Biotechnology* 16:757-61
323. Philippe S, Sarkis C, Barkats M, Mammeri H, Ladroue C, Petit C, Mallet J, Serguera C. 2006. Lentiviral vectors with a defective integrase allow efficient and sustained transgene expression in vitro and in vivo. *Proc. Natl. Acad. Sci. U. S. A* 103:17684-9
324. Yanez-Munoz RJ, Balaggan KS, MacNeil A, Howe SJ, Schmidt M, Smith AJ, Buch P, MacLaren RE, Anderson PN, Barker SE, Duran Y, Bartholomae C, von Kalle C, Heckenlively JR, Kinnon C, Ali RR, Thrasher AJ. 2006. Effective gene therapy with nonintegrating lentiviral vectors. *Nat. Med.* 12:348-53
325. Abordo-Adesida E, Follenzi A, Barcia C, Sciascia S, Castro MG, Naldini L, Lowenstein PR. 2005. Stability of lentiviral vector-mediated transgene expression in the brain in the presence of systemic antivector immune responses. *Hum. Gene Ther.* 16:741-51
326. Lowenstein PR, Mandel RJ, Xiong WD, Kroeger K, Castro MG. 2007. Immune responses to adenovirus and adeno-associated vectors used for gene therapy of brain diseases: the role of immunological synapses in understanding the cell biology of neuroimmune interactions. *Curr. Gene Ther.* 7:347-60
327. Peden CS, Burger C, Muzyczka N, Mandel RJ. 2004. Circulating anti-wild-type adeno-associated virus type 2 (AAV2) antibodies inhibit recombinant AAV2 (rAAV2)-mediated, but not rAAV5-mediated, gene transfer in the brain. *J. Virol.* 78:6344-59
328. Lowenstein PR. 2004. Input virion proteins: cryptic targets of antivector immune responses in preimmunized subjects. *Mol. Ther.* 9:771-4
329. Duan D, Yue Y, Yan Z, Yang J, Engelhardt JF. 2000. Endosomal processing limits gene transfer to polarized airway epithelia by adeno-associated virus. *J. Clin. Invest* 105:1573-87

330. Douar AM, Poulard K, Stockholm D, Danos O. 2001. Intracellular trafficking of adeno-associated virus vectors: routing to the late endosomal compartment and proteasome degradation. *J. Virol.* 75:1824-33
331. Yan Z, Zak R, Luxton GW, Ritchie TC, Bantel-Schaal U, Engelhardt JF. 2002. Ubiquitination of both adeno-associated virus type 2 and 5 capsid proteins affects the transduction efficiency of recombinant vectors. *J. Virol.* 76:2043-53
332. Cearley CN, Wolfe JH. 2006. Transduction characteristics of adeno-associated virus vectors expressing cap serotypes 7, 8, 9, and Rh10 in the mouse brain. *Mol. Ther.* 13:528-37
333. Bostick B, Ghosh A, Yue Y, Long C, Duan D. 2007. Systemic AAV-9 transduction in mice is influenced by animal age but not by the route of administration. *Gene Therapy* 14:1605-9
334. McCarty DM, Monahan PE, Samulski RJ. 2001. Self-complementary recombinant adeno-associated virus (scAAV) vectors promote efficient transduction independently of DNA synthesis. *Gene Ther.* 8:1248-54
335. Wang Z, Ma HI, Li J, Sun L, Zhang J, Xiao X. 2003. Rapid and highly efficient transduction by double-stranded adeno-associated virus vectors in vitro and in vivo. *Gene Therapy* 10:2105-11
336. Andino LM, Conlon TJ, Porvasnik SL, Boye SL, Hauswirth WW, Lewin AS. 2007. Rapid, widespread transduction of the murine myocardium using self-complementary Adeno-associated virus. *Genet. Vaccines. Ther.* 5:13
337. Petersen-Jones SM, Bartoe JT, Fischer AJ, Scott M, Boye SL, Chiodo V, Hauswirth WW. 2009. AAV retinal transduction in a large animal model species: comparison of a self-complementary AAV2/5 with a single-stranded AAV2/5 vector. *Mol. Vis.* 15:1835-42
338. Duan D, Yue Y, Yan Z, Engelhardt JF. 2000. A new dual-vector approach to enhance recombinant adeno-associated virus-mediated gene expression through intermolecular cis activation. *Nat. Med.* 6:595-8
339. Nakai H, Storm TA, Kay MA. 2000. Increasing the size of rAAV-mediated expression cassettes in vivo by intermolecular joining of two complementary vectors. *Nat. Biotechnol.* 18:527-32

340. Sun L, Li J, Xiao X. 2000. Overcoming adeno-associated virus vector size limitation through viral DNA heterodimerization. *Nat. Med.* 6:599-602
341. Yan Z, Lei-Butters DC, Zhang Y, Zak R, Engelhardt JF. 2007. Hybrid adeno-associated virus bearing nonhomologous inverted terminal repeats enhances dual-vector reconstruction of minigenes in vivo. *Hum. Gene Ther.* 18:81-7
342. Xu R, Janson CG, Mastakov M, Lawlor P, Young D, Mouravlev A, Fitzsimons H, Choi KL, Ma H, Dragunow M, Leone P, Chen Q, Dicker B, During MJ. 2001. Quantitative comparison of expression with adeno-associated virus (AAV-2) brain-specific gene cassettes. *Gene Therapy* 8:1323-32
343. Kumar M, Keller B, Makalou N, Sutton RE. 2001. Systematic determination of the packaging limit of lentiviral vectors. *Human Gene Therapy* 12:1893-905
344. Peel AL, Klein RL. 2000. Adeno-associated virus vectors: activity and applications in the CNS. *Journal of Neuroscience Methods* 98:95-104
345. Brenner M, Kisseberth WC, Su Y, Besnard F, Messing A. 1994. Gfap Promoter Directs Astrocyte-Specific Expression in Transgenic Mice. *Journal of Neuroscience* 14:1030-7
346. Weller ML, Stone IM, Goss A, Rau T, Rova C, Poulsen DJ. 2008. Selective overexpression of excitatory amino acid transporter 2 (EAAT2) in astrocytes enhances neuroprotection from moderate but not severe hypoxia-ischemia. *Neuroscience* 155:1204-11
347. Haberman RP, Mccown TJ, Samulski RJ. 2000. Novel transcriptional regulatory signals in the adeno-associated virus terminal repeat A/D junction element. *Journal of Virology* 74:8732-9
348. Kugler S, Meyn L, Holzmüller H, Gerhardt E, Isenmann S, Schulz JB, Bähr M. 2001. Neuron-specific expression of therapeutic proteins: evaluation of different cellular promoters in recombinant adenoviral vectors. *Mol. Cell Neurosci.* 17:78-96
349. Forsspetter S, Danielson PE, Catsicas S, Battenberg E, Price J, Nerenberg M, Sutcliffe JG. 1990. Transgenic Mice Expressing Beta-

- Galactosidase in Mature Neurons Under Neuron-Specific Enolase Promoter Control. *Neuron* 5:187-97
350. Kugler S, Lingor P, Scholl U, Zolotukhin S, Bahr M. 2003. Differential transgene expression in brain cells in vivo and in vitro from AAV-2 vectors with small transcriptional control units. *Virology* 311:89-95
351. Miller FD, Rogers D, Bamji SX, Slack RS, Gloster A. 1996. Analysis and manipulation of neuronal gene expression using the T alpha 1 alpha-tubulin promoter. *Seminars in the Neurosciences* 8:117-24
352. Lee Y, Messing A, Su M, Brenner M. 2008. GFAP promoter elements required for region-specific and astrocyte-specific expression. *Glia* 56:481-93
353. Chen H, McCarty DM, Bruce AT, Suzuki K, Suzuki K. 1998. Gene transfer and expression in oligodendrocytes under the control of myelin basic protein transcriptional control region mediated by adeno-associated virus. *Gene Therapy* 5:50-8
354. Yang C, Boucher F, Tremblay A, Michaud JL. 2004. Regulatory interaction between arylhydrocarbon receptor and SIM1, two basic helix-loop-helix PAS proteins involved in the control of food intake. *Journal of Biological Chemistry* 279:9306-12
355. Michaud JL, Rosenquist T, May NR, Fan CM. 1998. Development of neuroendocrine lineages requires the bHLH-PAS transcription factor SIM1. *Genes & Development* 12:3264-75
356. Woodson KG, Crawford PA, Sadovsky Y, Milbrandt J. 1997. Characterization of the promoter of SF-1, an orphan nuclear receptor required for adrenal and gonadal development. *Molecular Endocrinology* 11:117-26
357. Picon A, Bertagna X, de Keyser Y. 1999. Analysis of the human proopiomelanocortin gene promoter in a small cell lung carcinoma cell line reveals an unusual role for E2F transcription factors. *Oncogene* 18:2627-33
358. Brown AM, Mayfield DK, Volafova J, Argyropoulos G. 2001. The gene structure and minimal promoter of the human agouti related protein. *Gene* 277:231-8

359. Lin SL, Miller JD, Ying SY. 2006. IntronicMicroRNA (miRNA). *Journal of Biomedicine and Biotechnology*
360. McBride JL, Boudreau RL, Harper SQ, Staber PD, Monteys AM, Martins I, Gilmore BL, Burstein H, Peluso RW, Polisky B, Carter BJ, Davidson BL. 2008. Artificial miRNAs mitigate shRNA-mediated toxicity in the brain: implications for the therapeutic development of RNAi. *Proc. Natl. Acad. Sci. U. S. A* 105:5868-73
361. Shan Z, Lin Q, Deng C, Li X, Huang W, Tan H, Fu Y, Yang M, Yu XY. 2009. An efficient method to enhance gene silencing by using precursor microRNA designed small hairpin RNAs. *Mol. Biol. Rep.* 36:1483-9
362. Boudreau RL, Martins I, Davidson BL. 2009. Artificial microRNAs as siRNA shuttles: improved safety as compared to shRNAs in vitro and in vivo. *Mol. Ther.* 17:169-75
363. Boden D, Pusch O, Silbermann R, Lee F, Tucker L, Ramratnam B. 2004. Enhanced gene silencing of HIV-1 specific siRNA using microRNA designed hairpins. *Nucleic Acids Research* 32:1154-8
364. Stieger K, Belbellaa B, Le Guiner C, Moullier P, Rolling F. 2009. In vivo gene regulation using tetracycline-regulatable systems. *Advanced Drug Delivery Reviews* 61:527-41
365. Goverdhana S, Puntel M, Xiong W, Zirger JM, Barcia C, Curtin JF, Soffer EB, Mondkar S, King GD, Hu J, Sciascia SA, Candolfi M, Greengold DS, Lowenstein PR, Castro MG. 2005. Regulatable gene expression systems for gene therapy applications: Progress and future challenges. *Molecular Therapy* 12:189-211
366. Grill HJ. 2006. Distributed neural control of energy balance: contributions from hindbrain and hypothalamus. *Obesity. (Silver. Spring)* 14 Suppl 5:216S-21S
367. Patel HR, Qi Y, Hawkins EJ, Hileman SM, Elmquist JK, Imai Y, Ahima RS. 2006. Neuropeptide Y deficiency attenuates responses to fasting and high-fat diet in obesity-prone mice. *Diabetes* 55:3091-8
368. Korner J, Wardlaw SL, Liu SM, Conwell IM, Leibel RL, Chua SC, Jr. 2000. Effects of leptin receptor mutation on AgRP gene expression in fed and fasted lean and obese (LA/N-faf) rats. *Endocrinology* 141:2465-71

- 369. Torisu T, Sato N, Yoshiga D, Kobayashi T, Yoshioka T, Mori H, Iida M, Yoshimura A. 2007. The dual function of hepatic SOCS3 in insulin resistance in vivo. *Genes to Cells* 12:143-54
- 370. Shi H, Cave B, Inouye K, Bjorbaek C, Flier JS. 2006. Overexpression of suppressor of cytokine signaling 3 in adipose tissue causes local but not systemic insulin resistance. *Diabetes* 55:699-707
- 371. Di M, V, Matias I. 2005. Endocannabinoid control of food intake and energy balance. *Nat. Neurosci.* 8:585-9
- 372. Narayanan NS, Guarnieri DJ, Dileone RJ. 2009. Metabolic hormones, dopamine circuits, and feeding. *Front Neuroendocrinol.*
- 373. Havel PJ. 2001. Peripheral signals conveying metabolic information to the brain: short-term and long-term regulation of food intake and energy homeostasis. *Exp. Biol. Med. (Maywood.)* 226:963-77

OPTIMALISATIE VAN VIRALE VECTOR TECHNOLOGIE OM DE FUNCTIE VAN GENEN IN DE HYPOTHALAMUS TE BESTUDEREN

SAMENVATTING IN HET NEDERLANDS

Virale vectoren kunnen worden gebruikt om stukjes DNA in cellen te brengen en zo de expressie van een bepaald gen te verhogen (overexpressie) of te verlagen (knockdown). Door een virale vector coderend voor een bepaald gen in een specifiek weefsel te injecteren kan er bestudeerd worden welke functie een gen heeft in het weefsel. Zoals de naam doet vermoeden zijn virale vectoren afgeleid van virussen, maar ze zijn zo veranderd dat ze alleen nog de eigenschap van “infectie” (waardoor ze dus de cellen kunnen binnendringen) bezitten. Het binnendringen van virale vectoren in cellen wordt transductie genoemd, omdat virale vectoren zich niet kunnen vermenigvuldigen en dus ook niet door het lichaam heen verspreiden en een ziekte veroorzaken. Er zijn vele verschillende virale vectoren die allen hun eigen voor- en nadelen hebben. In dit proefschrift zijn 2 soorten virale vectoren gebruikt om DNA afgifte te bewerkstelligen in de hypothalamus, namelijk lentivirale (LV) vectoren en adeno-geassocieerde virale (AAV) vectoren. De hypothalamus is een gebied in de hersenen dat uit meerdere kernen bestaat en betrokken is bij de regulatie van energie inname en energie verbruik (energie balans). Bij de regulatie van energie balans zijn meerdere hersengebieden en eiwitten (neuropeptiden) betrokken, maar over de specifieke functies van de verschillende neuropeptiden in bepaalde hypothalamische kernen is nog onvoldoende bekend. Kennis over welke functie een bepaald gen in een specifieke kern van de hypothalamus heeft, kan nieuwe inzichten geven voor de ontwikkeling van therapieën voor obesitas en eetstoornissen. Daarom is in dit proefschrift bestudeerd welke functies het leptine en melanocortine systeem, in specifieke hypothalamische kernen, hebben op voedselinname en energieverbruik.

Om de effecten van bepaalde genen (uit het leptine en melanocortine systeem) op energie balans te kunnen bestuderen is eerst onderzocht welke virale vector, AAV of LV, het beste de hypothalamus transduceert om gen afgifte te bewerkstelligen. In hoofdstuk 2 wordt beschreven in welke mate AAV en LV vectoren de hersencellen (neuronen) in de laterale hypothalamus of in de amygdala van volwassen ratten transduceren. Uit de resultaten blijkt dat AAV-gemedieerde gen afgifte meer cellen in de laterale hypothalamus en amygdala transduceert dan LV-gemedieerde gen afgifte. Daarnaast kan de hoeveelheid geïnjecteerde AAV deeltjes eenvoudig verhoogd worden, omdat de stock 660 keer verdund was voor

injectie. Het geïnjecteerde aantal LV deeltjes, daarentegen, is moeilijk te verhogen omdat de stock maar 4 keer verdund was voor injectie. De verschillen in efficiëntie kunnen veroorzaakt zijn doordat AAV en LV vectoren een ander jasje om hun DNA/RNA hebben en daarom andere receptoren gebruiken om een cel te transduceren. Dus in andere hersengebieden/weefsels (andere cel soorten), in andere ontwikkelingsstadia (e.g. neonataal, adolescent) of in andere diersoorten kan het zijn dat LV vectoren juist een betere transductie efficiëntie hebben dan AAV.

De studie in hoofdstuk 2 laat zien dat AAV vectoren een betere methode zijn om de laterale hypothalamus van een volwassen rat te transduceren dan LV vectoren. Daarom is in hoofdstuk 3 het transductie profiel van AAV-gemedieerde genafgifte verder bestudeerd om de transductie efficiëntie te verbeteren. Een AAV-DNA construct is verpakt in verschillende eiwitjasjes (van andere AAV soorten (serotypes)) om te bestuderen welk jasje het beste zijn AAV-DNA construct afgeeft aan cellen in de hypothalamus. Hieruit blijkt dat het jasje van AAV1 de meeste cellen transduceert. Daarnaast is er gekeken of veranderingen in hoeveelheid van AAV1 verpakte AAV-DNA deeltjes (titers) of in injectievolume nog konden bijdragen aan een meer of mindere verspreiding van het aantal getransduceerde cellen in de hypothalamus. Hieruit bleek dat AAV1 verpakte AAV-DNA met een hoeveelheid van 1×10^9 deeltjes in een volume van 1 μ l (μ l is 1000x minder dan een ml) voldoende is om bijna alle cellen in hypothalamische kernen, zoals de laterale hypothalamus of de paraventriculaire hypothalamus, te transduceren en daar dus gen afgifte te bewerkstelligen. Er zijn heel veel AAV soorten en we hadden niet de mogelijkheid alle bestaande soorten te testen, dus het zou kunnen zijn dat er nog AAV soorten zijn die de hypothalamus beter transduceren dan AAV1 verpakte AAV-DNA constructen.

De optimale manier van gen afgifte die beschreven is in hoofdstuk 3 is gebruikt om de expressie van een neuropeptide dat eetlust opwekt (agouti-related peptide (AgRP)), te verhogen in specifieke hersengebieden van volwassen ratten. AgRP wordt normaal in bepaalde cellen (AgRP/NPY neuronen) van de arcuate nucleus (in de hypothalamus) gemaakt en afgegeven in veel hersengebieden, doordat de neuronen uitlopers (projecties) hebben naar die gebieden. In deze gebieden kan AgRP binden aan de melanocortine receptoren 3 en 4 en ervoor zorgen dat melanocortine signalering geremd wordt. Door verlaging van melanocortine signalering verhogen dieren en mensen hun voedselinname. Om te bestuderen wat de effecten van AgRP in bepaalde projectiegebieden op voedselinname en energieverbruik zijn, zijn AAV1-AgRP deeltjes geïnjecteed in een aantal van deze projectiegebieden in de hypothalamus (laterale hypothalamus (LH), paraventriculaire hypothalamus (PVN) of ventromediale hypothalamus (VMH)) of in de accumbens. De resultaten laten zien dat in ieder van de hypothalamische gebieden

(LH, PVN en VMH) remming van het melanocortine systeem, door AAV-AgRP, het lichaamsgewicht en hoeveelheid vet verhoogt ten opzichte van controles (AAV-GFP). Dit komt door een verhoging in voedselinname, via een vergroting van de maaltijdgrootte in zowel de licht- als donkerperiode. Daarnaast verhoogt AgRP in de PVN ook het aantal maaltijden dat genuttigd wordt in de lichtperiode (de normale slaaperperiode van ratten). De effecten van AAV1-AgRP in de hypothalamische kernen op energieverbruik (in deze studie de dagelijkse beweging en lichaamstemperatuur) zijn meer uiteenlopend. AgRP overexpressie in de PVN of VMH verhoogt lichaamstemperatuur in de donkerperiode op dag 40 na injectie, terwijl AgRP in de LH geen effecten had op lichaamstemperatuur. Remming van melanocortine signalering in de PVN verlaagt de hoeveelheid lichaamsbeweging in de donkerperiode op dag 20 en 40 na injectie van AAV-AgRP. Daarnaast zijn er kern-specifieke effecten op leptine en insuline concentraties in het bloed. Dus remming van melanocortine systeem (door AAV-gemedieerde AgRP expressie) in verschillende hypothalamische kernen verhoogt lichaamsgewicht en voedselinname door vergroting van maaltijd grootte, maar er zijn kernspecifieke effecten op energieverbruik en endocriene parameters. Overexpressie van AgRP in de accumbens had geen effecten op de voedselinname of energieverbruik van de ratten.

Deze AgRP overexpressie data is vergeleken met data van een experiment in ons lab waar neuropeptide Y (NPY) tot overexpressie was gebracht met AAV in de LH en PVN. AgRP en NPY worden namelijk gemaakt in dezelfde cellen in de arcuate nucleus en beide verhogen voedselinname. De vergelijking van effecten van NPY en AgRP laat duidelijk zien dat beide neuropeptiden leiden tot dik worden, maar dat dit via andere mechanismen gaat.

Een nadeel van de methode die in hoofdstuk 4 is gebruikt is dat het niet met 100% zekerheid te zeggen is dat al het uitgescheiden AgRP, uit AAV-AgRP getransduceerde cellen, daadwerkelijk in het projectiegebied is gebleven. Het is mogelijk dat in het projectiegebied cellen zijn geraakt die weer naar een ander gebied projecteren en dat AgRP daar uitgescheiden is. Daarom hebben we een nieuwe methode bedacht en getest in hoofdstuk 5 om de uitscheiding van AgRP bij het cellichaam te houden, zodat AgRP niet de projecties ingaat en bij die uiteinden uitgescheiden kan worden. Een korte, werkzame versie van AgRP, AgRP₈₃₋₁₃₂, werd in AAV gezet en getest. De resultaten lieten zien dat deze korte versie bij het cellichaam werd uitgescheiden en dat het na injectie in de PVN van ratten ook lichaamsgewicht en voedselinname verhoogde. Dus deze nieuwe methode kan in het vervolg gebruikt worden om neuropeptiden tot overexpressie te brengen en zo te bewerkstelligen dat het AAV-neuropeptide construct ook echt in het geïnjecteerde hersengebied wordt uitgescheiden.

Leptine is een hormoon dat gemaakt wordt in vetcellen naar ratio voor de hoeveelheid vet (meer vet dan meer leptine in het bloed). Normaal leiden hogere leptine concentraties tot verlaging van voedselinname door onder andere een verhoging van melanocortine signalering (verhoging van activator, POMC, en verlaging van de remmer, AgRP) en verlaging van NPY signalering (verlaging van NPY). Mensen en dieren met obesitas hebben hoge leptine concentraties, maar eten nog steeds teveel. Daarnaast reageren zij ook niet meer met een verlaging van voedselinname wanneer leptine wordt geïnjecteerd. Daarom lijkt obesitas geassocieerd met ongevoeligheid voor leptine (leptine resistentie). De huidige literatuur suggereert dat verhoging van Socs3 expressie in de arcuate nucleus een bijdrage heeft in het ontstaan van leptine ongevoeligheid, omdat Socs3 leptine signalering in de cel remt. In hoofdstuk 6 is bestudeerd wat het effect van verlaging van Socs3 in de mediobasale hypothalamus is op de ontwikkeling van dieet geïnduceerde obesitas. Normaal gaan ratten meer eten als zij beschikking hebben tot vet en sucrose water naast hun gewone voer en water en hierdoor kunnen ze obese worden, dit fenomeen wordt dieet geïnduceerde obesitas genoemd. Op basis van literatuur werd verwacht dat verlaging van Socs3 beschermend werkt tegen de ontwikkeling van dieet geïnduceerde obesitas. Maar de resultaten lieten zien dat verlaging van Socs3 (door middel van short hairpin RNA) in de mediobasale hypothalamus er juist voor zorgde dat ratten zwaarder werden dan hun controles. Dit kwam niet door een verhoging van inname van calorieën (wel een verschuiving in maaltijdpatronen), maar door een verlaging van lichaamsbeweging en lichaamstemperatuur in de donkerperiode. Het lijkt erop dat deze effecten veroorzaakt zijn door een verhoging van NPY expressie in de arcuate nucleus, als gevolg van de verlaging van Socs3. Deze resultaten suggereren dat leptine signalering complexer is dan gedacht en dat er een delicate balans is van moleculen, waaronder Socs3, die de expressie van genen zoals NPY kunnen beïnvloeden.

In hoofdstuk 7 worden de resultaten van dit proefschrift samengevat en aanbevelingen gegeven voor toekomstig onderzoek.

Dit proefschrift heeft laten zien dat virale vector technologie een valide methode is om lokaal gen expressie in het brein te veranderen en dat dit een mooie aanvulling is op al bestaande technieken om de functie van een gen in een specifiek gebied e/o gedrag te bestuderen.

CURRICULUM VITAE

Maria Wilhelmina Anna de Backer (Marijke) werd geboren op 25 november 1980 te 's-Hertogenbosch. In 1999 behaalde zij haar VWO diploma aan het Frederik Hendrik College te 's-Hertogenbosch, waarna zij in 2000 aan haar studie biomedische wetenschappen begon aan de Universiteit Utrecht. In 2003 begon ze aan de prestigieuze master Neuroscience and Cognition, in het programma Experimental and Clinical neuroscience, ook aan de Universiteit van Utrecht. Tijdens de master werden twee onderzoeksstages verricht. De eerste stage werd uitgevoerd bij de afdeling Neurowetenschappen en Farmacologie van het Rudolf Magnus Instituut voor Neurowetenschappen te Utrecht. Onder begeleiding van Dr. M.P. Smidt heeft zij het expressie patroon van metabotrope glutamaat receptoren tijdens de ontwikkeling van het muizen brein bestudeerd. De tweede stage werd uitgevoerd bij het Nederlands Instituut voor Hersenonderzoek te Amsterdam, waar zij heeft gewerkt aan de constructie van self-complementary adeno-associated viral vectors om neuroregeneratie te bevorderen, onder begeleiding van Prof. Dr. J. Verhaagen en Dr. F. Fallaux. In 2005 werd de master met goed gevolg afgesloten en werd zijn aangesteld als onderzoeker in opleiding bij de afdeling Neurowetenschappen en Farmacologie onder begeleiding van Prof. Dr. R.A.H. Adan. De resultaten van het onderzoek naar moleculaire mechanismen bij regulatie van energiebalans staan beschreven in dit proefschrift.

LIST OF PUBLICATIONS

van Hooijdonk LW, Ichwan M, Dijkmans TF, Schouten TG, **de Backer MW**, Adan RA, Verbeek FJ, Vreugdenhil E, Fitzsimons CP (2009). Lentivirus-mediated transgene delivery to the hippocampus reveals sub-field specific differences in expression. *BMC Neuroscience* 2009 Jan 13;10(1):2.

MWA de Backer, MAD Brans, MCM. Luijendijk, KM Garner, RAH Adan (2010). Optimization of adeno-associated viral vector mediated gene delivery to the hypothalamus. *Human Gene Therapy*. In press, Epub 14 jan. 2010
doi: 10.1089/hum. 2009.169.

Jethwa P, Warner A, Fowler M, Murphy M, **de Backer M**, Adan RAH, Barret P, Ebling F (2010). Short-days induce weight loss in Siberian hamsters despite overexpression of the agouti-related peptide (AgRP) gene. *Journal of Neuroendocrinology*. In press, Epub 27 March 2010
doi: 10.1111/j.1365-2826.2010.02001.x

MWA de Backer, RAH Adan. Recombinant adeno-associated viral vectors. Chapter 16 in *Neuropeptides: methods and protocols* in the serie *Methods in Molecular Biology*. In press.

MWA de Backer, MAD Brans, MCM Luijendijk, KM Garner, DMA van den Heuvel, RJ Pasterkamp, RAH Adan. A new method to deliver neuropeptides to the brain: a von Willebrand factor signal peptide to direct local neuropeptide secretion. Submitted.

MWA de Backer, CP Fitzsimons, MAD Brans, MCM Luijendijk, KM Garner, E Vreugdenhil, RAH Adan. An adeno-associated viral vector transduced the rat hypothalamus and amygdala more efficient than a lentiviral vector. Submitted.

MWA de Backer, SE la Fleur, MAD Brans, AJ van Rozen, MCM Luijendijk, M Merkestein, KG Garner, EM van der Zwaal, RAH Adan. Melanocortin receptor mediated effects on obesity are distributed over specific hypothalamic regions. Submitted.

MWA de Backer, MAD Brans, AJ van Rozen, EM van der Zwaal, MCM Luijendijk, KG Garner, M de Krom, O van Beekum, SE la Fleur[§], RAH Adan[§]. Suppressor of cytokine signaling (SOCS) 3 knockdown in the mediobasal hypothalamus: counterintuitive effects on energy balance. Submitted. [§] shared last authorship.

DANK JE WEL

De afgelopen jaren heb ik met veel plezier gewerkt aan het onderzoek dat in dit proefschrift is beschreven. Natuurlijk zijn bij het promoveren de mensen om je heen van groot belang, daarom wil ik hier graag de mensen bedanken die van belangrijke waarde zijn geweest.

Allereerst wil ik mijn promotor Roger Adan bedanken voor de supervisie en mogelijkheid om aan dit promotieonderzoek te werken. Voor overleg, advies en vragen kon ik op praktisch ieder moment bij je terecht. Ook al verliepen experimenten in het begin niet allemaal zoals verwacht, uiteindelijk zijn er mooie resultaten uitgekomen.

Susanne la Fleur, bedankt voor je steun, het enthousiast bestuderen van mijn gedragsdata, het geven van nieuwe inzichten en je goede adviezen.

Mariken de Krom bedankt voor je begeleiding met praktische dingen op het DNA-lab toen ik net begon en je goede adviezen later toen je geen postdoc meer was.

Maike en Mienke dankzij jullie was het mogelijk al het moleculaire werk op het lab te combineren met experimenten in ratten. Bedankt voor alle operaties en uitvoeren van veel van het dierwerk. Maike, ook erg bedankt voor de hulp bij het snijden van al die rattenbreintjes en het analyseren van de verspreiding van de AAV vectoren.

Rea, heel erg bedankt voor je hulp bij alle radioactieve in situ hybridisaties en het analyseren van al die data, zodat het toch ook nog op tijd allemaal klaar was voor dit boekje en al je gezelligheid.

Keith en Myrte, super dat jullie mijn paranimfen willen zijn. Keith bedankt voor alle inspirerende, maar ook gezellige gesprekken/discussies vanaf dag 1 en je hulp bij het opzetten van AAV productie op het RMI. Gezellig samen op de knieën voor de wetenschap! Myrte dank je wel voor je adviezen over dierwerk en natuurlijk voor alle gesprekken over van alles en nog wat op onze kamer.

Esther dank je wel voor de hulp bij dierwerk en alle (textuele) suggesties.

Ik heb ook veel te danken aan de bijdragen van collega's Dianne (RMI) en Jeroen (RMI), Miguel Sena-Esteves (University of Massachusetts), Carlos Fitzsimons (LUMC) en Erno Vreugdenhil (LUMC). Dank voor de fijne samenwerking.

Mijn studenten Margriet, Magdalena en Emmely, ik vond het heel leuk jullie te begeleiden. Margriet veel succes met je promotieonderzoek en als veelbelovende opvolger van mij. Magdalena success met je promotieonderzoek op het Hubrecht lab. Emmely veel succes met het maken van een keuze wat je wilt gaan doen na je stage in Aberdeen. Wetenschap of toch niet? Ik ben benieuwd.

Mijn kamergenootjes van kamer 4.219: Myrte, Dianne, Rou-Afza, Linda en Marijke A. dank voor alle gesprekken, gezelligheid en al het lekkers zoals de baksels. Jullie moeten snel weer eens pannenkoeken komen eten!

De rest van de Adan groep: Linda, Gitte, Judith, Yanina, Olivier, Ralph, Arjen, Sanna, Tom, Jan-Willem, Frank M. en Edwin. Dank voor de gesprekken en discussies over wetenschap en andere onderwerpen.

Afdeling neurowetenschappen en farmacologie van het RMI. Ik wil iedereen bedanken voor de geweldige tijd bij de afdeling! Dank voor alle steun, interesse en gezelligheid. Henk, dank je wel voor alle radioactiviteit voor al die southernns en voor de gezelligheid als we weer eens alleen met zijn tweeën op het grote DNA lab aan het werk waren. Heidi dank je wel voor je interesse en gezellige gesprekken over van alles en nog wat, super dat de lentivirale vectoren nu ook in jouw "nederlandse" muizen werken. Leo, Jan en Wout bedankt voor alle hulp met van alles en nog wat betreffende de 4^e en 5^e verdieping. En verder Ela, Eneda, Frank J., Elisa, Teresa, Anita, Lars, Youri, Raymond, Marina, Marije, Annemarie, Bert, Ellen, Maartje, Ria, Krista, Vicki, Joke, Marten, Roger2, Sandra, Hugo en de rest heel erg bedankt. Ik zal de Friday afternoon cookie missen.

Vrienden en familie. Pap en mam dank jullie wel voor jullie interesse en pogingen te snappen waar mijn onderzoek over ging en de mogelijkheid om überhaupt naar de universiteit te gaan. Paula en Johan dank jullie wel dat jullie een beetje probeerde te snappen wat ik deed. Myrthe dank je wel dat je me mijn beide benen op de grond zet om lekker buiten te spelen of te gaan sleeën en toen ik hard bezig was met schrijven. De rest van mijn familie (sinds oktober een stuk groter geworden) en vrienden, bedankt voor de interesse in mijn (waarschijnlijk soms onbegrijpelijke) werkzaamheden op het lab.

Marc, lieverd dank je wel voor alle liefde en het vertrouwen dat het allemaal goed zal komen. Ook heel veel dank voor je begrip als ik lange dagen maakte of weer eens naar Utrecht moest in het weekend en voor het eerste ontwerp van de omslag. Ik vind het heel fijn dat jij er altijd voor me bent.



